Water Research 213 (2022) 118053

Contents lists available at ScienceDirect

Water Research

journal homepage: www.elsevier.com/locate/watres

Ozonation of organic compounds in water and wastewater: A critical review

Sungeun Lim [a,†], Jiaming Lily Shi [b,†], Urs von Gunten [a,c,*], Daniel L. McCurry [b,*]

[a] Eawag, Swiss Federal Institute of Aquatic Science and Technology, Dübendorf CH-8600, Switzerland
[b] Department of Civil and Environmental Engineering, University of Southern California, Los Angeles, CA, United States
[c] School of Architecture, Civil and Environmental Engineering (ENAC), Ecole Polytechnique Fédérale de Lausanne (EPFL), Lausanne CH-1015, Switzerland

ARTICLE INFO

Keywords:
Organic contaminants
Kinetics
Mechanisms
Dissolved organic matter
Antibiotic resistance genes
Ozone

ABSTRACT

Ozonation has been applied in water treatment for more than a century, first for disinfection, later for oxidation of inorganic and organic pollutants. In recent years, ozone has been increasingly applied for enhanced municipal wastewater treatment for ecosystem protection and for potable water reuse. These applications triggered significant research efforts on the abatement efficiency of organic contaminants and the ensuing formation of transformation products. This endeavor was accompanied by developments in analytical and computational chemistry, which allowed to improve the mechanistic understanding of ozone reactions. This critical review assesses the challenges of ozonation of impaired water qualities such as wastewaters and provides an up-to-date compilation of the recent kinetic and mechanistic findings of ozone reactions with dissolved organic matter, various functional groups (olefins, aromatic compounds, heterocyclic compounds, aliphatic nitrogen-containing compounds, sulfur-containing compounds, hydrocarbons, carbanions, β-diketones) and antibiotic resistance genes.

1. Introduction

Ozonation has been applied in drinking water treatment for disinfection and oxidation for decades. Currently, as its application area is being further extended to wastewater treatment and potable water reuse, ozonation is facing new challenges associated with higher concentrations and new types of dissolved organic matter as well as a larger range of organic contaminants. This critical review provides the background of the current developments in ozonation applications (Section 2), addresses new challenges associated with the impact of dissolved organic matter on ozonation performance (Section 3), and provides a critical compilation of kinetic and mechanistic information necessary to evaluate abatement of organic compounds during ozonation (Section 4). Furthermore, the abatement of antibiotic resistance is discussed (Section 5) and compared to the abatement of micropollutants and bromate formation.

2. Ozonation in drinking water and wastewater treatments

2.1. Drinking water

2.1.1. From disinfection to oxidation

Ozonation has been applied in drinking water for more than a century, mainly for disinfection purposes (Fig. 1) (von Sonntag and von Gunten, 2012). It was considered as an equivalent to chlorine and in some cases an ozone residual was maintained in the distribution system for groundwaters with low DOC concentrations and with high carbonate alkalinity, conditions which warrant a high ozone stability (Courbat et al., 1999; Hoigné, 1998). In addition to its outstanding capacity for the inactivation of microorganisms, such as viruses, bacteria, and protozoa (von Sonntag and von Gunten, 2012; Wolf et al., 2018), ozone was also applied at an early stage to oxidatively abate inorganic compounds (e.g., Fe(II), Mn(II), NO_2^-, HS^-) and to control taste and odor issues (Fig. 1) (von Gunten, 2003b). Only in the 1970s and 1980s, the mechanism of ozone decomposition in water was elucidated and it was demonstrated that hydroxyl radicals ($^{\bullet}OH$) are formed during this process (Bühler et al., 1984; Hoigné and Bader, 1975; Staehelin et al., 1984;

* Corresponding authors.
E-mail addresses: urs.vongunten@eawag.ch (U. von Gunten), dmccurry@usc.edu (D.L. McCurry).
† Equal contributions from S.L. and J.L.S.

https://doi.org/10.1016/j.watres.2022.118053
Received 2 September 2021; Received in revised form 5 January 2022; Accepted 8 January 2022
Available online 10 January 2022

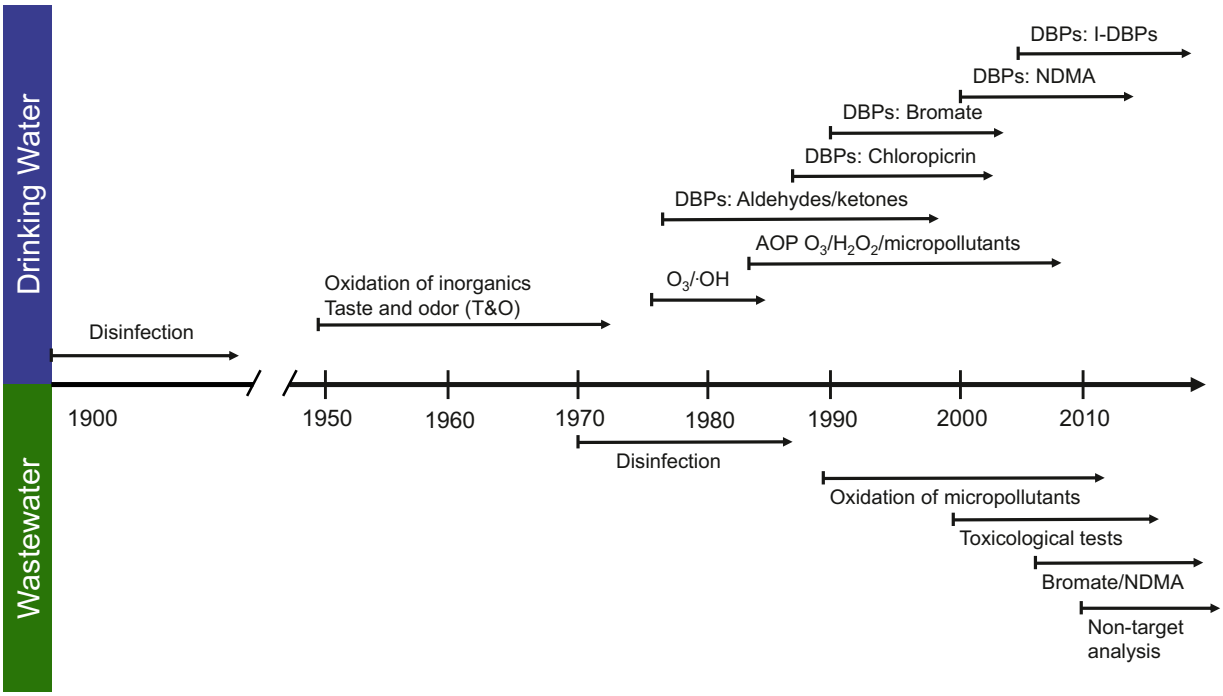

Fig. 1. Timeline of ozone applications in drinking water and wastewater: Challenges and solutions.

Staehelin and Hoigné, 1985). It was also shown that ozone transformation to •OH can be accelerated by hydrogen peroxide (H_2O_2), which opened up the possibility for ozone-based advanced oxidation processes (AOPs), which combine ozone and •OH oxidation and are applicable for oxidant-resistant micropollutant abatement (Fig. 1) (Aieta et al., 1988; von Gunten, 2018). As a consequence of this discovery, ozone-based AOPs were implemented in the 1990s especially in France to abate ozone-resistant pesticides (mainly atrazine) (Duguet et al., 1990). However, due to the drinking water regulations of the European Union in 1998 (EU, 1998), which included metabolites from pesticides as regulated products, this approach was no longer accepted in France and as a consequence, AOPs were banned for the abatement of pesticides and only admitted for the treatment of chlorinated solvents (von Gunten, 2018). The formation of transformation products during ozonation of micropollutants will be discussed in more detail in several sections below.

2.1.2. *Disinfection byproducts formation and mitigation*

In applications of chlorine, trihalomethanes (THMs) were reported as disinfection byproducts (DBPs) in the mid 1970s (Rook, 1974). However, it took much longer until DBPs were considered during ozonation processes (Hoigné, 1998; von Gunten, 2018). First the formation and removal (by biological post-filtration) of aldehydes, ketones and carboxylic acids was studied (Glaze et al., 1989; Hammes et al., 2006; Hammes et al., 2007; Nawrocki et al., 2003; Ramseier et al., 2011a; Swietlik et al., 2004; Swietlik et al., 2009; van der Kooij et al., 1989; Zürcher et al., 1978) and then the formation of trichloronitromethane (chloropicrin) during post-chlorination of ozonated waters was investigated (Fig. 1) (Hoigné and Bader, 1988; Thibaud et al., 1987). Even though bromate formation during ozonation of bromide-containing waters was already investigated in the early 1980s (Haag and Hoigné, 1983b), it only became an issue when it was found to be a possible human carcinogen in the early 1990s (Fig. 1) (WHO, 2017). The relatively stringent and quite universal drinking water standard for bromate (10 μg/L) often limits ozone applications for disinfection purposes. Therefore, several mitigation options were developed such as pH depression, ammonium addition, chlorine/ammonium or ammonium/-chlorine addition when disinfection is the main purpose and hydrogen peroxide addition when disinfection is not the primary target for ozonation (Buffle et al., 2004; Haag and Hoigné, 1983b; Krasner et al., 1993; Pinkernell and von Gunten, 2001; Song et al., 1996; Song et al., 1997; von Gunten and Hoigné, 1994; von Gunten and Oliveras, 1998; von Gunten, 2003a). An updated mechanism for bromate formation during ozonation is presented elsewhere (von Sonntag and von Gunten, 2012). With the discovery of the formation of *N*-nitrosamines during chlorination/-chloramination in the early 2000s (Mitch and Sedlak, 2002; Mitch et al., 2003b; Najm and Trussell, 2001), pre-oxidation by ozone was found to be an interesting option for the mitigation of these undesired compounds (Chen and Valentine, 2008; Krasner et al., 2018; Lee et al., 2007a; McCurry et al., 2015; Shah et al., 2012). However, numerous studies also reported *N*-nitrosamine formation during ozonation of individual target compounds (Andrzejewski et al., 2008; Lim et al., 2016; Marti et al., 2015; Oya et al., 2008; Schmidt and Brauch, 2008), including a case of bromide-catalysis for dimethylsulfamide (Trogolo et al., 2015; von Gunten et al., 2010) and real water matrices (Fig. 1) (Gerrity et al., 2015; Krasner et al., 2013; Pisarenko et al., 2015). Finally, with the discovery of toxic iodo-DBPs, which can be formed during oxidative processes in presence of iodide (Dong et al., 2019; Li et al., 2020), pre-ozonation was recognized as an efficient mitigation strategy to minimize iodo-DBPs by oxidizing iodide quickly to iodate (Fig. 1) (Allard et al., 2013; Bichsel and von Gunten, 1999).

2.2. *Wastewater*

2.2.1. *Disinfection*

Similar to drinking water, ozonation has been implemented in wastewater as a disinfectant before its discharge to the receiving water bodies (Fig. 1) (Gerrity et al., 2012; Janex et al., 2000; Paraskeva and

Graham, 2002; Xu et al., 2002). However, wastewater disinfection requires quite high doses and it is expected that disinfection, including inactivation of ozone-resistant microorganisms such as protozoa, will lead to the formation of bromate above the drinking water standard of 10 μg/L (Lee et al., 2016b; Schindler Wildhaber et al., 2015; Zimmermann et al., 2011).

2.2.2. *Oxidation of micropollutants for potable water reuse purposes (human health)*

Due to issues related to water scarcity and water security, potable water reuse projects are increasing with > 25 full-scale systems in operation worldwide (Marron et al., 2019). Potable water reuse requires a multibarrier approach to guarantee microbial and chemical drinking water safety (Gerrity et al., 2013; Marron et al., 2019). Currently, most of the water reuse facilities rely on systems which treat municipal wastewater effluent by a sequence of membranes (micro- or ultrafiltration and reverse osmosis (RO)) followed by an advanced oxidation process (most commonly UV/H_2O_2) and a disinfection step for the distribution system (Marron et al., 2019). This scheme can also include a pre-ozonation for disinfection as the primary treatment step (Gerrity et al., 2013). Often, an additional cycle through a natural or managed system (reservoir, groundwater) is used to condition the water in terms of temperature, mineral content and to remove biodegradable organic compounds. This approach, which is known as indirect potable reuse, also has reasonable consumer acceptance. Recently, more direct potable reuse projects have been implemented due to the lack of suitable systems or regulations for the storage/recharge of the treated water (Steinle--Darling, 2015). Even though these potable reuse systems provide high quality drinking water, the main drawback is the high waste stream from the concentrate of the RO (also containing antiscalants), which consists of about 20% of the treated water (Pérez-González et al., 2012). In coastal areas, this reject can be discharged to the ocean. However, for inland water reuse applications far from the ocean, such discharges are not possible and alternative treatment strategies have to be developed. Less tight membranes such as nanofiltration can ease this situation to a certain extent, but will still produce a significant waste stream and reject micropollutants to a smaller extent (Marron et al., 2019). Alternatively, treatment schemes involving activated carbon or ozonation combined with biological activated carbon (BAC) filtration were suggested, which reduce the problem of waste streams inherent to tight membrane-based systems significantly and can still provide a good drinking water quality, which was demonstrated in laboratory and pilot studies (Gerrity et al., 2011; Gerrity and Snyder, 2011; Gerrity et al., 2014; Hooper et al., 2020; Reungoat et al., 2012; Sundaram et al., 2020; Vaidya et al., 2019; Zhang et al., 2020). The first potable reuse system worldwide in Windhoek, Namibia comprised several treatment steps including the combination of ozonation with biological activated carbon filtration (Gerrity et al., 2013).

The assessment of ozone-based reuse systems was mainly based on the microbiological and the chemical quality related to micropollutants. Even though this approach seems quite promising, there are several critical points which need to be addressed more carefully for potable reuse systems: (i) Presence of ozone- and $^{\bullet}$OH-resistant compounds that are also not well removed during BAC treatment, (ii) formation of transformation products during ozonation of micropollutants, which are not abated during BAC treatment, (iii) formation of oxidation byproducts from dissolved organic matter (DOM) ozonation, which are not removed in BAC treatment, (iv) bromate formation during ozonation of bromide, which is often elevated in municipal wastewater effluent (see below), and (v) formation of precursors for disinfection byproduct during post-chlorination. Fig. 2 shows a summary of these different aspects.

Some of these issues are the same as for enhanced wastewater treatment for ecological reasons, however, in the context of potable water reuse, they become more critical:

(i) The occurrence of oxidant-resistant compounds such as per- and polyfluoroalkyl substances (PFAS) makes this class of toxic compounds a problem not only in drinking water resources but also in wastewater effluents (Crone et al., 2019; Gallen et al., 2018). Due to their resistance against oxidation, they are difficult to be abated by ozone and $^{\bullet}$OH (Lutze et al., 2018) and also limited removal efficiencies for activated carbon have been

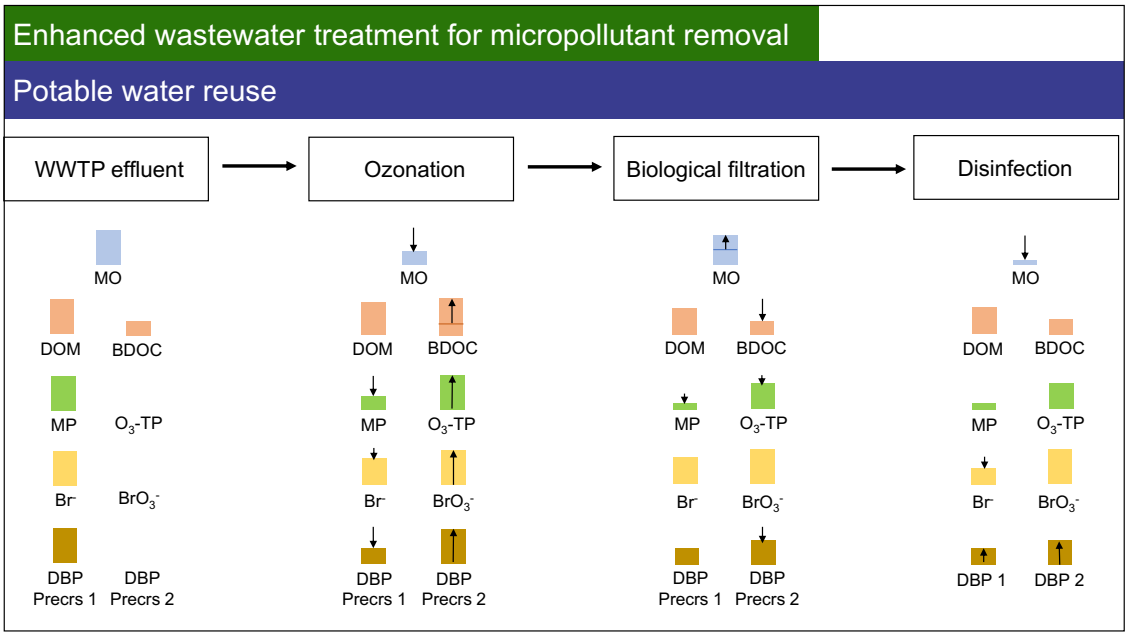

Fig. 2. Water quality aspects (relative concentrations shown with bar heights) for enhanced wastewater treatment with ozonation followed by biological post-treatment (BAC or sand filtration) for ecosystem protection or potable water reuse (additional disinfection step). MO: microorganisms; DOM: dissolved organic matter; BDOC: biologically degradable organic carbon; MP: micropollutant; O_3-TP: transformation product formed during ozonation; Br^-: bromide; BrO_3^-: bromate; DBP Precrs: disinfection byproduct precursors; Precrs1: Abated during ozonation; Precrs 2: Formed during ozonation; DBP: disinfection byproduct.

observed (Crone et al., 2019; Inyang and Dickenson, 2017; Sun et al., 2018).

(ii) Ozonation of micropollutants leads to the formation of transformation products, which are not necessarily biodegradable (Gulde et al., 2021a; Hübner et al., 2015) (Fig. 2). Predictive tools have been developed to assess their formation and it has been demonstrated that several to tens of transformation products can be formed per compound (Lee et al., 2017a). This has also been confirmed by non-target analysis, for which a huge increase in features has been observed during ozonation and only a partial abatement during biological post-filtration (Gulde et al., 2021a; Gulde et al., 2021b; Schollée et al., 2018). It can be assumed that the primary biological effects of the target compounds are abated, but it cannot be excluded that toxic compounds are formed, which are more problematic than the target compounds. However, due to the low concentrations of the micropollutants, it can be expected that the resulting toxicity will be minimal, since only very few classes of organic compounds are still toxic at such low levels.

(iii) Many of the oxygen-rich compounds formed during ozonation of DOM (e.g., aldehydes, ketones, carboxylic acids) are quite well biodegradable (Hammes et al., 2006; van der Kooij et al., 1989) (Fig. 2). In a recent study, α,β-unsaturated carbonyl compounds were detected after wastewater ozonation (Marron et al., 2020). Such electrophilic compounds are problematic because they can bind to DNA and proteins. Even though they are removed by about 90% in biological post-treatment, this class of compounds should be carefully monitored in potable water reuse systems.

(iv) So far in potable water reuse systems applying ozone, there is only limited information on bromate formation (Hooper et al., 2020). Based on the experiences from enhanced wastewater treatment, it can be expected that bromate will become a critical factor, especially if ozonation is applied to inactivate protozoa or bacterial spores (Morrison et al., submitted; Soltermann et al., 2016; Soltermann et al., 2017) (Fig. 2). However, if ozonation is applied for the inactivation of viruses or vegetative bacteria, significant disinfection credit can be achieved with limited bromate formation, because of the high second-order inactivation rate constants of such microorganisms (Hunt and Marinas, 1999; Morrison et al., submitted; Voumard et al., submitted; Wolf et al., 2018).

(v) Whereas ozonation alone may lead to an increase of the DBP precursors, a combination of ozonation with biological treatment is effective in DBP precursor control (Chuang et al., 2019; Krasner, 2009; Sun et al., 2018) (Fig. 2). One case in point is nitromethane formation during ozonation of municipal wastewater effluent, which then leads to the formation of trichloronitromethane during post-chlorination (Shi and McCurry, 2020). Nitromethane formed during wastewater ozonation was subsequently found to persist through membrane and advanced oxidation processes, but to be effectively removed by BAC (Shi et al., 2021). In addition to DBP concentrations, a toxicity-based approach has to be considered. It has been shown, that the combined effect of ozonation/BAC may lead to similar overall toxicity, because of a shift to more toxic DBPs (Chuang et al., 2019).

2.2.3. *Oxidation of micropollutants to reduce their discharge to water bodies (ecosystem health)*

With the development of the coupling of liquid chromatography with mass spectrometry, a new analytical window was established, which allowed the measurement of more polar compounds and led to the discovery of a wide range of (biologically active) organic micropollutants in municipal wastewater (Snyder, 2008; Ternes, 1998). These observations triggered environmental concerns and the ensuing ecological consequences were broadly investigated. Furthermore, the potential for abatement of micropollutants from municipal wastewaters by various strategies was explored, including membranes, activated carbon and chemical oxidation, which is the focus of this review (Fig. 1) (Joss et al., 2008; Ternes and Joss, 2006; Ternes et al., 2004). In these studies, several oxidation processes were investigated for enhanced wastewater treatment, including ferrate (VI) (Lee et al., 2009), chlorine dioxide (Huber et al., 2005b), UV/H_2O_2 and ozone (Huber et al., 2003; Huber et al., 2005a; Lee et al., 2013; Lee et al., 2016a; Ternes et al., 2003; Wert et al., 2009) and Fe-tetramido-macrocyclic ligands (TAML)/H_2O_2 (Jans et al., 2021). Based on these studies and other information from literature, ozonation was selected as the oxidation process of choice for enhanced wastewater treatment in Switzerland and in other countries, because of the broad spectrum of micropollutants which can be abated during ozonation (Domenjoud et al., 2017; Eggen et al., 2014; Gerrity et al., 2012; Hollender et al., 2009; Lee and von Gunten, 2010; Lee et al., 2013; Lee et al., 2014; Lee and von Gunten, 2016; Miklos et al., 2018; Ternes et al., 2003; Ternes et al., 2017; Zimmermann et al., 2011). This initiative triggered significant interest on the influence of oxidative treatment on biological effects of micropollutants and their transformation products (Prasse et al., 2015). It was shown that biologically active compounds such as estrogens, antibiotics, antivirals and pesticides lost their primary target effects during ozonation and other AOPs in laboratory *in vitro* studies (Dodd et al., 2009; Huber et al., 2004; Lange et al., 2006; Lee et al., 2008; Mestankova et al., 2011; Mestankova et al., 2012). During ozonation of real wastewaters in laboratory-, pilot- and full-scale studies, mixed results were obtained with various toxicological endpoints such as the fish early life stage toxicity test, the chironomid toxicity test, the Lumbriculus toxicity test, the *Ceriodaphnia dubia* toxicity test with mostly a reduction in toxicity but in some cases also an increase (Angeles et al., 2020; Escher et al., 2009; Magdeburg et al., 2014; Prasse et al., 2015; Stalter et al., 2010a; Stalter et al., 2010b; Völker et al., 2019; von Gunten, 2018). However, biological post-treatment by sand or activated carbon filtration led mostly to a significant reduction of the toxicity, wherefore, typically, a biological post-treatment step is implemented after ozonation of wastewater (Bourgin et al., 2018; Chys et al., 2017b; Itzel et al., 2020; Knopp et al., 2016; Reungoat et al., 2012). This observation can most likely be explained by potentially (eco)toxic DBPs such as aldehydes and ketones formed during ozonation of wastewater DOM, which are often easily biodegradable (see above). However, potential for the formation of (eco) toxic transformation products from micropollutants exists as mentioned in Section 2.2.2 (Schollée et al., 2018). From a theoretical study and experimental results, it is expected that mainly transformation products from olefins and aromatic compounds are biodegradable, whereas products from nitrogen-containing compounds are expected to be mostly persistent (Bourgin et al., 2018; Hübner et al., 2015; Zucker et al., 2018), however, often such a simplified approach is not justified (Gulde et al., 2021b). An additional benefit of biological post-treatment is a significant abatement of *N*-nitrosodimethylamine (NDMA), which is already present in the raw wastewater and/or formed during ozonation (Bourgin et al., 2018; Krauss et al., 2009). To assess the feasibility of ozonation of municipal wastewater effluents considering also toxicity, test procedures including chemical and toxicological methods have been developed and applied (Itzel et al., 2017; Schindler Wildhaber et al., 2015). Bromide levels in municipal wastewaters can be significantly higher than in drinking waters, occasionally reaching levels of tens of mg/L (Lee et al., 2013; Schindler Wildhaber et al., 2015; Soltermann et al., 2016). This may lead to significant bromate formation during ozonation of municipal wastewaters, especially for specific ozone doses > 0.5 $gO_3/gDOC$, which are typical for enhanced wastewater treatment for micropollutant abatement (Soltermann et al., 2016; Soltermann et al., 2017). Under oxic conditions, which are prevalent after ozonation, bromate persists in biological post-treatment (see Fig. 2 and below).

3. Challenges in wastewater matrices and characterization of DOM by surrogate parameters

3.1. Water matrix: differences between drinking water and wastewater

Ozonation of secondary municipal wastewater effluents entails some challenges, which are not serious issues during drinking water treatment: (i) higher concentrations and different types of DOM, (ii) potential presence of nitrite, and (iii) higher and variable concentrations of bromide.

(i) As a consequence of the higher DOM concentrations, higher concentrations of ozone and $^{\bullet}OH$ are consumed by reactive DOM sites and lead to higher concentrations of AOC/BDOC and low molecular weight oxygen-containing compounds (aldehydes, carboxylic acids) (Marron et al., 2020; Wert et al., 2007; Zimmermann et al., 2011). Because these compounds may lead to enhanced toxicity, a biological post-treatment is necessary for their removal (Prasse et al., 2015; Stalter et al., 2010b). Furthermore, the concentration of dissolved organic nitrogen is typically much higher in secondary municipal wastewater effluent (Chon et al., 2013; Parkin and McCarty, 1981; Pehlivanoglu-Mantas and Sedlak, 2006; Shon et al., 2006) and may lead to nitro and nitroso moieties (Pehlivanoglu-Mantas and Sedlak, 2008; Shi and McCurry, 2020) (see below).

(ii) In secondary wastewater effluents which are not or incompletely nitrified, elevated nitrite concentrations can be found. Since ozone reacts readily with nitrite ($k_{O3} = 3.7 \times 10^5$ $M^{-1}s^{-1}$, (Hoigné et al., 1985)), its presence leads to a stoichiometric consumption of ozone. Furthermore, it has been shown that nitro compounds can be formed as side reactions during ozonation of nitrite-containing waters (Hu et al., 2010; Manasfi et al., In prep.; Thibaud et al., 1987).

(iii) Similar to drinking waters, ozonation of bromide-containing wastewaters leads to bromate formation (Bourgin et al., 2018; Schindler Wildhaber et al., 2015; Wu et al., 2019). Compared to typical drinking waters, the bromide concentrations in secondary wastewater effluents are more variable and can also be significantly higher. This may be caused by discharge from industry, municipal incineration plants, fracking wastewaters, seawater intrusion, etc. (Dong et al., 2017; Harkness et al., 2015; Soltermann et al., 2016). Bromate is only removable under anaerobic conditions (van Ginkel et al., 2005), which are unlikely during biological post-treatment after ozonation. Nevertheless, there are several options to minimize bromate formation during ozonation of secondary municipal wastewater effluent, such as addition of hydrogen peroxide or a distributed dosing of ozone, each of which entails certain limitations and needs to be tested on a case-by-case basis (Merle et al., 2017; Soltermann et al., 2017).

3.2. Control of ozonation systems for enhanced municipal wastewater treatment

Compared to typical drinking water ozonation with ozone lifetimes in the range of tens of minutes, the lifetime of ozone in municipal wastewater effluents is much smaller (Acero and von Gunten, 2001; Buffle et al., 2006b). Therefore, ozone monitoring and control in drinking waters, which is based on direct ozone concentration and decay measurements (Kaiser et al., 2013), is not applicable to municipal wastewater, for which specialized equipment such as stopped-flow or quench-flow is needed to monitor kinetics (Buffle et al., 2006b).

Due to this shortcoming and the lack of fast monitoring systems for micropollutants and microorganisms, empirical methods have been developed, which correlate the abatement of microorganisms or micropollutants to surrogate parameters. It has been shown that the natural logarithm of the relative abatement of the UV absorption at 285 nm is correlated to the ozone exposure (Buffle et al., 2006a). Since the ozone exposure is the relevant parameter for disinfection and oxidation, this opens up the possibility to use UV absorption to assess the efficiency of wastewater ozonation. In addition to UV, changes in fluorescence have been tested as descriptors for micropollutant abatement during ozonation (Chys et al., 2017a; Park et al., 2017). A recently developed method to characterize the electron donor properties of the DOM is the electron donating capacity (EDC) (see below). Table 1 summarizes selected studies in which surrogate parameters have been applied to predict micropollutant abatement and inactivation of microorganisms. A detailed discussion of these proxies is provided in the sections below.

3.2.1. Characterization of DOM and derived surrogate parameters

DOM plays a crucial role during ozonation in several ways: (i) direct consumption of ozone, (ii) acceleration of ozone decomposition by radical-type chain reactions (Staehelin and Hoigné, 1985), (iii)

Table 1
Summary of selected studies that applied UV, fluorescence or EDC measurements to predict micropollutant abatement or inactivation of microorganisms in drinking waters or municipal wastewaters.

Parameter	Scale	Targets	Correlation coefficient[6] R^2	Reference
UV (254 nm)	Pilot	16 micropollutants, 2 fecal indicator, bacteria, bromate	0.56 – 0.95, 0.57 – 0.79	(Bahr et al., 2007)
UV (254 nm)	Laboratory	12 micropollutants	0.91	(Nanaboina and Korshin, 2010)
UV (254 and 366 nm)	Laboratory (3)[1] Pilot (1)[1]	24 micropollutants	Sigmoidal approach	(Wittmer et al., 2015)
UV (254 nm)	Pilot	16 micropollutants	0.28 – 0.92	(Stapf et al., 2016)
UV (254 nm)	Laboratory (3)[2] Pilot (1)[3]	2 viruses (MS2, coxsakievirus B5)	Logarithmic correlation	(Wolf et al., 2019)
UV (254 nm) or fluorescence (excitation 254 nm)	Laboratory (9)[1] Pilot (7)[1] Full-scale (1)[1]	18 micropollutants, *E. coli*, MS2, *B. subtilis spores*	0.50 – 0.83, 0.46 – 0.78	(Gerrity et al., 2012)[4]
UV (254 nm) or fluorescence	Laboratory (5)[1]	13 micropollutants	> 0.8	(Park et al., 2017)
UV (254 nm) or fluorescence	Laboratory (1)[5]	9 micropollutants	No correlation, k_{O3}-based approach	(Chys et al., 2017a)
EDC or UV (254 nm)	Laboratory (2)[1]	6 micropollutants, bromate	0.78 – 1.00, 0.82 – 0.83	(Chon et al., 2015)
EDC and UV (255 nm)	Full-scale (1)[1]	22 micropollutants, bromate	No linearcorrelations	(Walpen et al., 2022)

[1] Number of wastewaters tested at this scale;
[2] two surface waters and one wastewater;
[3] lake water;
[4] also predicted hydroxyl radical exposure based on ΔUV or Δfluorescence;
[5] One wastewater was collected 3 times;
[6] Linear regression correlation coefficient for the Δparameter versus the relative abatement of micropollutants or microorganisms.

formation of oxygenated disinfection byproducts (Hammes et al., 2007; Nawrocki et al., 2003; van der Kooij et al., 1989; Wert et al., 2007), (iv) abatement or formation of precursors for the formation of disinfection byproducts during post-disinfection (Fig. 2) (Hoigné and Bader, 1988; Hua and Reckhow, 2013; McCurry et al., 2016; Reckhow and Singer, 1984; Reckhow et al., 1986; Wert and Rosario-Ortiz, 2011), and (v) changes in photochemical and photophysical DOM properties (Leresche et al., 2019; Leresche et al., 2021).

To better understand the reactions of ozone with DOM, various DOM characterization methods have been developed with surrogate parameters (e.g., UV absorbance, fluorescence excitation-emission spectra, molecular weight distributions, relative intensities of different chemical shift regions in NMR, EDC, Table 1) rather than attempting to characterize individual moieties in highly heterogeneous mixtures (Beggs et al., 2013; Chen et al., 2003; Her et al., 2003; Lyon et al., 2014; Weishaar et al., 2003). In addition, oxidative titration methods with chlorine, chlorine dioxide and ozone have been developed to estimate the concentrations of oxidant-reactive moieties in DOM (Essaïed et al., 2022; Houska et al., 2021). Finally, high-resolution mass spectrometry can been applied to characterize molecular features of DOM (see below).

3.2.2. *Specific UV absorption - SUVA*

One of the first methods to characterize changes in DOM upon ozonation is based on optical properties, in particular UV measurements at various wavelengths and a derived parameter, the specific UV absorbance (SUVA), which is the UV absorbance normalized to the dissolved organic carbon (DOC) concentration. The UV absorbance typically decreases during ozonation, due to bleaching of the DOM (Wenk et al., 2013). This effect is caused by the oxidation of activated aromatic systems, leading to moieties with lower UV absorbances. Other optical methods based on fluorescence measurements are also applied to characterize DOM during ozonation (Gerrity et al., 2012; Swietlik and Sikorska, 2004), which allows a qualitative classification of DOM moieties (McKay et al., 2018).

3.2.3. *Electron donating capacity - EDC*

Another tool for characterization of DOM is based on its EDC. This can be measured by electrochemical or spectrophotometric methods (Aeschbacher et al., 2010; Önnby et al., 2018b; Walpen et al., 2020; Walpen et al., 2022), by the radical cation of 2,2-azino-bis(3-ethylbenzothiazo-line-6-sulphonate) ($ABTS^{\bullet+}$), which can be produced electrochemically or by oxidation with chlorine (Aeschbacher et al., 2010; Önnby et al., 2018b). $ABTS^{\bullet+}$, which absorbs light at various wavelengths in the visible range is reduced by reaction with electron donating moieties to ABTS, which is non-colored (Pinkernell et al., 1997). The EDC can be derived from the decoloration of $ABTS^{\bullet+}$ and allows a semi-quantitative determination of the availability of electrons, which can be abstracted by oxidants such as ozone, chlorine and chlorine dioxide (Wenk et al., 2013). EDC has also been shown in laboratory and full-scale experiments with a continuous online system to be a useful proxy for the abatement of micropollutants and the formation of bromate during ozonation of municipal wastewater effluents (Chon et al., 2015; Walpen et al., 2022). Furthermore, it has been shown that the combination of UV and EDC measurements can provide valuable insights into the DOM functional groups which are oxidized and formed. Typically, a more efficient decrease of the EDC was observed compared to the UV absorbance (Önnby et al., 2018a; Wenk et al., 2013). This can be interpreted by the oxidation of phenolic moieties leading to quinone-type and ring-opening products, which have a limited capacity to donate electrons to $ABTS^{\bullet+}$ but might still have UV absorption properties (Mvula and von Sonntag, 2003; Önnby et al., 2018a; Ramseier and von Gunten, 2009; Tentscher et al., 2018; Wenk et al., 2013).

3.2.4. *High Resolution Mass Spectrometry - HRMS*

Recent increases in the accessibility of high resolution mass spectrometry (HRMS) instruments, including Fourier-transform ion cyclotron resonance (FT-ICR) and bench-top Orbitrap instruments with mass resolution of up to 1,000,000 have led to molecular-level characterization of natural organic matter (NOM). Rather than attempting to connect peaks on a mass spectrum to specific molecular structures, these efforts generally make empirical formula assignments, and draw conclusions based on those. Most commonly, H:C and O:C ratios are compared in van Krevelen diagrams (Andersson et al., 2020; Gonsior et al., 2014; Lavonen et al., 2015; Zhang et al., 2012) to infer functional group abundances and degrees of oxidation and to calculate the number of double bond equivalents (DBE) in the molecules.

HRMS has been applied to study the transformation of DOM by ozone in NOM isolates (Remucal et al., 2020; These and Reemtsma, 2005), solid phase extracts from surface waters (Phungsai et al., 2018; 2019), and wastewaters (Phungsai et al., 2016). Such studies typically find several thousand molecular features (i.e., mass spectral signals corresponding to putative molecules) and infer information about DOM composition and reactivity from trends in van Krevelen diagrams and DBE changes as a function of ozonation and/or advanced oxidation processes. The strongest effect of ozone is to increase the O:C ratio of molecular features, by up to 35% at 1.3 mg O_3/mg C in DOM isolates (Remucal et al., 2020) and by a factor of 3.5 at 2.5 mg O_3/mg C in Suwannee River Fulvic Acid (These and Reemtsma, 2005), indicating oxygen transfer reactions, in both the presence and absence of *tert*-butanol, pointing to a role for both ozone and $^{\bullet}OH$ (Fig. 3) (Remucal et al., 2020). Double bond equivalents have been generally found to decrease slightly, but not as strongly as UV signals (Phungsai et al., 2018; Remucal et al., 2020) and H:C ratios are largely unchanged or slightly

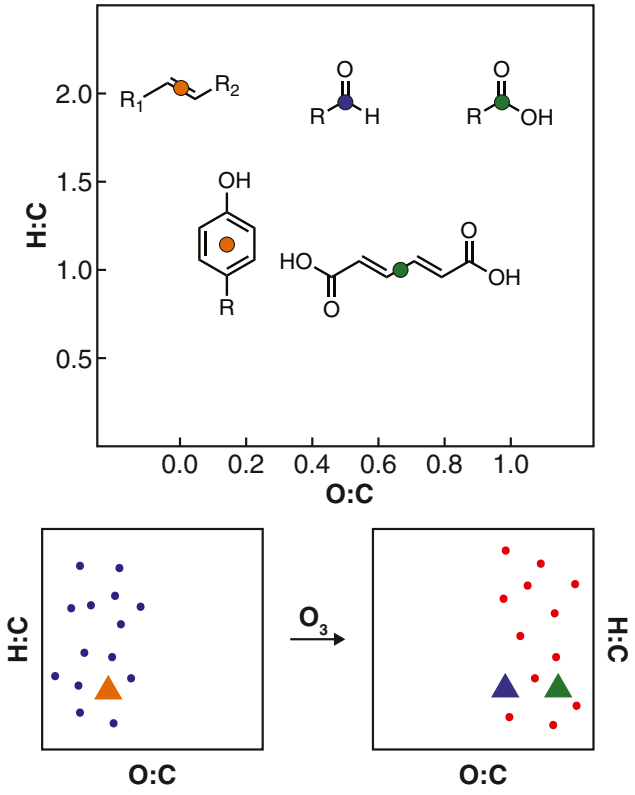

Fig. 3. Top: Example van Krevelen diagrams showing representative functional groups occupying different regions of which exact locations are specified by colored circles. Bottom: Shifts in DOM van Krevelen positioning as a function of ozonation. Blue and red dots represent molecular formulas detected before and after ozonation, respectively. Triangles represent hypothetical phenolic target compounds (orange) and products (blue, green) during ozonation. Possible structures corresponding to the colored triangles in Fig. 3 are shown in Fig. 4, with the corresponding colors.

increased (Phungsai et al., 2018; Remucal et al., 2020; These and Reemtsma, 2005), consistent with ozonation of phenol-type functional groups to highly oxygenated, lower molecular weight products (Fig. 3). Among partially abated compounds, those with lower H:C ratios (i.e., more aromatic) favor reactions with ozone, while those with high H:C ratios (i.e., more aliphatic) favor •OH reactions (Remucal et al., 2020). Finally, •OH has been shown to be a more potent initiator of decarboxylation reactions than ozone, with loss of CO_2 seen from ~3 – 5 × more molecular features ozonated under •OH-promoting conditions than in the presence of a radical scavenger (Remucal et al., 2020).

3.2.5. *Use of multiple characterization methods*

Because single methods are not suitable to fully characterize DOM, a combination of bulk techniques (e.g. UV, EDC) and HRMS can be applied to get further insights into DOM reactive moieties (Phungsai et al., 2016; Remucal et al., 2020). Fig. 4 shows the change of various DOM parameters for the ozonation of DOM.

UV absorbance at 254 nm decreases strongly upon exposure to ozone, but less so when •OH formation is promoted, likely due to the preference of ozone for attacking conjugated and aromatic functional groups that are also often chromophores, whereas •OH can react with the same functional groups through insertion reactions that might not lead to loss of UV absorbance (Fig. 4). UV signal losses greatly exceed the degree of mineralization (~10%) measured as DOC loss (Remucal et al., 2020). EDC and $SUVA_{254}$ significantly decrease by ozone attack, possibly by fragmentation of phenolic groups to ring-opening products or oxidation of them to quinone-type structures (Fig. 4), while •OH does not change EDC significantly. Ozone and •OH both modestly increase the oxygen:carbon ratio of DOM, presumably through oxygen transfer and insertion reactions, respectively. Neither ozone nor •OH substantially affect the hydrogen:carbon ratio (Fig. 4). Finally, the number of double bond equivalents is modestly decreased by both ozone and •OH, likely due to loss of alkene and phenolic structures by reactions with ozone (Fig. 4), and loss of double bonds to •OH through addition reactions. Overall, available evidence is consistent with the bulk of ozone-reactive sites in DOM being phenolic, and that they react analogously to phenol with ozone leading to oxygen addition and a decrease in molecular weight (Fig. 4). However, reactions between ozone and other functional groups, as well as reactions with •OH, likely make some contribution to these bulk phenomena as well.

3.2.6. *Chemical Derivatization*

Chemical derivatization has long been used in environmental analytical chemistry, such as derivatization of charged haloacetic acids to neutral methyl esters for analysis via gas chromatography (Domino et al., 2003), and derivatization of small polar compounds such as dimethylamine to improve retention on hydrophobic stationary phases prior to liquid chromatography (Mitch et al., 2003a). However, most applications to date have been to aid in targeted quantification of known compounds. More recently, progress has been made in using derivatization techniques, often borrowed from the synthesis or biochemistry literature, to characterize DOM and its reactions with oxidants, including ozone, leading to unwanted byproducts.

In one example, a derivatization reaction was used to block specific ozone-reactive functional groups in water to establish the importance of compounds with those functional groups as DBP precursors. A reaction used synthetically to protect primary and secondary amines, addition of a *tert*-butoxycarbonyl group with di-*tert*-butyl-dicarbonate (Einhorn et al., 1991), was applied to DOM extracts prior to ozonation (McCurry et al., 2016). The resulting carbamates are much less reactive with ozone than the parent amine compounds, which was demonstrated with control experiments using model amines. Post-chlorination (after ozone) of derivatized DOM formed ~90% less chloropicrin than in controls, establishing primary and/or secondary amines as the principal chloropicrin precursors in water sequentially treated with ozone and chlorine. A similar approach has been applied for chlorine titrations with and without derivatization of amines to quantify primary and secondary amine moieties in DOM (Essaïed et al., 2022). In a more recent study, another derivatization reaction was applied to identify amines in water. Amines in DOM extracted by SPE were derivatized with either light

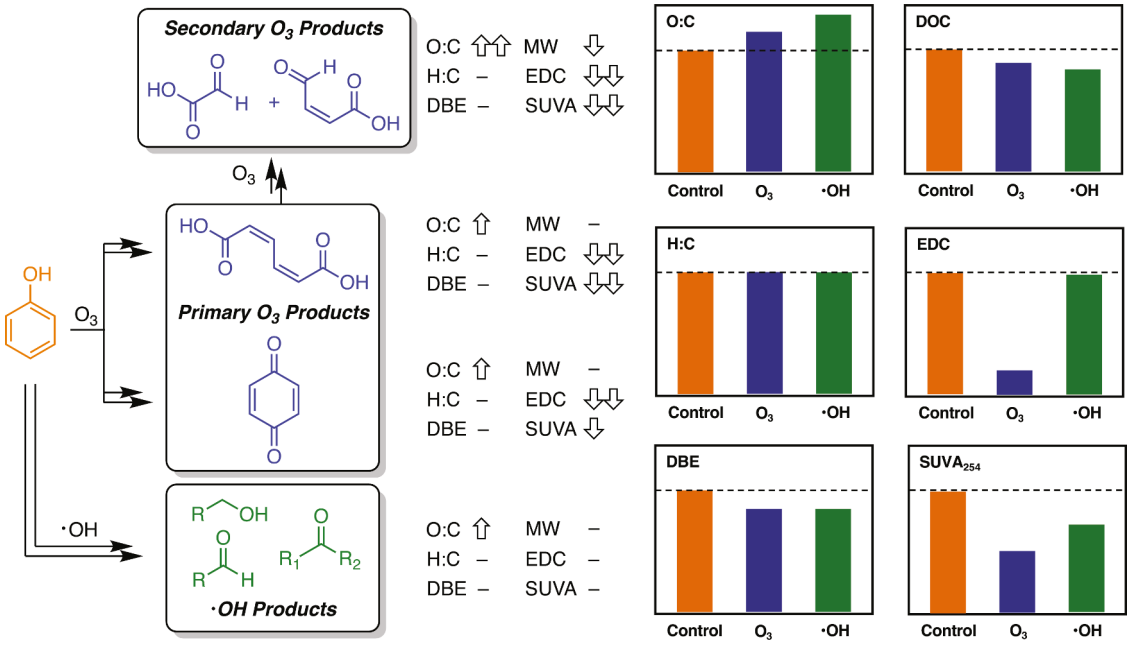

Fig. 4. Left side: reactions of ozone and •OH with phenolic moieties in e.g. DOM and the development of bulk properties and HRMS parameters of the corresponding example products. Up or down arrows correspond to an increase or decrease in the value of the associated bulk property. Horizontal dash lines indicate no significant change to bulk property. Right side: general trends observed as a function of ozonation of NOM isolates under conditions to suppress (blue bars) or promote (green bars) •OH reactions in parallel to direct ozonation reactions. Bars are approximately to scale. Trends primarily obtained based on data reported by (Remucal et al., 2020) on ozonation of Suwanee River NOM and Upper Mississippi River NOM.

(ordinary) or heavy (deuterated) isotopes of formaldehyde prior to analysis with HRMS (Liu et al., 2019). The mass difference between the heavy and light isotopes of the resulting derivatives (4.025 Da) was used to pinpoint amines among the noise of other compounds in the DOM mass spectrum. Further, because primary amines were dimethylated, while secondary amines were monomethylated, information about amine order could also be extracted from the mass spectra. The authors used this technique to identify several dipeptides in water, which were then confirmed with analytical standards (Liu et al., 2019).

Derivatization was also applied to waters disinfected with chlorine, chloramines, or ozone to identify carbonyl-containing compounds. Suwannee River Fulvic Acid was derivatized with a hydrazine compound which was either partially deuterated or unlabelled, then analyzed via HRMS to search for peaks showing characteristic mass differences, as described above in (Liu et al., 2019). Prior to disinfection, most identified compounds in DOM (before oxidation) were polyoxygenated with between five and ten double bond equivalents, and were proposed to be lignin-type structures (Liu et al., 2020). Ozonation led to a greater disappearance of putative lignin structures than chlorine or chloramines (Liu et al., 2020), consistent with selective reactivity toward activated aromatic compounds. Ozone increased the number of carbonyl-containing products relative to controls, whereas chlorine and chloramines led to their loss. Ozone tended to reduce the size of detected carbonyl compounds relative to controls, consistent with molecular fragmentation (e.g., via Criegee-type reactions) (Liu et al., 2020). In another study, phenolic moieties in DOM were derivatized with acetic anhydride to the phenylacetates. The latter have a very low reactivity with chemical oxidants and this approach can be used to block phenolic moieties from reaction with e.g., ozone or chlorine dioxide (Houska et al., 2021). Even though this approach works well for synthetic chemicals, only part of the electron rich sites could be derivatized, potentially due to steric effects (Houska et al., 2021). Overall, derivatization shows promise as a means of reducing the complexity of analyzing reactions between DOM and oxidants by (i) allowing attribution of oxidation byproduct formation to specific precursor functional groups, regardless of the identity of individual precursor molecules, and (ii) adding characteristic functional group-specific tags to oxidation reaction precursors and products, to deconvolute their signals from analytical noise in complex matrices.

4. Ozone reaction kinetics and mechanisms

4.1. Introduction

4.1.1. General kinetic considerations

Understanding reaction kinetics is important for predicting micropollutant abatement efficiency during ozonation process (von Sonntag and von Gunten, 2012). The abatement kinetics for a micropollutant (MP) results from the concurrent oxidation by ozone and $^{\bullet}$OH (formed from ozone decomposition reactions) and can be formulated by the following integrated rate law (Eq. 1) (Lee and von Gunten, 2016):

$$-\ln\left(\frac{[MP]_t}{[MP]_0}\right) = k_{O_3}\int_0^t [O_3]dt + k_{^{\bullet}OH}\int_0^t [^{\bullet}OH]dt \quad (1)$$

with k_{O3} and $k_{\bullet OH}$ as second-order rate constants for the reactions of micropollutant with ozone and $^{\bullet}$OH, respectively, and with $\int_0^t [O_3]dt$ and $\int_0^t [^{\bullet}OH]dt$ as ozone and $^{\bullet}$OH exposures, respectively (Lee and von Gunten, 2016). The oxidant exposure is experimentally determined for a given water matrix and for a specific ozone dose. Matrix components such as DOM, nitrite, and carbonate significantly influence the stability of ozone and $^{\bullet}$OH and thereby their exposures. Ozone and $^{\bullet}$OH exposures have been determined for various types of wastewater (e.g., municipal wastewater, industrial wastewater, landfill leachate) and their correlations with the specific ozone doses (normalized by DOC concentration) has been determined (Lee and von Gunten, 2016; Wildhaber et al., 2015; Wolf et al., 2019). Based on this empirical model, the micropollutant abatement for a specific ozone dose can be predicted. Compounds with k_{O3} higher than 10^3 $M^{-1}s^{-1}$ are considered to be well abated during ozonation for typical municipal wastewater, with > 80% abatement (Bourgin et al., 2018). To determine the fraction of a micropollutant reacting with ozone or $^{\bullet}$OH, respectively, the R_{ct} concept has been developed (Elovitz and von Gunten, 1999). It has been experimentally observed that the ratio of the $^{\bullet}$OH and ozone exposures (R_{ct}) is constant for most of the duration of ozone decomposition (Elovitz and von Gunten, 1999; Elovitz et al., 2000a; b) (Eq. 2):

$$R_{ct} = \frac{\int_0^t [^{\bullet}OH]dt}{\int_0^t [O_3]dt} \Rightarrow \int_0^t [^{\bullet}OH]dt = R_{ct}\int_0^t [O_3]dt \quad (2)$$

Substituting $\int_0^t [^{\bullet}OH]dt$ in Eq. 1 by $R_{ct}\int_0^t [O_3]dt$ yields a rate law for the abatement of a MP, which only depends on the ozone exposure and the R_{ct} (Eq. 3):

$$-\ln\left(\frac{[MP]_t}{[MP]_0}\right) = k_{O_3}\int_0^t [O_3]\,dt + k_{^{\bullet}OH}R_{ct}\int_0^t [O_3]\,dt = \int_0^t [O_3]\,dt\left(k_{O_3} + k_{^{\bullet}OH}R_{ct}\right) \quad (3)$$

Based on Eq. 3, the fraction of the oxidation occurring by reacting with $^{\bullet}$OH can be calculated from Eq. 4 (Elovitz and von Gunten, 1999):

$$f_{^{\bullet}OH} = \frac{k_{^{\bullet}OH}R_{ct}}{k_{^{\bullet}OH}R_{ct} + k_{O_3}} \quad (4)$$

The fraction of the MP reaction with $^{\bullet}$OH as a function of the R_{ct} and for selected values of k_{O3} is shown in Fig. 5 (Elovitz and von Gunten, 1999).

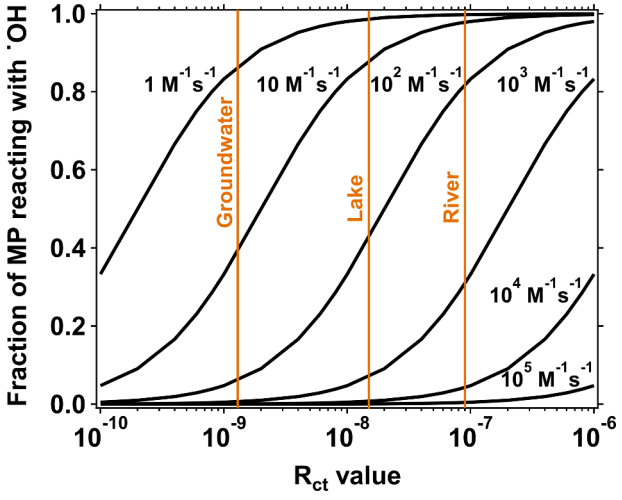

Fig. 5. Fraction of a micropollutant (MP) reacting with $^{\bullet}$OH as a function of the R_{ct} according to Eq. 4. The curves are representative for second-order rate constants for the reaction with ozone (1-10^5 $M^{-1}s^{-1}$). The second-order rate constant for the reaction with $^{\bullet}$OH is assumed to be 5×10^9 $M^{-1}s^{-1}$. The vertical lines show measured R_{ct} values for a karstic groundwater (Porrentruy, Switzerland), a lake water (Zurich, Switzerland) and a river water (Sihl, Switzerland) (Elovitz et al., 2000b).

4.1.2. Determination of reaction kinetics

Second-order rate constants for the reactions of ozone with inorganic and organic compounds have been determined experimentally by directly monitoring the decrease of ozone or substrate over time under pseudo first-order conditions or by using competition kinetics methods (von Sonntag and von Gunten, 2012). To date, k_{O3} for several hundred organic and inorganic compounds have been compiled (von Sonntag and von Gunten, 2012). Based on this wealth of information, regression models employing quantitative structure-activity relationships (QSAR) have been developed to predict unknown k_{O3} for target compounds (Lee et al., 2015; Lee and von Gunten, 2012; Sudhakaran and Amy, 2013). Hammett and Taft constants are common molecular descriptors, which showed reliable prediction results for diverse ozone-reactive functional groups (Lee and von Gunten, 2012). However, empirical parameters such as Hammett and Taft constants are not always available. To overcome this limitation, quantum chemically computed molecular descriptors such as orbital energies or average local ionization energies have been assessed, showing promising results (see Fig. 8 and ensuing discussion) (Lee et al., 2015; Tentscher et al., 2019). An *in silico* pathway prediction tool has been developed, which includes a module for quantum chemically based prediction of k_{O3} for target compounds (Lee et al., 2017a). The current computed descriptors also have certain caveats (e.g., failing to account for steric effects) (Tentscher et al., 2019) and an effort for building better QSAR models should be continued. A multivariate model containing complementary quantum chemical variables may enhance the model performance. Additionally, *ab initio* calculations of barrier height ($\Delta G^{\ddagger}$) could be alternative QSAR variables, which have been successfully applied for predicting $k_{\cdot OH}$ (Minakata and Crittenden, 2011). However, for ozone reactions, *ab initio* calculations suffer from serious uncertainties of up to 5 orders of magnitude (Trogolo et al., 2015); the cause and possible solutions of this issue are worthy of further investigations.

As an electrophilic agent, ozone attacks moieties with high electron density, thus any modifications that alter the electron density of the moieties change their ozone reactivity. Typical examples are dissociating compounds. When protonated, a dissociating compound has a much lower k_{O3} (than when deprotonated), because the electrons of the dissociating center are shared with the proton and less available for ozone (see e.g., aliphatic amines in Section 4.5). The protonation can also decrease the electron density inductively or by prohibiting resonance structures available to the deprotonated molecule (e.g., phenolic compounds in Section 4.3). Another example is compounds substituted by electron-donating/withdrawing groups. Typically, electron-donating groups such as alkyl groups increase k_{O3}, whereas electron-withdrawing groups like carbonyl groups decrease k_{O3} (e.g., olefins with various substituents in Section 4.2). An exception exists for heterocyclic compounds, some of which have higher k_{O3} with the addition of carbonyl groups to the ring than without (Section 4.4). Substitution with electron-withdrawing groups can result in an increased apparent k_{O3} at circumneutral pH ($k_{O3,app,pH7}$), for dissociating compounds bearing a pK_a in the alkaline pH range (e.g., phenolic compounds in Section 4.3).

4.1.3. Transformation products and reaction mechanisms

Over the last few decades, many studies have investigated

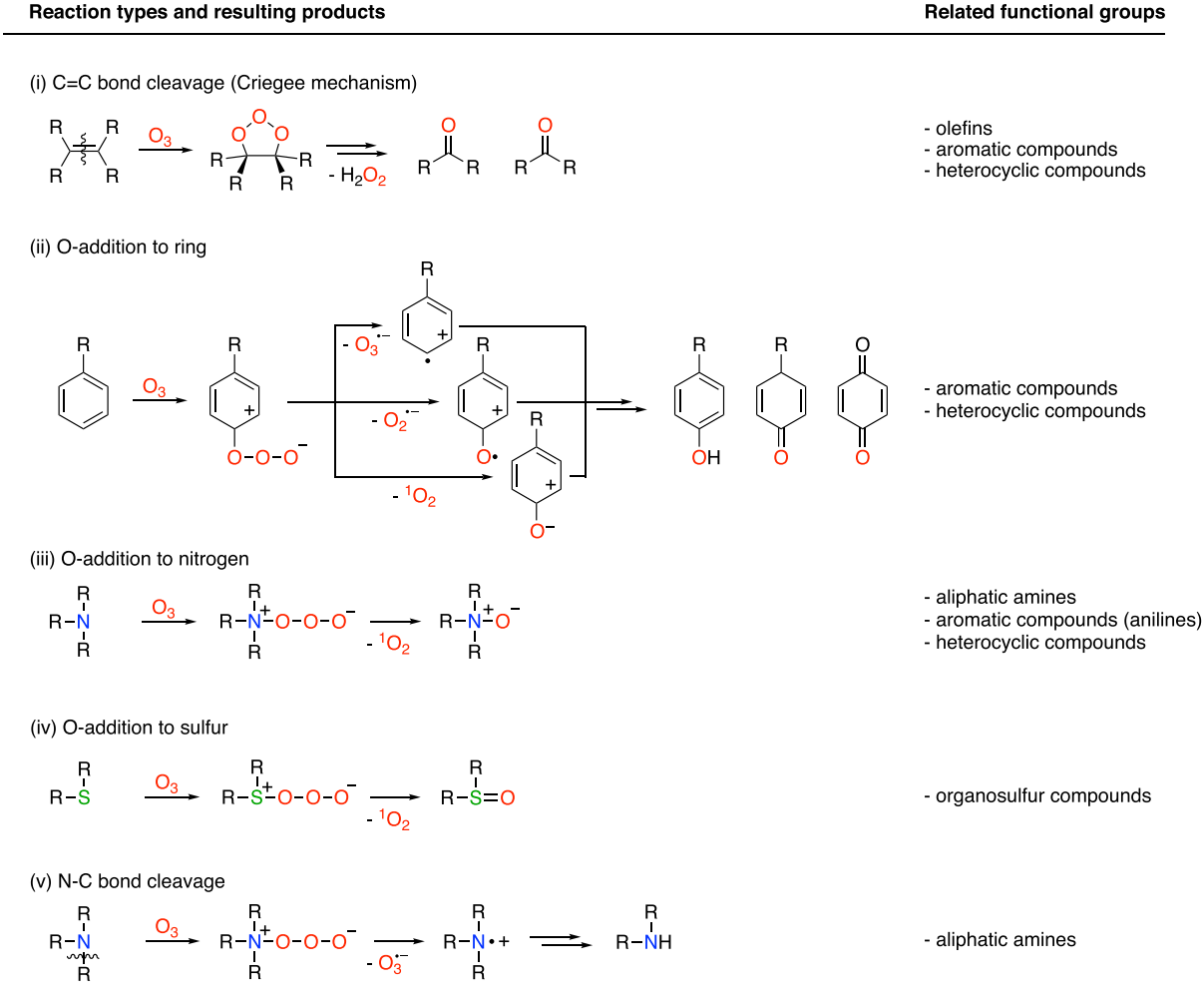

Scheme 1. Conceptual scheme for the principal ozone reactions based on the target sites and the resulting products.

transformation products formed during ozonation and elucidated ozone reaction mechanisms. The principal ozone reaction mechanisms and the corresponding products are summarized in Scheme 1. The reaction type (i) is a carbon-carbon double bond cleavage based on the well-known Criegee mechanism (Criegee, 1975). An ozone molecule is added to a double bond to create an ozonide as a key intermediate, which subsequently degrades into carbonyl products. This type of reaction is also observed during the reaction of aromatic/heterocyclic compounds with ozone, opening the ring structure and forming aliphatic products with carbonyl groups. Aromatic and heterocyclic compounds also undergo reaction type (ii), leading to the oxygen-added ring products via radical intermediates (von Sonntag and von Gunten, 2012). Reaction types (iii) and (iv) show oxygen-transfer to the heteroatoms nitrogen and sulfur, respectively, resulting in the corresponding *N*-oxygenated and *S*-oxygenated products (von Sonntag and von Gunten, 2012). Nitrogen-containing compounds can also react with ozone via electron-transfer, forming an aminyl radical cation and subsequently a dealkylated amine, as shown by reaction type (v) (von Sonntag and von Gunten, 2012). Each reaction type is also characterized by the formation of distinct reactive oxygen species. For example, hydrogen peroxide, singlet oxygen, and $^{\bullet}$OH are known as byproducts for the Criegee mechanism (i), O-addition to heteroatoms (iii/iv), and N-C bond cleavage (v), respectively (Leitzke and von Sonntag, 2009; Muñoz et al., 2001; von Gunten, 2003b). Thus, identifying/quantifying reactive oxygen species can provide additional evidence for certain reaction pathways. Alternatively, reaction mechanisms can be explored by quantum chemical computations. An increasing number of studies employs quantum chemical computations to corroborate experimental findings. Quantum chemical computations can predict initial reaction sites in a given molecular structure by computing molecular descriptors such as orbital energies or assess the thermodynamic feasibility of a proposed reaction mechanism by computing the Gibbs free energy (Tentscher et al., 2019). In addition, quantum chemical computations can provide insights related to unstable reaction intermediates, which escape experimental identification. A case in point is the formation of NDMA during ozonation of bromide- and dimethylsulfamide-containing waters, for which a detailed mechanism has been proposed based on experimental evidence and quantum chemical computations (Trogolo et al., 2015).

In Sections 4.2 to 4.9, ozone reaction kinetics and mechanisms are discussed on the basis of ozone-reactive functional groups. Direct ozone reactions are the main focus for most reaction mechanisms, as the role of $^{\bullet}$OH is minimal for the first generation transformation products for compounds with high ozone reactivity (Fig. 5). The majority of the recent findings in product analyses were obtained by HRMS. To discuss HRMS results in a clear manner, the confidence level system (from level 1 to 5) defined by (Schymanski et al., 2014) is employed. Briefly, confidence level 1 indicates a confirmed structure with a reference standard, level 2 indicates a probable structure by e.g., a MS library match, level 3 provides some structural information by MS data and compound class, level 4 provides an unequivocal molecular formula and level 5 provides an exact mass.

4.2. Olefins (and alkynes)

Olefins are well-known ozone-reactive functional groups. In the 1970s, Rudolf Criegee revealed the key mechanism of the reaction of olefins with ozone, characterized by a cycloaddition of ozone to a carbon-carbon double bond to form carbonyl compounds as final products via ozonide as a cyclic intermediate (reaction type (i) in Scheme 1) (Criegee, 1975). On the basis of this landmark study, olefin-ozone reactions have been extensively studied in organic solvents, and later on, the knowledge has been transferred to aqueous solutions (von Sonntag and von Gunten, 2012). This section focuses on recent findings on k_{O3} and summarizes briefly the olefin-ozone reaction mechanisms and ozonation products of aliphatic olefins. Cyclic olefins (or olefin moieties included in aromatic rings) are discussed in separate Sections 4.3 (Aromatic compounds) and 4.4 (Heterocyclic compounds).

4.2.1. Kinetics

4.2.1.1. Kinetics of Alkene-ozone reactions. Unsubstituted olefins react fast with ozone with k_{O3} of approximately 10^5 $M^{-1}s^{-1}$ (e.g., ethene: k_{O3} = 1.8 × 10^5 $M^{-1}s^{-1}$ (Dowideit and von Sonntag, 1998)). In contrast, substituted olefins have a wide range of k_{O3} from 10^1 to 10^6 $M^{-1}s^{-1}$ (Table S1, Supporting Information, SI), depending on the nature of the substituents (von Sonntag and von Gunten, 2012) (Fig. 6). Addition of electron-donating alkyl groups increases k_{O3} (e.g., propene: k_{O3} = 8.0 × 10^5 $M^{-1}s^{-1}$ (Dowideit and von Sonntag, 1998)), but the magnitude of this effect is generally smaller than for electron-withdrawing groups as shown in Fig. 6 (Dowideit and von Sonntag, 1998). This is consistent with induction effects (Anslyn and Dougherty, 2006). Olefins with multiple electron-withdrawing substituents exhibit further decrease in reactivity (e.g., trichloroethene: k_{O3} = 14 $M^{-1}s^{-1}$ (Dowideit and von Sonntag, 1998), tetrachloroethene: k_{O3} < 0.1 $M^{-1}s^{-1}$ (Hoigné and Bader, 1983b)). Such additive effects of electron-withdrawing groups on k_{O3} were also found in a study on polychloro-1,3-butadienes (e.g., tetrachloro-1,3-butadienes: k_{O3} = 1.6 × 10^2 – 7.8 × 10^3 $M^{-1}s^{-1}$, pentachloro-1,3-butadienes: k_{O3} = 0.8 and 10 $M^{-1}s^{-1}$, and hexachloro-1,3-butadiene: k_{O3} < 0.1 $M^{-1}s^{-1}$ (Lee et al., 2017b)).

Differences in k_{O3} also exist among the olefins substituted by the same number of electron-withdrawing groups but in different positions, i.e., stereoisomers. Examples are *cis*-1,2-dichloroethene (k_{O3} = 5.4 × 10^2 $M^{-1}s^{-1}$) vs. *trans*-1,2-dichloroethene (k_{O3} = 6.5 × 10^3 $M^{-1}s^{-1}$) (Dowideit and von Sonntag, 1998) and (*E*)-1,1,3,4-tetrachlorobutadiene (k_{O3} = 1.1 × 10^3 $M^{-1}s^{-1}$) vs. (*Z*)-1,1,3,4-tetrachlorobutadiene (k_{O3} = 4.0 × 10^2 $M^{-1}s^{-1}$) (Lee et al., 2017b). These significant differences in ozone reactivity between seemingly similar compounds may be explained by the geometry of the transition state in the rate-limiting step. Based on the reaction mechanism discussed in Section 4.2.2, the rate limiting step of the ozonolysis reaction likely requires the sp^2 carbon(s) in the double bond to rehybridize to sp^3, resulting in a decrease of the C-Cl or C-C bond angle from 120° (planar geometry) to 109.5° (tetrahedral geometry). This geometry brings the substituents in the *cis* position closer to each other, and if both substituents are bulky chlorines, rather than one chlorine and one methyl group, repulsion between these two chlorines in the transition state may potentially explain the lower k_{O3} observed from the *cis* isomer of 1,2-dichloroethene.

Besides the induction effects from electron-donating/withdrawing groups, steric effects from bulky substituents can also affect k_{O3}. An example is *cis*-1,2-dichloroethene (k_{O3} = 5.4 × 10^2 $M^{-1}s^{-1}$ (Dowideit and von Sonntag, 1998)) vs. endrin (k_{O3} < 0.02 $M^{-1}s^{-1}$ (Yao and Haag, 1991)). Endrin also has a *cis*-1,2-dichloroethene moiety, but the ozone attack is hindered by the presence of the neighboring chlorinated carbons, resulting in a much lower k_{O3} (Yao and Haag, 1991).

4.2.1.2. Kinetics of Alkyne-ozone reactions. Alkynes can react with ozone through a similar reaction mechanism as olefins, but with generally lower k_{O3}. For example, the k_{O3} for the reaction of 1-ethinyl-1-cyclohexanol with ozone ($k_{O3} = 2.0 \times 10^2$ $M^{-1}s^{-1}$ (Huber et al., 2004)) is much lower than for buten-3-ol ($k_{O3} = 7.9 \times 10^4$ $M^{-1}s^{-1}$ (Dowideit and von Sonntag, 1998)), both of which feature the reactive moiety geminal to a substituted alcohol. To date, there is lack of information on ozonation kinetics of alkynes to make further generalizations about their reactivity.

4.2.2. Reaction mechanisms

The predominant pathway for the reaction of olefins with ozone is through pathway (i) in Scheme 2, in which the first zwitterion (A) formed in aqueous solutions (von Sonntag and von Gunten, 2012) leads to an ozonide (B), which subsequently forms a second zwitterion (C), or decomposes via a concerted reaction to the third zwitterion (D) and a carbonyl product. Zwitterion (D) is the branching point where aqueous reactions deviate from reactions in organic solvents. In aprotic solvents, the zwitterion (D) recombines with the carbonyl product to produce a Criegee ozonide (E) (Criegee, 1975). In water, the zwitterion D rapidly hydrates to α-hydroxyalkylhydroperoxide (F), which reversibly dissociates to hydrogen peroxide and the second carbonyl product. Complete mass balances were achieved by the corresponding carbonyl products for the reactions of ozone with simple olefins like ethene and propene (Dowideit and von Sonntag, 1998).

There are minor pathways leading to the formation of partial cleavage products from zwitterion (A), such as a carbonyl product (G), a glycol (H) and an epoxide (I), all of which contain the two initial olefin carbons still linked by a single bond after ozonation. Partial cleavage products were observed in early studies in organic solvents, typically for sterically-hindered compounds like 3,3-dimethyl-2-*tert*-butyl-butene and 3.3-dimethyl-2-isoproyl-butene in methylene chloride (Bailey and Lane, 1967) and 1,1,2-trichloro-1,2,2-trifluoroethene in dichloromethane (Agopovich and Gillies, 1980; Keay and Hamilton, 1976). Dichloroacetaldehyde was identified as a minor product from ozonating dichloroethane (Scheme 2 (ii)) (Dowideit and von Sonntag, 1998). Glycol and carbonyl compounds (with two carbon atoms linked) were quantified in aqueous ozone reactions from tetramethylethene, dichloroethenes, and trichloroethene, with yields <15% (Dowideit and von Sonntag, 1998) (Scheme 2 (iii)). Epoxides were suggested as intermediates in aqueous ozone reactions mostly for olefin moieties in aromatic/heteroaromatic compounds, but with limited experimental

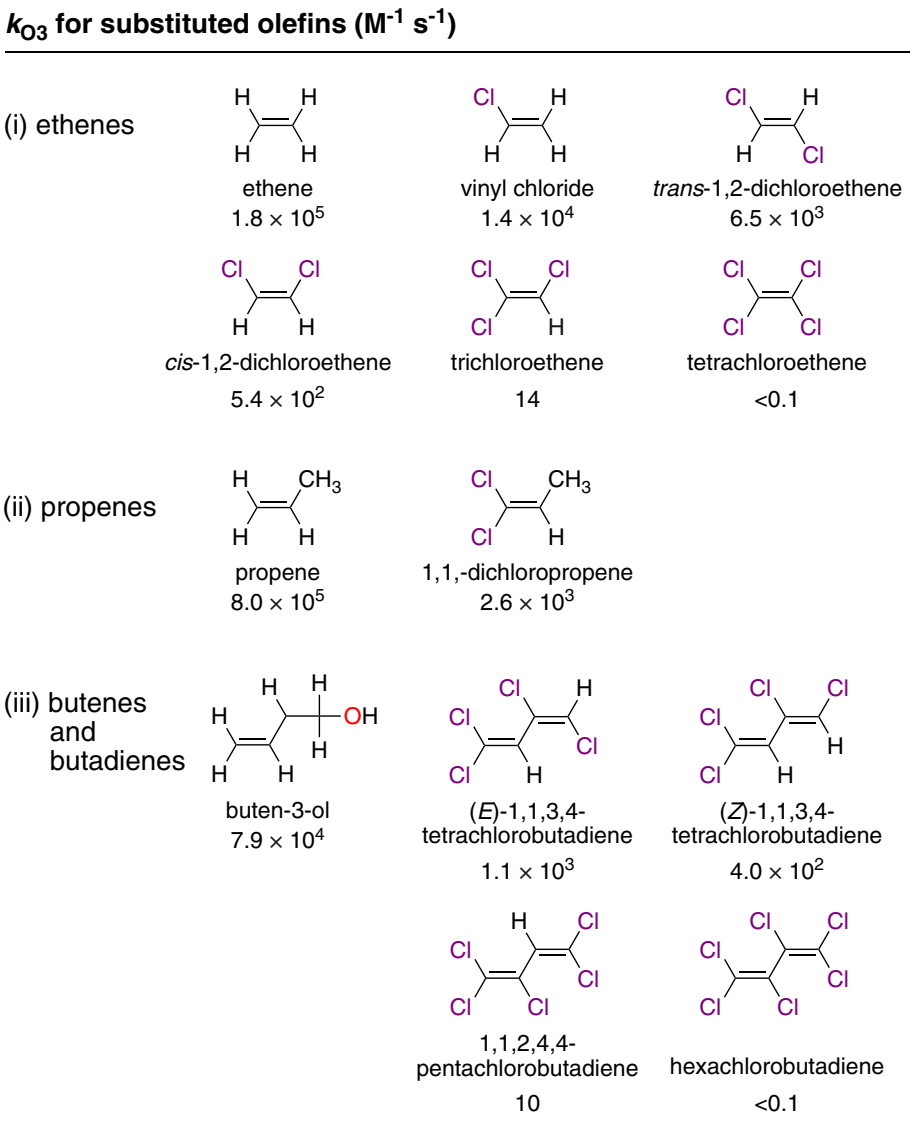

Fig. 6. Effects of substitution by chlorine and hydroxyl groups on k_{O3} for (i) ethene, (ii) propene, and (iii) butene and butadiene derivatives (Dowideit and von Sonntag, 1998; Lee et al., 2017b).

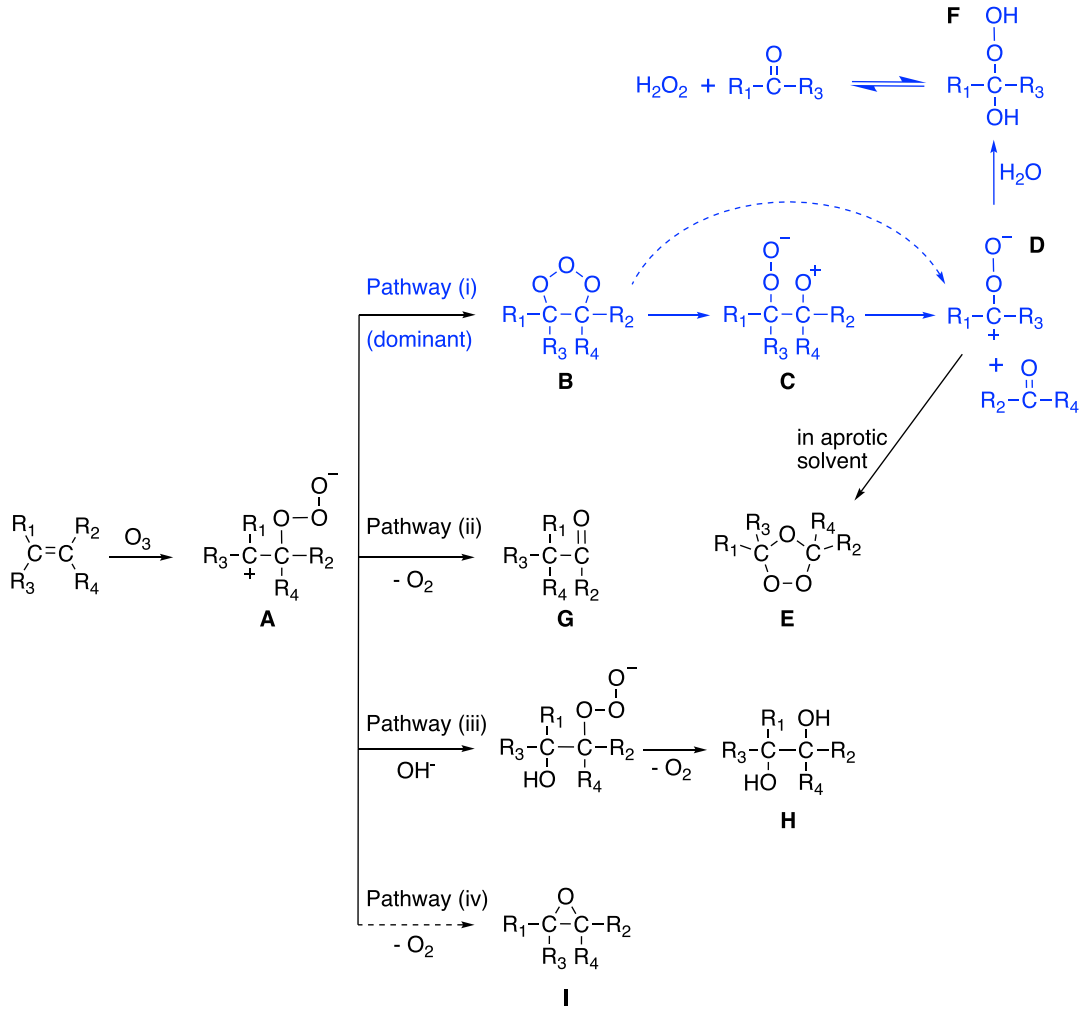

Scheme 2. Reactions of olefins with ozone: The predominant pathway in water is highlighted in blue. Some minor pathways are shown in black and a hypothesized pathway to an epoxide (iv) is indicated by a dashed arrow.

evidence (see Section 4.2.3).

4.2.3. *Micropollutants*

Many ozone-reactive micropollutants in water feature olefin functional groups. Some important taste and odor compounds in drinking water contain an olefin moiety. They can be quickly inactivated during ozonation, because of their high k_{O3} for the reactions with ozone (Table S1, SI). Examples are 3-hexen-1-ol ($k_{O3} = 5.4 \times 10^5\ M^{-1}s^{-1}$), β-ionone ($k_{O3} = 1.6 \times 10^5\ M^{-1}s^{-1}$), 2,6-nonadienal ($k_{O3} = 8.7 \times 10^5\ M^{-1}s^{-1}$) and 1-penten-3-ol ($k_{O3} = 5.9 \times 10^4\ M^{-1}s^{-1}$) (Peter and von Gunten, 2007).

Microcystins are a class of compounds with multiple ozone-reactive sites. The olefin moieties are the main ozone reaction sites for most microcystins except the ones with tyrosine and tryptophan substituents (MC-YR and MC-LW, respectively) (Kim and Lee, 2019; Onstad et al., 2007). As a result, primary ozonation products of MC-YR and MC-LW are likely to contain undamaged olefins and to retain toxicity for small specific ozone doses (note that the conjugated olefins of the base structure of microcystins are responsible for hepatotoxicity) (Kim and Lee, 2019). See Section 4.9 for more discussions on compounds with multiple reaction sites.

The ozone reactions of natural olefinic compounds have also been investigated in the aqueous phase of the atmosphere such as clouds and fogs. Examples are β-caryophyllonic acid ($k_{O3,app} = 4.8 \times 10^5\ M^{-1}s^{-1}$ at pH 2 (Witkowski et al., 2019)), limononic acid ($k_{O3,app} = 4.2 \times 10^5\ M^{-1}s^{-1}$ at pH 2 (Witkowski et al., 2018)), and α-terpineol ($k_{O3} = 9.9 \times 10^6\ M^{-1}s^{-1}$ in the absence of radical scavenger (Leviss et al., 2016)).

Full mineralization of micropollutants is typically not achieved during ozonation. Olefin-containing micropollutants react with ozone leading to the formation of transformation products through pathways listed in Scheme 2. The chemical structures of the major transformation products from ozone reactions of selected olefin-type micropollutants are provided in Table S2 (SI). Ozonation of micropollutants containing an olefin moiety such as imazalil (Genena et al., 2011), octinoxate (Hopkins et al., 2017), tamoxifen and toremifene (Knoop et al., 2018), and carbamazepine (Hübner et al., 2014; McDowell et al., 2005) follow the predominant pathway (Scheme 2 (i)) because there is no steric hindrance on the olefin group. This leads to the formation of expected carbonyl compounds such as aldehydes and ketones. Keto-limononic acid was semi-quantified by LC-MS with a surrogate standard (30% yield), after ozonation of limononic acid (Witkowski et al., 2019). For ozonation of α-terpineol, more than 90% of a primary aldehyde product was expected based on the yields of the subsequent products (*trans*- and *cis*-lactol by rearrangement of the aldehyde) quantified by NMR (Leviss et al., 2016).

For micropollutants containing olefin moieties that are less accessible, hindering formation of the initial ozonide, such as carotenoids (Henry et al., 2000), acyclovir (Prasse et al., 2012), acetamidoantipyrine (Favier et al., 2015), carbamazepine (Hübner et al., 2014) and tetracycline (Khan et al., 2010), partial cleavage products such as glycol or epoxides have been suggested to be formed (Scheme 2 (iv)) (Table S2, SI). However, these reports were based on confidence level 2b (by diagnostic evidence), and there is no direct confirmation with reference

standards of epoxide formation in aqueous ozone reactions.

Alkyne-containing micropollutants react with ozone through a mechanism analogous to Criegee ozonation of alkenes. Without any bulky substituent groups nearby, complete cleavage products, including ketones and carboxylic acids are formed (Huber et al., 2004).

4.3. Aromatic compounds

4.3.1. Kinetics

Aromatic compounds react with ozone with a large range of second-order rate constants ($k_{O3,app} < 0.1$ to $\sim 10^9$ $M^{-1}s^{-1}$) (basic structures and recently reported examples in Table S3, SI), depending on the substituents. Unsubstituted arenes react with ozone slowly (e.g., benzene: $k_{O3} = 2$ $M^{-1}s^{-1}$ (Hoigné and Bader, 1983b)). Electron-donating alkyl substituents modestly increase k_{O3} (e.g., 14 $M^{-1}s^{-1}$ for toluene (Hoigné and Bader, 1983b)). As with olefins, electron-withdrawing substituents reduce k_{O3} (e.g., 0.57 $M^{-1}s^{-1}$ for 1,3-dichlorobenzene (Hoigné and Bader, 1983b)). Ring substituents featuring lone pairs of electrons which can delocalize into the ring somewhat increase k_{O3} (e.g., 2.9×10^2 $M^{-1}s^{-1}$ for methoxybenzene) (Hoigné and Bader, 1983b)). One exceptional class are polycyclic aromatic hydrocarbons, which have significantly higher k_{O3} than benzene or alkylbenzenes (e.g., 3×10^3 $M^{-1}s^{-1}$ for naphthalene (Hoigné and Bader, 1983b)), for reasons which have never been fully elucidated.

Phenol and phenol-derived compounds have high k_{O3} (Table S3, SI). Even in a wastewater matrix with strong scavenging of ozone, phenolic compounds can be abated to a large extent by ozone at relatively low specific ozone doses (Chedeville et al., 2009; Lee and von Gunten, 2010). The apparent k_{O3} for the reaction of phenol with ozone increases with increasing pH because of greater electron density of phenolate than phenol, due to the delocalization of phenolate electron lone pair into the ring. The k_{O3} is 1.3×10^3 $M^{-1}s^{-1}$ for phenol, which is 6 orders of magnitude lower than for phenolate (1.4×10^9 $M^{-1}s^{-1}$) (Hoigné and Bader, 1983a). This corresponds to a half-life of ~12 s at pH 2 and ~10 μs at pH 12 for an ozone concentration of 2 mg/L.

The pK_a of phenol and phenol derivatives is a critical parameter for determining $k_{O3,app}$, the apparent second-order rate constant at a given pH. It is influenced by electron-withdrawing or donating groups on the ring. For example, substitution by halogen or nitro groups decreases the pK_a of the hydroxyl group (e.g., the pK_a of dibromo-phenol is 6.67 (Serjeant and Dempsey, 1979) compared to 9.98 for phenol (Gross and Seybold, 2001). The $k_{O3,app}$ for the reactions of phenols at different pH can be expressed as (Eq. 5):

$$k_{O3,\ app} = k_{O3,phenolate} \times \frac{K_a}{K_a + [H^+]} + k_{O3,phenol} \times \frac{[H^+]}{K_a + [H^+]} \quad (5)$$

where K_a is the acid dissociation constant. For a pK_a decrease, the apparent second-order rate constant increases at a given pH. Even though electron withdrawing groups such as halogens will reduce the electron density of the substituted phenolate relative to the unsubstituted phenolate, the net effect can be an increased reactivity at neutral pH. The tradeoff effect can be observed by comparing the $k_{O3,app}$ of phenol (pK_a = 9.98), 4-chlorophenol (pK_a = 9.2) and 4-nitrophenol (pK_a = 7.2) as a function of pH (Fig. 7). For substituted phenols with lower pK_a than the pK_a of phenol, the $k_{O3,app}$ can be higher at neutral pH than for phenol, while at low or high pH the $k_{O3,app}$ are lower. A similar trend in $k_{O3,\ app}$ at neutral pH is observed for substituted nitrogen-containing compounds, discussed in Section 4.6 (Fig. 12).

The ozone reactivity of anilines is also influenced by pK_a and given pH conditions. Aniline (pK_a of conjugate acid = 4.6) reacts readily with ozone ($k_{O3,app} = 1.4 \times 10^7$ $M^{-1}s^{-1}$ at pH 6.5), but under acidic conditions the positively charged anilinium has a significantly lower ozone reactivity ($k_{O3,app} = 5.9 \times 10^4$ $M^{-1}s^{-1}$ at pH 1.5) (Hoigné and Bader, 1983a; Pierpoint et al., 2001), because the nitrogen lone pair is unable to delocalize into the ring when protonated. Substituted anilines have a

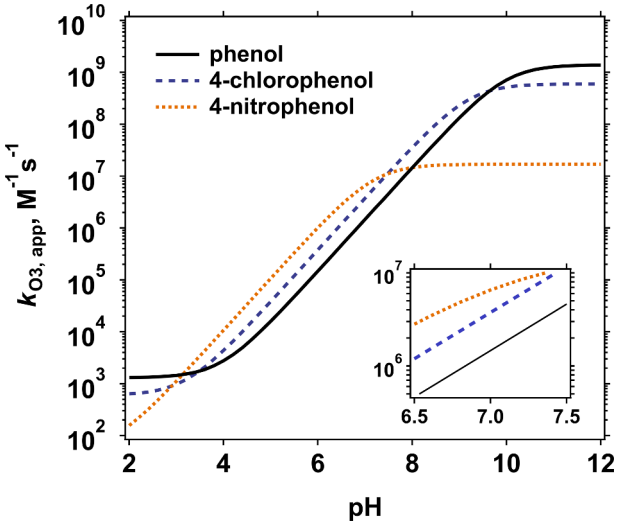

Fig. 7. pH-effect on the apparent second-order rate constants for the reactions of ozone with phenol and substituted phenols (Hoigné and Bader, 1983a). Even though the k_{O3} values for phenol and phenolate are higher than for their substituted analogues, the $k_{O3,app}$ for the substituted phenols are higher at neutral pH (see also insert).

range of k_{O3} values depending on the ring substituents (Table S3), within approximately two orders of magnitude (Pierpoint et al., 2001; Tekle-Röttering et al., 2016c).

QSAR methods have been applied to predict k_{O3} for aromatic compounds based on empirically determined Hammett and Taft constants (Lee and von Gunten, 2012) and quantum chemically computed energies of the highest occupied molecular orbital (E_{HOMO}) (Lee et al., 2015; Tentscher et al., 2019). Other tested descriptors include the number of bonds, dipole moment, partial charge distribution, and 3D configuration of the molecule (Cheng et al., 2018; Huang et al., 2020; Jiang et al., 2010; Zhu et al., 2014; Zhu et al., 2015).

In Fig. 8, k_{O3} for aromatic compounds are plotted as a function of the E_{HOMO} (Tentscher et al., 2019). It shows an overall good correlation for various types of aromatic compounds, suggesting E_{HOMO} as a promising quantum molecular descriptor for aromatic ring systems. Generally, for aromatic compounds the predicted k_{O3} based on both E_{HOMO} and Hammett and Taft constants agree well with the experimentally

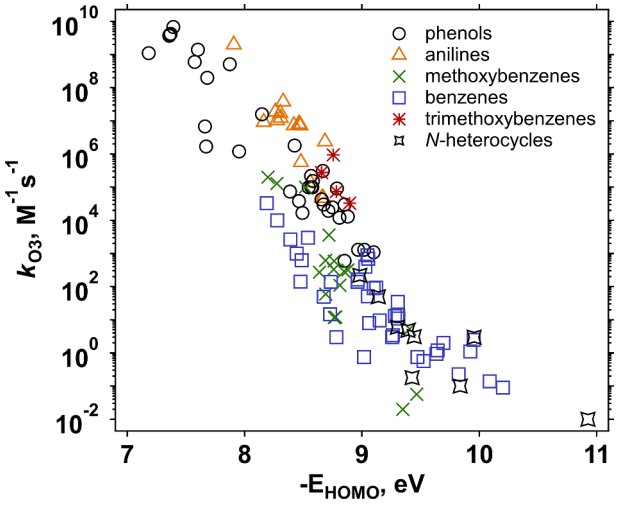

Fig. 8. QSAR-type correlation between the k_{O3} for the reactions of ozone with aromatic compounds and the E_{HOMO} values obtained by DFT calculations employing the M11/6-311+G(d,p) methods with the SMD implicit solvation model (for details of calculations, see Tentscher et al. 2019).

determined k_{O3} within a factor of 4 (Lee et al., 2015; Lee and von Gunten, 2012).

4.3.2. Reaction mechanisms

The three major pathways for oxidation of aromatic compounds by ozone are oxygen addition, electron transfer and the Criegee-type mechanism (Scheme 3). Of these, the most common reaction is oxygen addition to the ring (reaction type (ii) in Scheme 1 and pathway (i) in Scheme 3). For activated aromatic compounds with high k_{O3} (e.g., phenols), ozone adduct formation occurs in ortho/para position, which has an elevated electron density. The ozone adduct can then lose singlet oxygen and form a hydroxylated product (Scheme 3 (i)) (Mvula and von Sonntag, 2003). Hydroquinones and catechol are the major products through this pathway for phenolate (Mvula and von Sonntag, 2003; Ramseier and von Gunten, 2009; Tentscher et al., 2018). For aniline, the major products are *p*-hydroxyaniline and *o*-hydroxyaniline, with the sum of all hydroxyanilines accounting for ~40% of the initial aniline (Tekle-Röttering et al., 2016c).

The second pathway is electron transfer (Scheme 3 (ii)). It is unclear if this occurs via an ozone adduct formation or a direct electron transfer. Phenolate reacts with ozone to phenoxyl radical that can further react to benzoquinone (Ramseier and von Gunten, 2009). The coupling product (4,4-dihydroxybiphenyl), is an artefact of high phenol concentrations in laboratory experiments. Similar dimerization products were hypothesized from aniline such as 2-amino-5-anilino-benzochinon-anil and 2, 5-dianilino-*p*-benzochinon-imin, which are only expected at high initial concentrations of aniline (Tekle-Röttering et al., 2016c).

Finally, aromatic compounds can react through a Criegee-type mechanism (Scheme 3 (iii)), producing ring opening products such as muconic acid (Ramseier and von Gunten, 2009). Similar products were also observed from the ozone reaction with anisole, 1,2-dimethoxybenzene and 1,3,5-trimethpxylbenzene (Mvula et al., 2009). 2-Pyridine-carboxylic acid is a Criegee-type product detected from ozone reactions with aniline (Sarasa et al., 2002), however it cannot be confirmed that ozone is responsible for its formation, because $^{\bullet}$OH was not scavenged in this study.

For aniline-type compounds, the sites of ozone attack can also be the nitrogen, producing nitrosobenzene, nitrobenzene, azobenzene and azoxybenzene as products (Chan and Larson, 1991; Sarasa et al., 2002), but these reactions are minor based on the observed low yields (< 8%) (Tekle-Röttering et al., 2016c). Ozonation of nitrogen-containing compounds will be further discussed in Sections 4.5 and 4.6.

Ring substitution can affect the final products from the reactions of phenol with ozone. In a systematic study of phenol substituent effects on

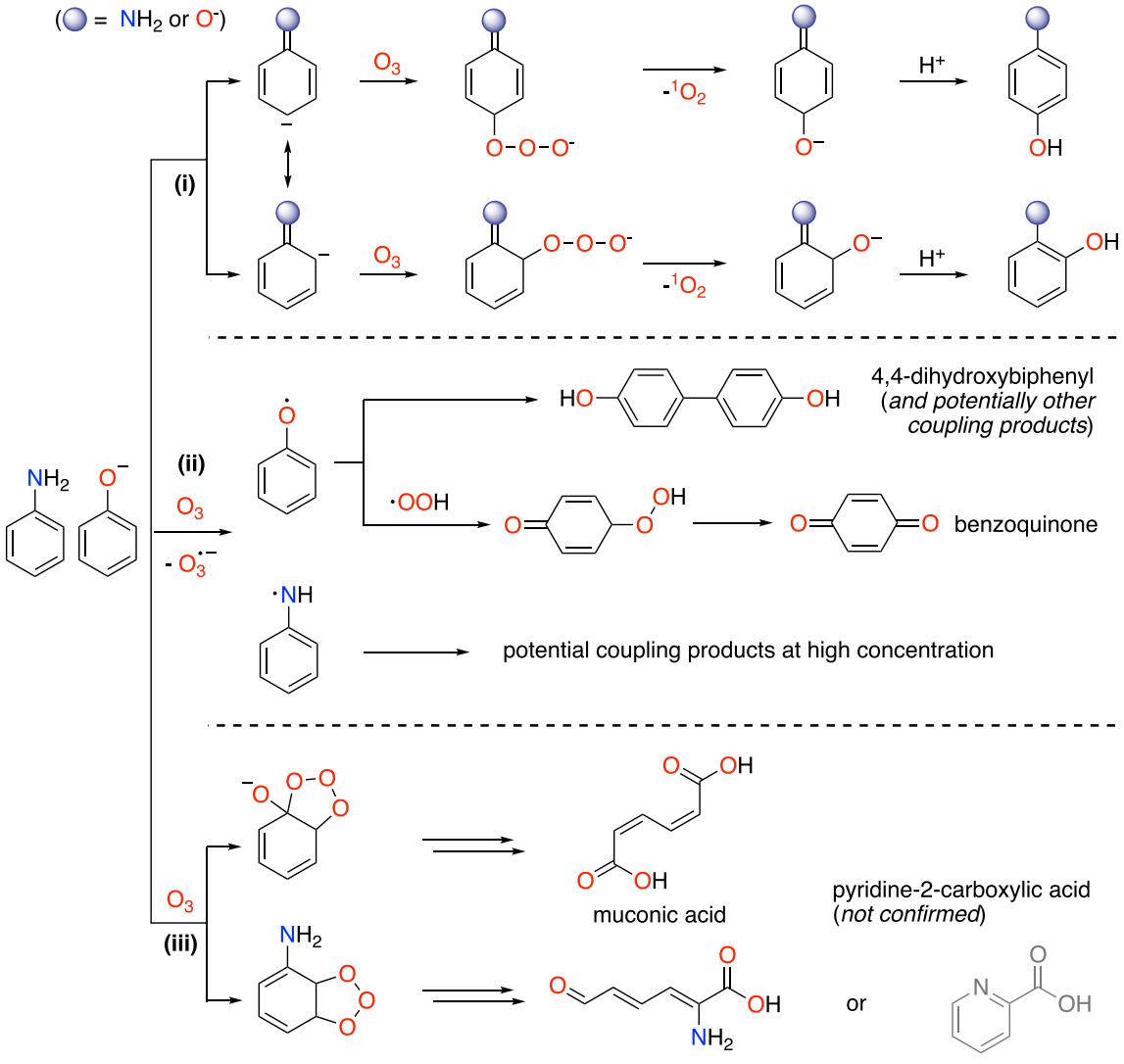

Scheme 3. Ozone reaction pathways for phenolate and aniline. (i) Hydroxylation, (ii) electron transfer with formation of an ozonide radical, (iii) Criegee ozonide formation leading to ring opening. (Mvula and von Sonntag, 2003; Mvula et al., 2009; Ramseier and von Gunten, 2009; Tekle-Röttering et al., 2016c)

product distribution, *para*-substituted catechols were found to be the most common products at pH 7, quantified from ozonation of *para*-substituted phenols (Tentscher et al., 2018), but with no obvious trend in their yields with respect to substitution. Somewhat surprisingly, many *para*-substituted phenols formed 1,4-benzoquinone, indicating loss of the substituent group during ozonation (Tentscher et al., 2018). Quinones have been previously observed as products of chlorophenol ozonation (Hong and Zeng, 2002; Qiu et al., 2004; Tentscher et al., 2018; Utsumi et al., 1998), and the dechlorination achieved by ozone (Tentscher et al., 2018) may increase the biodegradability (Adams et al., 1997; Hong and Zeng, 2002; Pi et al., 2007; Qiu et al., 2004; Utsumi et al., 1998). For two *para*-alkylated phenols, formation of the corresponding 4-hydroxy-4-alkylcyclohexadienone was observed, but not for any other phenols, possibly due to the poor leaving group properties of the alkyl substituents preventing further transformation to benzoquinones. Hydroquinones were only detected as ozonation products from 4-methoxyphenol (mequinol) and 4-formylphenol, and were attributed to reactions other than direct attack by ozone (Tentscher et al., 2018).

4.3.3. Micropollutants

Micropollutants and biomolecules bearing aromatic moieties generally react with ozone to produce hydroxylated and/or ring opening products analogously to Scheme 3. Because many of the hydroxylated moieties have higher ozone reactivities than the parent compounds, these primary products often escape detection (Gulde et al., 2021a). Reported ozone-induced transformation products of aromatic micropollutants are provided in Table S4 (SI).

Hydroxylated products such as hydroquinone and catechols are expected products of micropollutants (Scheme 3 (i)). For 17α-ethinylestradiol, estrone and 5,6,7,8-tetrahydro-2-naphthol, ozone was proposed to attack the phenolic moieties to form catechols by an oxygen transfer (Huber et al., 2004; Lee et al., 2008). Benzoquinone formation results from an electron transfer pathway (Scheme 3 (ii)). Ozonation of bisphenol A, a widely used industrial chemical, forms benzoquinone as the main product, along with 3-cyclohexene-1-carboxylic acid-ethyl ester and benzaldehyde (Deborde et al., 2008; Mutseyekwa et al., 2017). The formation of benzoquinones may be of toxicological relevance (Tentscher et al., 2021). One case in point is ozonation of *N*-(1,3-dimethylbutyl)-*N*'-phenyl-*p*-phenylenediamine, a widely applied tire antiozonant, forming a quinone product highly toxic to aquatic organisms (Tian et al., 2021).

Many ring opening products are expected from ozone reactions with aromatic compounds such as muconic acid or muconic aldehyde (Scheme 3 (iii)), which can potentially explain dicarbonyl compound formation. It has been shown that triazole-4,5-dicarbaldehyde is a product from the ozone attack of benzotriazole (Mawhinney et al., 2012). Formation of a dicarbonyl compound was reported from the ozone reaction with bezafibrate (Dantas et al., 2007). When ozone is in excess, further oxidation of the muconic-type compounds is expected to form small carbonyl species and carboxylic acids such as formic acid (Ramseier and von Gunten, 2009). The final products of the ozone oxidation of benzophenone-2, a common photo inhibitor, include oxalic acid and formic acid (Wang et al., 2017). These polar and low molecular weight compounds may escape detection for analysis with solid phase extraction and LC-HRMS/MS (Gulde et al., 2021a).

4.4. Heterocyclic compounds

Heterocyclic compounds are an important class of functional groups in micropollutants as well as in DOM. They usually consist of five-membered, six-membered, or fused rings and include at least one heteroatom (e.g., N, O, S) in the ring. For *N*-containing heterocyclic compounds, only unsaturated compounds are discussed in this section. The reactions of *N*-containing saturated heterocyclic compounds with ozone are similar to aliphatic amines, their acyclic analogues (Tekle-Röttering et al., 2016a). Aromatic rings without heteroatoms are discussed in the Section 4.3.

4.4.1. Kinetics

Heterocyclic compounds are characterized by extraordinarily diverse chemical properties and therefore undergo a wide range of reaction types: some react readily with electrophiles while others do not (Joule and Mills, 2012). Their reactivity with ozone varies widely, with reported k_{O3} from $< 0.1\ M^{-1}s^{-1}$ to $\sim 10^8\ M^{-1}s^{-1}$ (Table S5, SI).

4.4.1.1. N-containing heterocyclic compounds. Six-membered *N*-containing heterocyclic compounds like pyridine and pyrazine react slowly with ozone with $k_{O3} \leq 3\ M^{-1}s^{-1}$ (Tekle-Röttering et al., 2016b), whereas five-membered rings such as pyrrole and imidazole react much faster with ozone with $k_{O3} > 10^5\ M^{-1}s^{-1}$ (Tekle-Röttering et al., 2020). The surprisingly large difference in k_{O3} between six- and five-membered heterocycles seems attributable to the electron distribution in the rings. In pyridine, resonance withdraws electron density from carbons to the nitrogen (Fig. 9). As a result, pyridine carbons become π-deficient and thus less reactive towards ozone. Resonance in pyrrole works in the opposite way, pushing the electron density from the nitrogen towards carbons, making carbon-carbon double bonds more susceptible to an electrophilic ozone attack.

Heterocycles consist often of complex structures with diverse substituents. Effects of substituents on k_{O3} for selected heterocyclic compounds are shown in Fig. 10. (i) Pyrimidine and (ii) purine derivatives: the addition of a carbonyl or an amino group to the pyrimidine or purine significantly increases k_{O3}. All derivatives have higher k_{O3} than the simple heterocycles, by up to 7 orders of magnitude (pyrimidine vs. 2,4-

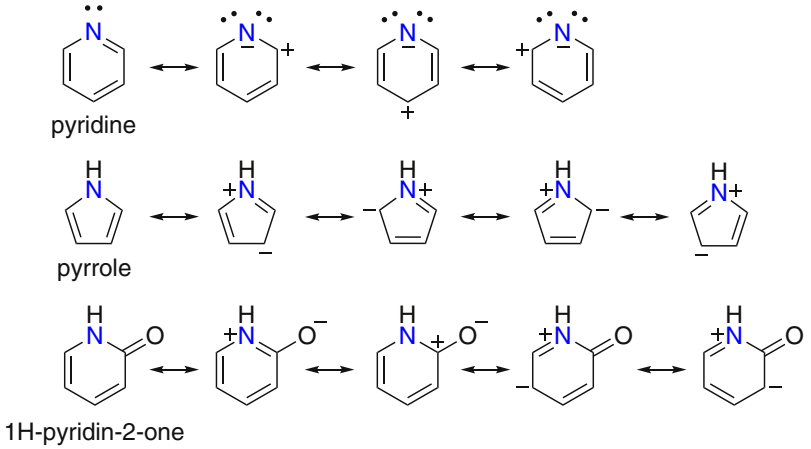

Fig. 9. Resonance structures of pyridine, pyrrole, and 1H-pyridin-2-one.

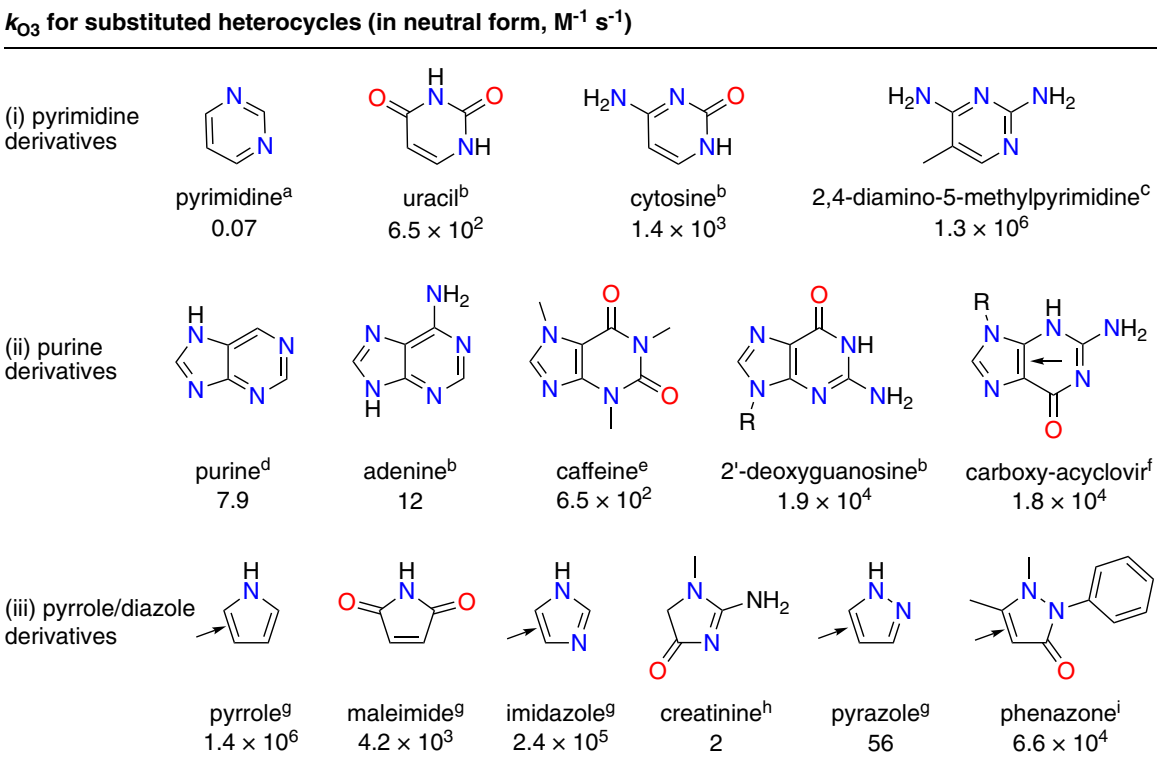

Fig. 10. Effects of carbonyl and amino group substitution on second-order rate constants for the reactions of ozone with (i) pyrimidine, (ii) purine, and (iii) pyrrole/diazole derivatives. Arrows indicate the ozone attack sites based on identified products in presence of *tert*-butanol, for the compounds with product information. References: [a](Tekle-Röttering et al., 2016b), [b](Theruvathu et al., 2001), [c](Dodd et al., 2006), [d](Legube et al., 1987), [e](Broséus et al., 2009), [f](Prasse et al., 2012), [g](Tekle-Röttering et al., 2020), [h](Hoigné and Bader, 1983a), and [i](Favier et al., 2015).

diamine 5-methylpyrimidine). (iii) Pyrrole/diazole derivatives: unlike pyrimidines and purines, pyrrole and imidazole derivatives with a carbonyl or amino group show lower k_{O3} (imidazole vs. creatinine). For pyrazole derivatives, k_{O3} seems to increase by a carbonyl group (pyrazole vs. phenazone) as for pyrimidines and purines, but the benzene ring on a nitrogen of phenazone may also contribute to the increase in k_{O3}. To confirm this, it is necessary to compare pyrazole with pyrazole derivatives substituted only by a carbonyl group, however, kinetic information of such derivatives is currently not available. The higher k_{O3} of uracil than for pyrimidine is especially interesting, as the substitution by an electron-withdrawing carbonyl group is expected to reduce the ozone reactivity. One way to explain these unusual cases with carbonyl substituents is by their resonance structures (Fig. 9). While pyridine lacks in electron density in the ring as discussed above, a 1H-pyridin-2-one (pyridine with a carbonyl substituent) develops a higher negative charge on the ring by resonance, suggesting a possibly higher k_{O3}.

4.4.1.2. O-containing heterocyclic compounds. Generally, there is little information on the ozone reactivity of heterocyclic compounds containing heteroatoms other than nitrogen. Furans, five-membered heterocyclic rings containing oxygen, show high reactivity towards ozone with $k_{O3,app,pH\ 7} > 10^4\ M^{-1}s^{-1}$ (Table S5, SI) (Jeon et al., 2016; Zoumpouli et al., 2021). Depending on the type of substituents (e.g., methyl, carboxyl groups) and their locations on the ring (e.g., α-, β-carbons), the $k_{O3,app,pH7}$ varied from $8.5 \times 10^4\ M^{-1}s^{-1}$ for furan-2,5-dicarboxylic acid to $3.2 \times 10^6\ M^{-1}s^{-1}$ for 3-(2-furyl)propanoic acid (Zoumpouli et al., 2021).

4.4.2. Reaction mechanisms

Heterocyclic compounds react with ozone by various types of mechanisms, mostly by reaction type (i) in Scheme 1, which opens the ring by carbon-carbon double bond cleavage (Criegee-type mechanism). As a result, ring-opened primary products with two carbonyl groups on each end are formed. The ring-opened products undergo subsequent reactions, sub-categorized as (i-a), (i-b), and (i-c) in Scheme 4. They are subject to further transformation by ozone to form secondary products with typically a shorter chain length (i-a). Examples of such secondary products are quinolinic acid from quinoline with 65% yield (Andreozzi et al., 1992b) and glyoxal from pyrrole with 5% yield (Tekle-Röttering et al., 2020). In a rarer case, ring-opened products are fully fragmented without further oxidation (i-b). A case in point is imidazole, which is transformed to formamide, cyanate, and formate, with 100% yields, respectively, by a single ozone attack (Tekle-Röttering et al., 2020).

Ring-opened products are also susceptible to an intramolecular cyclization (i-c). This results in the formation of products with smaller ring size as the parent heterocyclic compounds. For example, hydantoins with a five-membered ring were identified after the reactions of ozone with six-membered heterocyclic compounds like uracil (Matsui et al., 1990) and thymine (Flyunt et al., 2002), at yields of ~30%. Although it is unclear whether these products resulted from direct ozone reactions (because of lack of information on the use of radical scavengers), similar ring products with reduced size were also identified in more controlled experiments (in the presence of *tert*-butanol) for 2-hydroxypyridine (Andreozzi et al., 1992a) and thymidine (confidence level 3) (Funke et al., 2021). The reaction type (i) was also suggested for reactions of furans with ozone, based on the formation of ring-opened products, α,β-unsaturated dicarbonyl compounds (Zoumpouli et al., 2021). However, the products were identified in absence of radical scavengers. Therefore, experimental evidence under more controlled conditions is required to confirm the proposed mechanism of the furan-ozone reaction.

Some heterocyclic compounds react with ozone via reaction type (ii) (Scheme 1 and Scheme 4), in analogy to typical reactions of aromatic compounds with ozone (Section 4.3.2). In this case, oxygen-added ring products with the same ring structure as the parent heterocycle are formed. The formation of maleimide (34% yield) from the reaction of

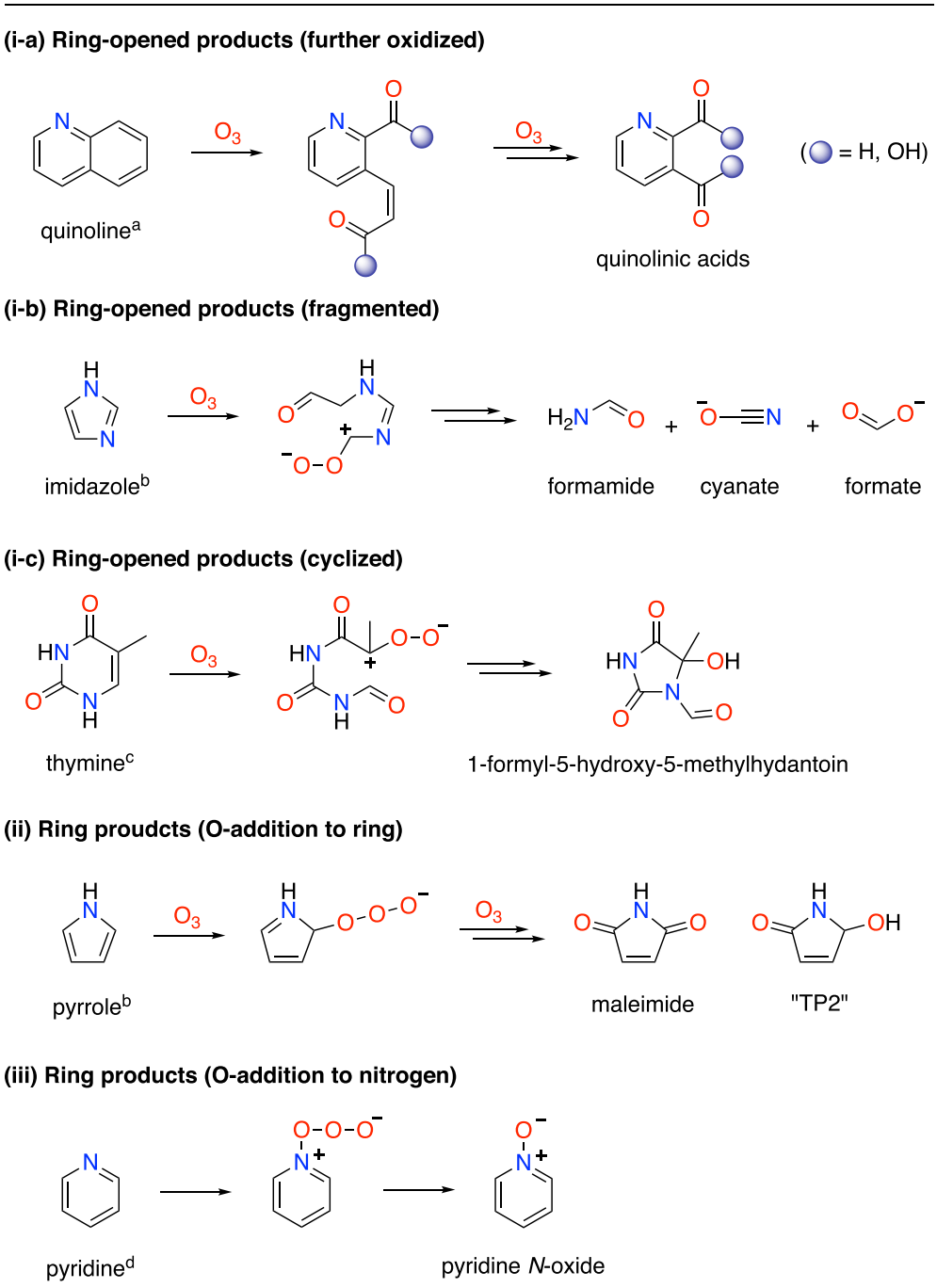

Scheme 4. Ozone reactions with heterocyclic compounds categorized based on the resulting transformation products. References: [a](Andreozzi et al., 1992b), [b](Tekle-Röttering et al., 2020), [c](Flyunt et al., 2002), [d](Andreozzi et al., 1991; Tekle-Röttering et al., 2016b).

pyrrole with ozone supports an oxygen-addition mechanism (Tekle-Röttering et al., 2020). Another ring product structurally close to maleimide (called TP2 in the original study) was also identified but with unknown yield. One heterocyclic compound can react through multiple reaction types, as for pyrrole, which reacts with ozone via reaction types (i) and (ii) in Scheme 4 (Tekle-Röttering et al., 2020).

Ozone attack on the heteroatom instead of a carbon-carbon double bond is rarely reported during ozonation of heterocyclic compounds (Scheme 4, (iii)). Pyridine and pyridazine are transformed to *N*-oxides with yields of $\leq$ 93% (Andreozzi et al., 1991; Tekle-Röttering et al., 2016b). This *N*-oxide formation is similar to reactions of tertiary amines with ozone, as illustrated in reaction type (iii) in Scheme 1. Nevertheless, high yields of *N*-oxides from heterocycles are unlikely under realistic ozonation conditions, because of the low ozone reactivity of pyridine and pyridazine ($k_{O3} \sim 2\ M^{-1}s^{-1}$ for both (Tekle-Röttering et al., 2016b)). Such ozone-refractory compounds are mainly oxidized by $^{\bullet}OH$ (Fig. 5), which consequently leads to a different spectrum of transformation products. During ozonation in absence of *tert*-butanol ($^{\bullet}OH$ reaction possible), pyridine was transformed to ring-opened products like formamido(oxo)acetic acid and oxamic acid (Andreozzi et al., 1991).

4.4.3. *Micropollutants*

Micropollutants often contain heterocyclic moieties, which are the

main site of ozone attack. Acesulfame is attacked on the carbon-carbon double bond in the ring to form ring-opened products susceptible to further oxidation, as described in (i-a) in Scheme 4. The resulting products are a hydrated form of a carbonyl product and carboxylic acid, with ~50% and 80% yields, respectively (Scheurer et al., 2012). Phenazone derivatives (Favier et al., 2015) and benzotriazole (Mawhinney et al., 2012) were also reported to form ring-opened products upon ozonation, with sufficient MS evidences (confidence level 2) but with unknown yields. Furosemide and ranitidine, both of which feature a furan moiety, were also suggested to be oxidized at a carbon-carbon double bond of furan to form the corresponding ring-opened products based on MS results (confidence level 2) (Zoumpouli et al., 2021). Caffeine was found to be oxidized by ozone to form five- and six-membered ring products with 20 – 30% yields, resulting from the intramolecular cyclization of an initial ring-opened product ((i-c) in Scheme 4) (Kolonko et al., 1979). In this study, however, ozonation experiments were conducted in absence of $^{\bullet}$OH scavengers and thus an impact of $^{\bullet}$OH cannot be excluded (Kolonko et al., 1979). Carboxy-acyclovir, containing a purine moiety, was attacked by ozone at the carbon-carbon double bond shared by the fused six- and five-membered rings (Prasse et al., 2012). The resulting ozonide intermediate underwent rearrangement of the ring and hydrolyzed to form a final product containing a five-membered ring with 100% yield (similar to (i-c) in Scheme 4) (Prasse et al., 2012). Zidovudine, a thymidine derivative, reacted with ozone at the carbon-carbon double bond of the thymine moiety. Ring-opened products via (i-a) as well as ring products by rearrangement via (i-c) were proposed by MS analyses (confidence level 3) (Funke et al., 2021). Lamotrigine, containing a 1,2,4-triazine moiety, was oxidized by ozone at the nitrogen to form a *N*-oxide ((iii) in Scheme 4), which underwent subsequent oxidation (Bollmann et al., 2016).

4.5. Aliphatic amines

4.5.1. Kinetics

Aliphatic amines are present in natural waters as part of the dissolved organic nitrogen pool (Westerhoff and Mash, 2002). They are also common functional groups of micropollutants (Bourgin et al., 2018). The lone electron pair on the nitrogen of aliphatic amines is susceptible to an electrophilic attack by ozone. As a result, aliphatic amines in the neutral form react fast with ozone with k_{O3} ranging from 10^3 to 10^8 $M^{-1}s^{-1}$ (von Sonntag and von Gunten, 2012). Because of this high ozone reactivity, aliphatic amines are considered key ozone-reactive moieties. At neutral pH, aliphatic amines are mostly present in the protonated form because the pK_a of the protonated form of aliphatic amines typically lies in the range of 9 – 11. Amines in their protonated form have low reactivities with ozone ($k_{O3} < 0.1$ $M^{-1}s^{-1}$) due to the lack of a lone electron pair (Hoigné and Bader, 1983a). Consequently, apparent second-order rate constants at pH 7 ($k_{O3,app,pH7}$) decrease by 3 – 4 orders of magnitude relative to k_{O3} of the neutral form, resulting in typical $k_{O3,app,pH7}$ values of 10 to 10^3 $M^{-1}s^{-1}$ (von Sonntag and von Gunten, 2012). The ozone reactivity of aliphatic amines is affected by the nature of substituents that can increase or decrease the electron density of the nitrogen. For example, an alkyl substituent generally increases ozone reactivity by inductive effects. Therefore, tertiary amines typically have higher second-order rate constants for the reaction with ozone than primary and secondary amines (von Sonntag and von Gunten, 2012). In contrast, amides are practically unreactive towards ozone due to the presence of the electron withdrawing carbonyl group. Halogen substituents typically decrease the ozone reactivity by an electron withdrawing effect, as is shown for methylamine ($k_{O3} < 1 \times 10^5$ $M^{-1}s^{-1}$ (Hoigné and Bader, 1983a)), methylchloramine ($k_{O3} = 8.1 \times 10^2$ $M^{-1}s^{-1}$ (Haag and Hoigné, 1983a)), and dichloromethylamine ($k_{O3} < 1 \times 10^{-2}$ $M^{-1}s^{-1}$ (Haag and Hoigné, 1983a)). However, exceptional cases exist, as for monochloramine ($k_{O3} = 26$ $M^{-1}s^{-1}$ (Haag and Hoigné, 1983a)) and monobromamine ($k_{O3} = 40$ $M^{-1}s^{-1}$ (Haag et al., 1984)), in comparison to ammonia ($k_{O3} = 20$ $M^{-1}s^{-1}$ (Hoigné and Bader, 1983a)). The reason why the electron withdrawing effect by halogens is not as pronounced as expected is not clear. In the case of dimethylsulfamide (DMS), the effect of halogenation is even more pronounced. For the reactions of DMS and Br-DMS with ozone, $k_{O3,app} \approx 20$ $M^{-1}s^{-1}$ and $k_{O3,app} \geq 5 \times 10^3$ $M^{-1}s^{-1}$ were determined at pH 8, respectively, by kinetic modeling of experimental data (von Gunten et al., 2010). This is due to a depression of the pK_a of Br-DMS, which results in a partially deprotonated amine moiety. More aliphatic amine derivatives containing substituents other than alkyl and carbonyl groups are discussed in Section 4.6.

4.5.2. Reaction mechanisms

Ozonation of tertiary amines has been studied extensively. *N*-oxides were identified as major products with high yields (> 90%) for simple tertiary amines with short alkyl chains and micropollutants containing a tertiary amine moiety (von Sonntag and von Gunten, 2012) (Scheme 5 and reaction type (iii) in Scheme 1).

Besides *N*-oxides, dealkylated products were also identified from the reaction of tertiary amines with ozone, but as minor products with yields ≤ 10% (Lange et al., 2006; Lim et al., 2019; Zimmermann et al., 2012). While *N*-oxides are products formed via an oxygen-transfer pathway,

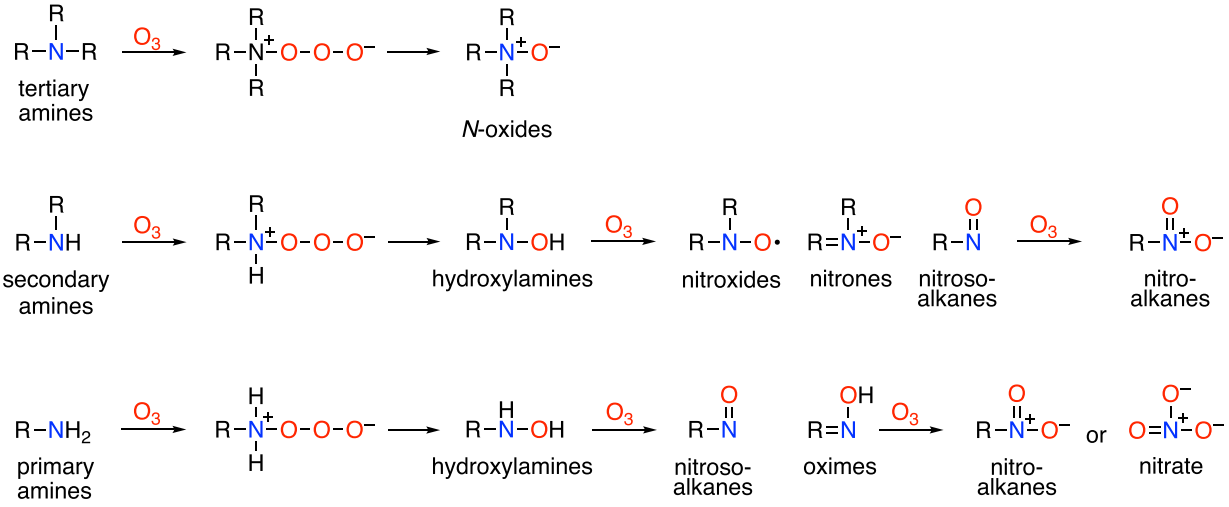

Scheme 5. Reactions of aliphatic amines with ozone.

dealkylated products result from an electron-transfer pathway involving an amine radical cation as a reaction intermediate (von Sonntag and von Gunten, 2012) (reaction type (v) in Scheme 1).

The mechanisms of the reactions of primary and secondary amines with ozone have also been investigated (de Vera et al., 2017; Essaïed et al., 2022; Lim et al., 2019; McCurry et al., 2016; Shi and McCurry, 2020; Tekle-Röttering et al., 2016a). Nitroalkanes were identified as major products (yields up to 100%) from simple primary and secondary amines (Lim et al., 2019; McCurry et al., 2016) (Scheme 5). A potentially undesirable outcome associated with the formation of nitroalkanes is discussed in Section 2.2.2.

Hydroxylamines were suggested as ozonation products of secondary amines (Benner and Ternes, 2009a; Benner and Ternes, 2009b; Tekle-Röttering et al., 2016a; von Gunten, 2003b), in analogy to *N*-oxides as ozonation products of tertiary amines. However, recent studies identified hydroxylamines not as end products but as reaction intermediates that further react with ozone to eventually form nitroalkanes (Scheme 5; see also Section 4.6). This occurs especially under neutral pH conditions, where the ozone reactivity of hydroxylamines is typically much higher than the ozone reactivity of amines, because of the lower pK_a of protonated hydroxylamines compared to protonated amines. Besides hydroxylamines, nitroxides, nitrones, and nitrosoalkanes have been suggested as other reaction intermediates, but only the formation of nitrone was confirmed by an analytical standard during ozonation of a secondary amine (Lim et al., 2019).

Nitrate is also a final product for ozonation of aliphatic amines along with carbonyl products originating from the carbonaceous part of the amine compounds. It was shown that the yields of nitrate were highly variable for primary and secondary amines with a 20-fold molar ozone excess (17-100%) (de Vera et al., 2017; Essaïed et al., 2022). Amino acids showed consistently high yields of nitrate under similar ozonation conditions (Essaïed et al., 2022). Under these extreme conditions, nitroalkanes and *N*-oxides were possibly further oxidized to nitrate. Certain primary amines form nitrate more efficiently. Glycine was transformed into nitrate with a $>$ 80% yield with a 5-fold ozone excess (Berger et al., 1999). This is in contrast to ethylamine, forming nitroethane as the only product under similar ozonation conditions (Lim et al., 2019). Nitrate formation during continuous ozonation was used as a surrogate for the potential formation nitro and/or nitroso compounds from DOM. It could be shown that the nitrate formation potential during ozonation was in the range of 13-45 % of the dissolved organic nitrogen for 6 different DOM sources (Essaïed et al., 2022).

Overall, all types of aliphatic amines (primary, secondary, and tertiary) are transformed into products containing N-O bonds (nitroalkanes, *N*-oxides, and nitrate) with high yields. This indicates that aliphatic amines react with ozone mainly via oxygen-transfer pathways (reaction type (iii) in Scheme 1). Additional evidence is provided by high yields of singlet oxygen (a byproduct of the oxygen-transfer pathway) and quantum chemically computed Gibbs free energy favoring an oxygen-transfer over an electron-transfer pathway (Lim et al., 2019). However, the reaction pathway can be shifted to some extent under real ozonation conditions where $^{\bullet}$OH is formed as a secondary oxidant and plays a role in oxidizing aliphatic amines (Fig. 5), due to the relatively low $k_{O3,app}$ at neutral pH. In this case, aliphatic amines undergo hydrogen atom abstraction to form *N*-centered radicals that are subsequently degraded into dealkylated products and ultimately ammonia (reaction type (v) in Scheme 1) (de Vera et al., 2017; Le Lacheur and Glaze, 1996).

4.5.3. Micropollutants

The formation of *N*-oxides during ozonation has been reported for many pharmaceuticals containing a tertiary amine moiety such as clarithromycin, tramadol, venlafaxine, tamoxifen, and toremifene (Knoop et al., 2018; Lange et al., 2006; Lester et al., 2013; Zimmermann et al., 2012). Pharmaceuticals containing a tertiary amine moiety in a saturated heterocyclic form, such as cetirizine (containing piperazine), fexofenadine (piperidine), sulpiride (pyrrolidine), and amisulpride (pyrrolidine), were also transformed into *N*-oxides upon ozonation (Bollmann et al., 2016; Borowska et al., 2016). The formation of *N*-oxides has been also observed in pilot- and full-scale wastewater treatment plants with ozonation of secondary wastewater effluent (Bourgin et al., 2018; Merel et al., 2017; Zucker et al., 2018). Once formed, *N*-oxides are persistent in the treated water. They are not biodegradable during typical aerobic biological post-treatments after ozonation (Bourgin et al., 2018; Hübner et al., 2015; Knopp et al., 2016; Zucker et al., 2018).

In contrast to the ample evidence of the *N*-oxide formation, the formation of hydroxylamines from the oxidation of micropollutants containing secondary/primary amines by ozone has been reported to a lesser extent (e.g., propranolol (Benner and Ternes, 2009a)). This is probably because of the further oxidation of hydroxylamines, ultimately forming nitro compounds, as is shown for sitagliptin, a pharmaceutical containing a primary amine moiety (Hermes et al., 2020). The corresponding nitro product of sitagliptin was also detected in pilot-scale and full-scale ozonation process (Gulde et al., 2021a; Hermes et al., 2020).

4.6. Other aliphatic nitrogen-containing compounds

4.6.1. Kinetics

Various derivatives are related to aliphatic amines by substitution of the nitrogen with heteroatoms (e.g., O, N, S). The k_{O3} of these compounds are in the range from $<$ 1 to ~10^6 $M^{-1}s^{-1}$. Currently available information on k_{O3} is summarized in Fig. 11, categorized by characteristic chemical bonds found in the functional groups. Differences in pK_a values result in a different trend in $k_{O3,\ app}$ as a function of the pH for substituted nitrogen-containing compounds in comparison to aliphatic amines (Fig. 12).

(i) N-O bond: compounds containing N-O bonds, e.g., *N*-oxides, hydroxylamines, nitrones, and nitroalkanes, are common ozonation products of aliphatic amines (Section 4.5.2). They show a wide range of k_{O3}, from slow-reacting *N*-oxides and nitroalkanes ($k_{O3,app,pH7} < 10$ $M^{-1}s^{-1}$) to fast-reacting nitrones and hydroxylamines ($k_{O3,app,pH7} > 10^3$ $M^{-1}s^{-1}$). It should be noted that the reported k_{O3} for the fexofenadine *N*-oxide is associated with other moieties (Borowska et al., 2016) and therefore k_{O3} of the *N*-oxide moiety would be even lower than 6 $M^{-1}s^{-1}$. Hydroxylamines are especially reactive because of their pK_a values, 3 – 5 units lower than the pK_a of the amine analogous (Table S6, SI). Therefore, unlike aliphatic amines, hydroxylamines remain highly reactive towards ozone at pH 7 where they are dominantly present in the neutral form (Fig. 12).

(ii) N-N bond: hydrazines and hydrazides react fast with ozone with high k_{O3}. Similarly to hydroxylamines, their protonated forms have a lower pK_a than protonated aliphatic amines (Table S6, SI), resulting in high $k_{O3,app,pH7}$ (Fig. 12). Daminozide reacts fast with ozone over a wide pH-range ($k_{O3} \geq 10^5$ $M^{-1}s^{-1}$ for pH 3 – 9), due to its low pK_a of 3.7.

(iii) N-N=O bond: nitrosamines and nitroamines react very slowly with ozone with most $k_{O3} \leq 0.5$ $M^{-1}s^{-1}$ (Mestankova et al., 2014).

(iv) N-C(=N)-N bond: The nitrogen of guanidine derivatives is present in the protonated form under most pH conditions because of the high pK_a (e.g., 13.6 for guanidine (Table S6, SI)). As a consequence, their k_{O3} are likely to be low, as shown for metformin (1.2 $M^{-1}s^{-1}$) and creatine (0.5 $M^{-1}s^{-1}$) (Hoigné and Bader, 1983a; Jin et al., 2012).

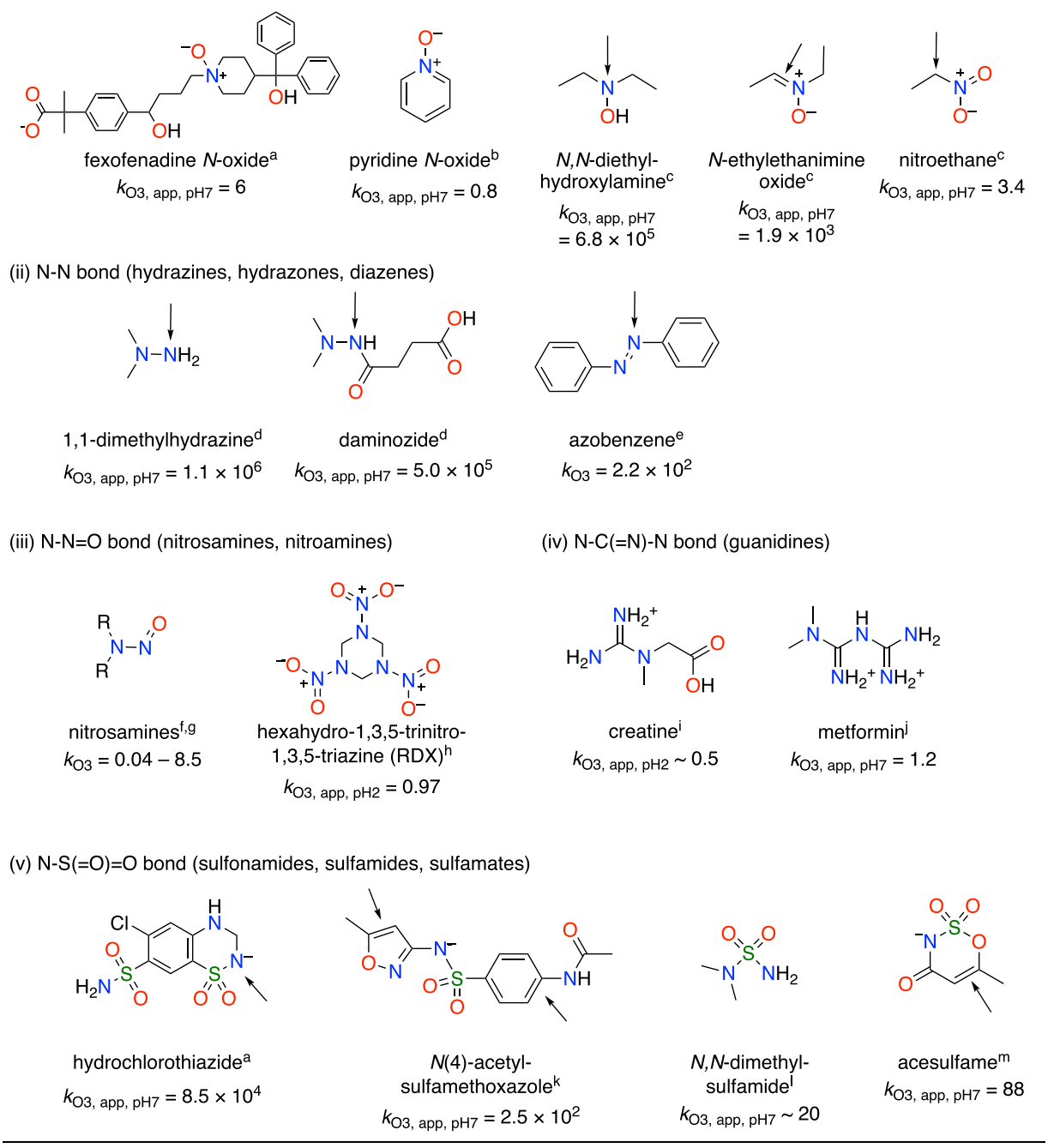

Fig. 11. Second-order rate constants k_{O3} for the reactions of ozone with selected *N*-containing compounds: (i) N-O bond, (ii) N-N bond, (iii) N-N=O bond, (iv) N-C(=N)-N bond, and (v) N-S(=O)=O bond. Arrows indicate the sites of ozone attack. Structures of major species at given pH are depicted based on the pK_a summarized in Table S6, SI, except hydrochlorothiazide (shown as deprotonated species) for which the major species at the given pH is unclear because of its ill-defined pK_a. References: [a](Borowska et al., 2016), [b](Tekle-Röttering et al., 2016b) [c](Lim et al., 2019), [d](Lim et al., 2016), [e](Yao and Haag, 1991), [f](Lee et al., 2007b), [g](Mestankova et al., 2014), [h](Chen et al., 2008), [i](Hoigné and Bader, 1983a), [j](Jin et al., 2012), [k](Dodd et al., 2006), [l](von Gunten et al., 2010), and [m](Kaiser et al., 2013).

(v) N-S(=O)=O bond: The nitrogen adjacent to sulfur in sulfonamides, sulfamides, and sulfamates undergoes acid-base speciation from the neutral to the deprotonated, anionic form (Table S6, SI) and therefore k_{O3} strongly depends on the pH. k_{O3} of the deprotonated forms are ~3 × 10^5 $M^{-1}s^{-1}$ for hydrochlorothiazide (Borowska et al., 2016), 2.6 × 10^2 $M^{-1}s^{-1}$ for *N*(4)-acetyl-sulfamethoxazole (Dodd et al., 2006), >10^3 $M^{-1}s^{-1}$ for *N,N*-dimethylsulfamide (von Gunten et al., 2010), and 88 $M^{-1}s^{-1}$ for acesulfame (Kaiser et al., 2013). Only hydrochlorothiazide with a pK_a ~ 7.0 remains ozone-reactive at neutral pH with $k_{O3, app,pH7}$ = 8.5 × 10^4 $M^{-1}s^{-1}$, while the other compounds show low to moderate $k_{O3,app,pH7}$.

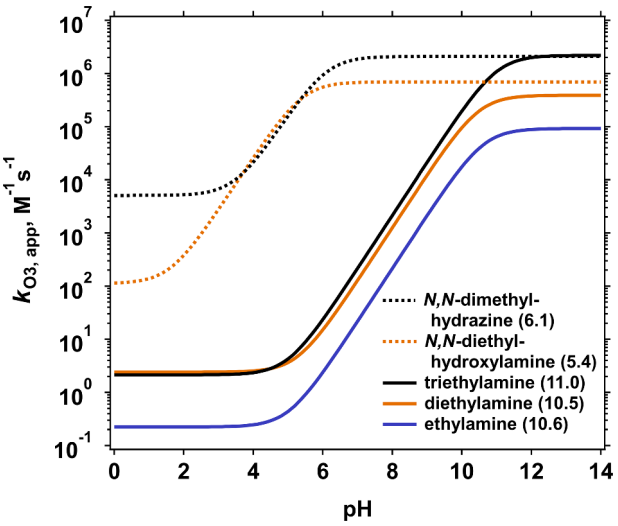

Fig. 12. pH-dependent apparent second-order rate constants ($k_{O3, app}$) for the reactions of ethylamine, diethylamine, triethylamine, *N,N*-diethylhydroxylamine, and 1,1-dimethylhydrazine with ozone, based on the results from (Lim et al., 2016; Lim et al., 2019) and the reported pK_a values (shown in parentheses).

4.6.2. *Reaction mechanisms*

Depending on the substituents, the reactions of aliphatic amine derivatives with ozone differ significantly. Some are attacked by ozone on the nitrogen, e.g., 1,1-dimethylhydrazine, whereas others shift the main attack site to an α-carbon, e.g., nitroethane (Section 4.8.1). The reactions for which nitrogen is the main ozone-reactive site are summarized in Scheme 6. Systematic investigations on product formation and reaction mechanisms for this group of compounds are scarce. Because of the lack of information with model compounds, some of the mechanisms are discussed for micropollutants.

(i) Compounds with N-O bond: hydroxylamines are quantitatively transformed to nitroalkanes upon ozonation, forming nitrones as reaction intermediates (Lim et al., 2019; Shi and McCurry, 2020). This supports that hydroxylamines are likely involved in the reactions of primary/secondary amines with ozone, which also form nitroalkanes as final products.

(ii) Compounds with an N-N bond: hydrazine/hydrazide-ozone reactions have been studied mainly with regard to the formation of *N*-nitrosodimethylamine (NDMA), a probable human carcinogen. Upon ozonation, one of the two nitrogen atoms is directly attacked by ozone and forms a new N=O bond. NDMA was quantified as final product with high molar yields for 1,1-dimethylhydrazine and daminozide (Lim et al., 2016), and industrial chemicals containing semicarbazides (Kosaka et al., 2009; Kosaka et al., 2014). Hydrazides are also found in heterocycles (Section 4.4), e.g., phenazone-type pharmaceuticals (Favier et al., 2015). In this case, however, the main ozone attack site is not the hydrazide-nitrogen but an endocyclic double bond.

(iii) and (iv) Compounds with N-N=O and N-C(=N)-N bonds: There is little information on the direct ozone reactions with nitrosamines, nitroamines, and guanidines, mostly because of their low ozone reactivity, which will promote an $^{\bullet}$OH oxidation under realistic ozonation conditions (Fig. 5).

(iv) Compounds with a N-S(=O)=O bond: Typically, substitution by electron-withdrawing groups reduces the ozone reactivity of the nitrogen. In certain cases, if the electron-withdrawing effect is strong enough that the substituted nitrogen becomes acidic, the deprotonated nitrogen is the favorable target site for ozone. This was observed for hydrochlorothiazide of which the sulfonamide-nitrogen was oxidized by ozone via electron transfer and transformed into chlorothiazide as a primary product (Borowska et al., 2016). In contrast, *N*(4)-acetyl-sufamethoxazole, with the aniline-nitrogen deactivated by an amide, is likely oxidized by ozone on the isoxazole or the aniline ring, rather than on the sulfonamide (Dodd et al., 2006). Acesulfame, containing a nitrogen substituted by both sulfonyl and amide groups, reacts with ozone mainly via an oxidation on the endocyclic double bond (Scheurer et al., 2012). The presence of the second substitution group or other ozone-reactive moieties seems a determining factor for assessing the sulfonamide-ozone reaction. The reaction of *N,N*-dimethylsulfamide with ozone was studied in detail because of its potential to form NDMA (Schmidt and Brauch, 2008; Trogolo et al., 2015; von Gunten et al., 2010). The ozone reaction is slow and does not lead to NDMA formation. However, in presence of bromide, *N,N*-dimethylsulfamide (DMS) reacts fast with hypobromous acid (HOBr) ($k_{HOBr,DMS} = 8.1 \times 10^8$ $M^{-1}s^{-1}$ with the deprotonated form of *N,N*-dimethylsulfamide (Heeb et al., 2017)) to a bromamine. HOBr is formed as a secondary oxidant from the reaction of bromide with ozone (Haag and Hoigné, 1983b). This intermediate is then further transformed to NDMA with a yield of about 50% ((von Gunten et al., 2010); see above for kinetic assessment).

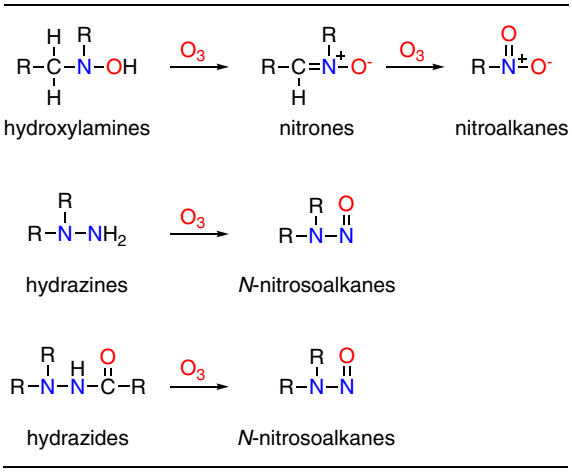

Scheme 6. Mechanisms for the reactions of hydroxylamines, hydrazines, and hydrazides with ozone.

4.7. *Organosulfur compounds*

4.7.1. *Kinetics*

Ozonation of sulfur has been observed for at least 75 years, such as the reaction of aqueous 2-chloroethyl sulfide with ozone to produce the corresponding sulfoxide (Price and Bullitt, 1947). Sulfur compounds can exist in oxidation states between (-II) and (VI) (Fig. 13). S(VI) compounds such as sulfate do not react with ozone (von Sonntag and von Gunten, 2012). Sulfur-containing functional groups in oxidation states < VI (with the exception of sulfones and analogues) react with ozone, with generally higher k_{O3} with increasing sulfur electron density. Sulfoxides react sparingly with ozone (e.g., dimethylsulfoxide: $k_{O3} = 8$ $M^{-1}s^{-1}$ (Pryor et al., 1984), and compounds with sulfur bonded to carbonyls are moderately reactive (e.g., molinate: $k_{O3} = 5 \times 10^2$ $M^{-1}s^{-1}$; *S*-Ethyl-*N,N*-dipropylthiocarbamate: $k_{O3} = 5 \times 10^2$ $M^{-1}s^{-1}$) (Chen et al., 2008). However, sulfurous functional groups in lower oxidation states such as thiols, thioethers, and disulfides react readily with ozone.

Thiols and thioethers react very fast with ozone (cysteine: $k_{O3} = 4 \times 10^4$ $M^{-1}s^{-1}$, methionine: $k_{O3} = 4 \times 10^6$ $M^{-1}s^{-1}$) (Pryor et al., 1984). Thioglycolic acid was found to be completely oxidized within 9 minutes of exposure to 12 mg/L ozone (Gilbert and Hoffmann-Glewe, 1990), but $^{\bullet}$OH was not suppressed, so the k_{O3} cannot be determined.

Reactions with disulfides are generally fast (e.g., bis(2-hydroxyethyl)

Sulfur groups	Structures	Oxidation state of S	Typical k_{O3}	Examples	
sulfones		+2	low		
sulfoxides		0	low		dimethylsulfoxide k_{O3} = 8 $M^{-1}s^{-1}$
thiocarbamates	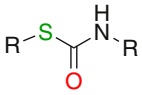	0	moderate	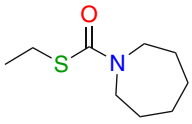	molinate k_{O3} = 500 $M^{-1}s^{-1}$
disulfides	R–S–S–R	-1	high	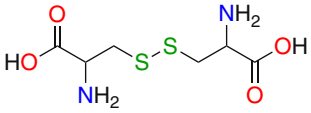	cystine $k_{O3,app,pH3}$ = 1×10^3 $M^{-1}s^{-1}$
thiols	R–SH	-2	high	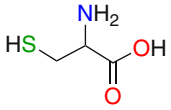	cysteine k_{O3} = 4×10^4 $M^{-1}s^{-1}$
thioethers	R–S–R	-2	high	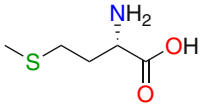	methionine k_{O3} = 4×10^6 $M^{-1}s^{-1}$

Fig. 13. Typical species-specific second-order rate constants for the reactions of organosulfur functional groups with ozone. References: (Chen et al., 2008; Hoigné and Bader, 1983a; Muñoz et al., 2001; Pryor et al., 1984)

disulfide: $k_{O3} = 1.7 \times 10^5$ $M^{-1}s^{-1}$; *trans*-1,2-dithiane-4,5-diol: $k_{O3} = 2.1 \times 10^5$ $M^{-1}s^{-1}$) (Muñoz et al., 2001), with final products being *S*-alkyl sulfinates (Muñoz et al., 2001). Cystine is an unusual outlier as a slower-reacting disulfide ($k_{O3} = 1 \times 10^3$ $M^{-1}s^{-1}$) (Hoigné and Bader, 1983a), a difference for which no explanation has been proposed.

Thioether-containing β-lactam antibiotics react quickly with ozone. Penicillin and cephalexin were both observed to react quickly with ozone at pH 7 with high $k_{O3,app,pH7}$ of 4.8×10^3 $M^{-1}s^{-1}$ and 8.7×10^4 $M^{-1}s^{-1}$, respectively (Dodd et al., 2006). Penicillin has no other clearly oxidizable functional groups, so the $k_{O3,\ app}$ was interpreted as the species-specific k_{O3} for the reaction with the thioether, but cephalexin also features olefin and primary amine functional groups, complicating the kinetic interpretation. Lincomycin and methicillin also react quickly at their thioether sites with $k_{O3,app,pH7}$ of 6.75×10^5 $M^{-1}s^{-1}$ and 3.9×10^4 $M^{-1}s^{-1}$, respectively (Qiang et al., 2004; Jin et al., 2012). The thioether of ranitidine was reported to be highly reactive with ozone, with a species-specific k_{O3} of 2.0×10^5 $M^{-1}s^{-1}$ (Jeon et al., 2016).

Data on ozone reactions with aromatic sulfur are scarce. Benzothiazole and analogues were reportedly abated during ozonation of synthetic wastewater (Derco et al., 2011). However, no studies to date have reported species-specific k_{O3} or products for benzothiazole reactions with ozone or •OH. Therefore, it cannot be determined whether the site of ozone attack was at the sulfur, the nitrogen, or an aromatic carbon site. Increased abatement rates at pH 8.5 compared to 5.8 suggested that •OH may have been responsible for the benzothiazole degradation, implying a low second-order rate constant for the reaction with ozone. One study measured second-order rate constants for benzothiazole reactions with ozone and •OH and found them to be $k_{O3} = 2.3$ $M^{-1}s^{-1}$ and $k_{•OH} = 6 \times 10^9$ $M^{-1}s^{-1}$, respectively (Valdés et al., 2004). The measurements were made in a solution with continuous ozone sparging, during which the concentration of ozone and •OH may be somewhat unstable. Nevertheless, these measurements are useful as preliminary estimates. After ozonation of secondary municipal wastewater effluent at ~0.6 mg O_3/mg DOC, the benzothiazole concentration was found to decrease by 70% in one study (Hollender et al., 2009), but in another after ozonation at 0.81 mg O_3/mg DOC, benzothiazole was observed to be abated by only 7% (Margot et al., 2013), and the reason for the discrepancy is unclear.

4.7.2. *Reaction Mechanisms*

Information on the mechanisms and products of sulfur reactions with ozone are relatively scarce, but available evidence points to oxygen transfer reactions as the dominant pathway, with sulfoxides being the most commonly-reported product functional groups (reaction type (iv) in Scheme 1). Ozonation of methionine was found to convert the thioether to the corresponding sulfoxide as the quantitative product (Muñoz et al., 2001). Ozonation of thioglycolic acid was reported to first lead to a dimerization to the corresponding thioether, thiodiglycolic acid, although no mechanism was proposed (Gilbert and Hoffmann-Glewe, 1990). This thioether was then reported to undergo a series of further ozonation reactions, first to the sulfoxide, then the corresponding sulfone, then to the sulfonic acid. Finally at high pH, fragmentation and further oxidation produced sulfate and oxalic acid (Gilbert and Hoffmann-Glewe, 1990). Because no •OH scavenger was used, involvement of •OH in the fragmentation reaction seems likely. The thioether of penicillin G was reported to be ozonated quantitatively to the corresponding sulfoxide, while for cephalexin the Criegee product is also observed from alkene scission in addition to oxidation of the thioether (Dodd et al., 2010; von Sonntag and von Gunten, 2012).

Ozonation of reduced sulfur seems to occur generally via stepwise oxygen transfer reactions, increasing the oxidation state by +2 at each step (Scheme 1 (iv)). However, it is currently unknown why some reduced sulfur compounds appear to stop at the sulfoxide as a stable product, while others proceed further in the presence of ozone to the

sulfone, sulfonic acid, and possibly sulfate. In experiments with •OH scavenging, direct ozone oxidation beyond sulfones (to sulfonic acids and sulfate) has not yet been conclusively established. The role of ozone versus •OH in breaking C-S bonds to fragment sulfones is also unclear at present, however, •OH involvement seems likely, as sulfones have no obvious available sites for ozone reactions.

4.8. Other functional groups

While the majority of research on ozonation of organic compounds has focused on electron rich moieties such as olefins, activated aromatic compounds, reduced nitrogen and reduced sulfur, ozone may attack other functional groups as well. Comparatively less is known about these reactions, but ozone has been shown to oxidize carbanions produced by the deprotonation of relatively strong carbon acids, to react fast with a β-diketone, and to directly functionalize certain carbon-hydrogen bonds by hydride transfer or other mechanisms.

4.8.1. Carbanions

Despite a lack of obviously oxidizable functional groups (i.e., no carbon-carbon double bonds, no activated aromatic moieties, no lone pairs on N or S), some alkyl compounds with electron-withdrawing substituents have been observed to react with ozone. However, these reactions are typically slow and under realistic ozonation conditions, the reactions with •OH will dominate (Fig. 5).

Nitroethane was reported to have a $k_{O3,app}$ of 3.4 $M^{-1}s^{-1}$ at pH 7 (Lim et al., 2019). Ozonation of the amino acids serine (Le Lacheur and Glaze, 1996) and glycine (Berger et al., 1999; de Vera et al., 2017; McCurry et al., 2016) and other amino acids and amines (Essaïed et al., 2022), produces nitrate upon exposure to excess ozone, potentially implicating further oxidation of an oxime (de Vera et al., 2017; Lim et al., 2019) or nitro intermediate (McCurry et al., 2016), the latter of which lacking any clear ozone attack sites.

One explanation for these reactions is an ozone attack of a carbanion conjugate base of electron-deficient structures such as nitroalkanes (pK_a < 14) (Anslyn and Dougherty, 2006). Aqueous oxidation of carbanions has been reported for chlorine (Orvik, 1980), and has been proposed to explain halonitromethane formation from nitromethane (McCurry et al., 2016; Orvik, 1980; Shi and McCurry, 2020), and halonitroalkane formation from the ε-nitro analogue of lysine during chlorination (McCurry et al., 2016). Less is known about carbanion reactions with ozone, but carbanion intermediates have been proposed in the synthesis literature as sites for electrophilic ozone attack. The carbanion resonance structure of nitrones was invoked to explain electrophilic attack of ozone on nitrone carbon (Erickson and Myszkiewicz, 1965), leading to aldehydes and *C*-nitroso compounds. Ozone reactions with deprotonated secondary nitro compounds to ketones were rationalized by invoking a nitronate structure (McMurry et al., 1974), which is in resonance with the corresponding nitroalkyl anion (Scheme 7). Deprotonation of a malonate derivative to the corresponding carbanion and subsequent carbanion oxidation was proposed to explain the hydroxylation of the central (acidic) carbon by ozone (White and Egger, 1984).

Kinetic data on carbanion oxidation are scarce. Based on reported *k* for the reaction with chlorine, the deprotonation of nitromethane (pK_a = 10.2) to nitromethyl anion is the rate-limiting step below pH ~11.5, rather than oxidation of the corresponding carbanion (Orvik, 1980). It is unclear why deprotonation is the rate limiting step during neutral oxidation of nitromethane, in contrast to other weak acids in which the conjugate base is more reactive (e.g., phenol), for which the reaction can be successfully modeled assuming base in equilibrium with acid. Regardless, it appears likely that deprotonation of nitromethane will also be rate-limiting at neutral pH for the reaction with ozone, given that ozone reactions generally proceed with higher k_{O3} than reactions with chlorine (Deborde and von Gunten, 2008; von Gunten, 2003b). The species-specific second order rate constant for HOCl reacting with the nitromethyl anion was reported to be 9.5 × 10^3 $M^{-1}s^{-1}$ (Orvik, 1980), which is likely a lower bound for its reaction rate constant with ozone. To date, the only reported k_{O3} for carbanions are for nitroethane ($k_{O3,app}$ = 3.4 $M^{-1}s^{-1}$ at pH 7; (Lim et al., 2019)) and malonate (k_{O3} = 7 ± 2 $M^{-1}s^{-1}$; (Hoigné and Bader, 1983a)), wherefore determining structure-activity relationships is not possible. However, it is likely that as with phenols/phenolates or amines, carbanions and their conjugate acids will be subject to a tradeoff, in which increasing electron-withdrawing substituents will decrease the pK_a and shift speciation from the unreactive neutral acid to the reactive base, while also decreasing electron density at the nucleophilic site (Scheme S1, SI). To date, the net effect of these competing phenomena is not clear and should be investigated further. However, in each of these pathways, ozone would be competing against •OH for reactive sites, and ozone reactions will rarely be more important than •OH reactions, because at R_{ct} values typical of water and wastewater (10^{-8} – 10^{-9}) (von Sonntag and von Gunten, 2012), ozone reactions with an apparent second-order rate constant below ~5 – 50 $M^{-1}s^{-1}$ will be less important than •OH reactions with the same compound (Fig. 5).

4.8.2. β-Diketones

Despite the presence of electron-withdrawing carbonyl groups, simple β-diketones (e.g., acetylacetone, dimedone) exhibit generally high reactivities towards various oxidants such as chlorine, chlorine dioxide, and permanganate (Deborde and von Gunten, 2008; Hoigné and Bader, 1994; Jáky et al., 2006). Acetylacetone shows very high reactivity towards ozone with $k_{O3,app,pH7}$ = 5.1 × 10^5 $M^{-1}s^{-1}$ (Houska et al., 2021). The reason for the unusually high reactivity for β-diketones is not entirely clear. Like the nitroalkanes discussed in the previous

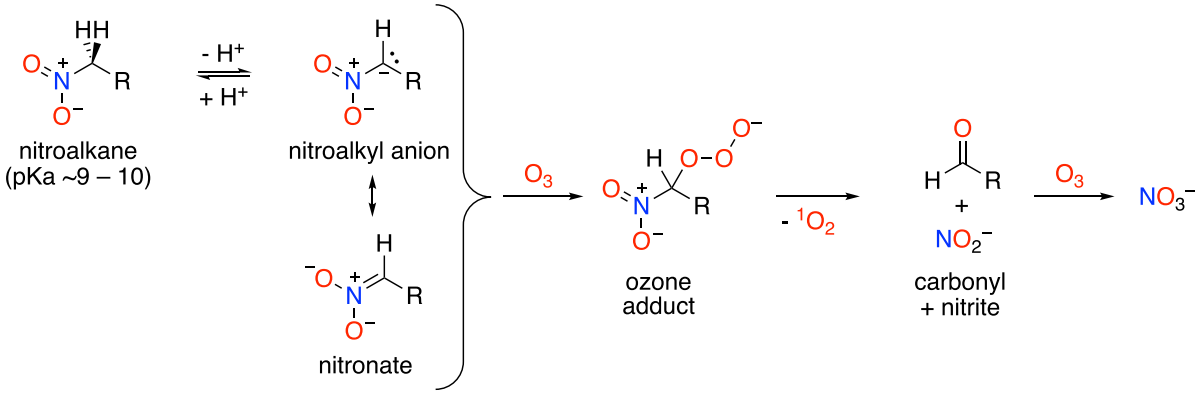

Scheme 7. Potential pathway for the formation of nitrate from the ozonation of nitroalkanes.

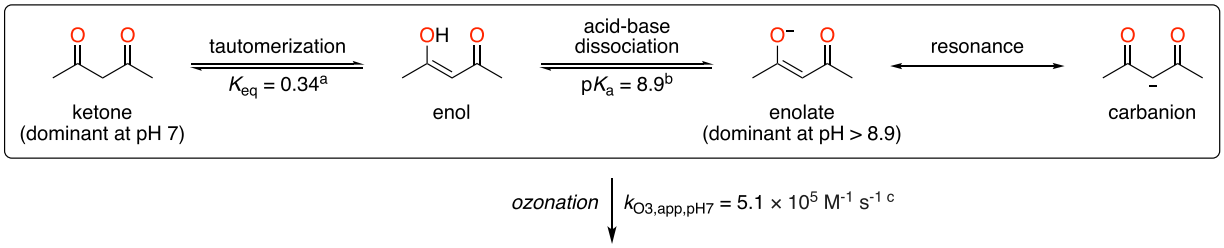

Scheme 8. Different forms of acetylacetone by tautomerization, acid-base dissociation, and resonance, and the reported $k_{O3,app,pH7}$ for acetylacetone. References are [a](Moriyasu et al., 1986), [b](Eidinoff, 1945), [c](Houska et al., 2021).

section, β-diketones are present in different forms in aqueous solution due to tautomerization (keto and enol form) and dissociation (enol and enolate), with the enolate featuring a carbanion resonance structure (Scheme 8). The relative contributions of these different forms to ozone reactivity should be carefully assessed. Because β-diketones are common moieties of DOM, understanding the kinetics and mechanisms of their reactions with ozone is highly relevant to predict potential oxidation byproducts and warrants further investigation.

4.8.3. Hydrocarbons

For compounds with no ozone-reactive moieties, limited ozone reactivity has still been observed at the site of carbon-hydrogen bonds. Four possible mechanisms have been proposed, including H-abstraction, direct electron transfer, hydride transfer, and insertion (von Sonntag and von Gunten, 2012). k_{O3} spanning seven orders of magnitude ($\leq$ 50 M^{-1}s^{-1}), have been reported for more than 25 of such compounds (von Sonntag and von Gunten, 2012). The most ozone-reactive compound in this category, formate, has been reported to have a species-specific k_{O3} of 46 ± 5 M^{-1}s^{-1} when measured with careful $^{\bullet}$OH scavenging (Reisz et al., 2014). This reaction proceeds primarily through hydride transfer, with some contribution from H-abstraction, leading to CO_2 as the primary product. However, the reason for the unusually high k_{O3} for a hydrocarbon is still unknown (Reisz et al., 2014). Ozonation of *tert*-butanol (k_{O3}= 10^{-3} M^{-1}s^{-1}; von Sonntag and von Gunten 2012) was found to proceed to butan-2-one, via hydride transfer from one of the methyl groups, followed by methyl transfer to the carbanion and oxygen deprotonation (Reisz et al., 2014). Likewise, hydride transfer was found to be the dominant mechanism of 2-propanol (k_{O3}= 2.7 ± 0.1 M^{-1}s^{-1}) (Reisz et al., 2018) and 1-propanol (k_{O3}= 0.64 ± 0.02 M^{-1}s^{-1}) (Reisz et al., 2019) oxidation, leading to acetone and propionaldehyde acid as the major products, respectively. While direct C–H bond oxidation with ozone is possible, because the corresponding k_{O3} are low, under most circumstances relevant to water treatment, $^{\bullet}$OH reactions will dominate transformation of these compounds (Fig. 5).

4.9. Compounds with multiple ozone reaction sites

The ozone-reactive moieties, discussed individually throughout Section 4, can be present simultaneously within a molecule. One way to determine the main reaction site is by studying the moiety-specific reactivity with model compounds representing key substructures of a target compound. This approach was applied to study the reaction of ozone with compounds with complex structures such as pharmaceuticals (Dodd et al., 2006; Huber et al., 2004; Jeon et al., 2016) and cyanotoxins (Onstad et al., 2007).

If a compound contains multiple ozone-reactive moieties including ionizable groups such as aliphatic amines or phenols, the reactivity of the main reaction site alters as a function of the pH. For example, ozone attacks mainly at an amine moiety at a pH higher than the protonated amine's pK_a, i.e., where the neutral amine is dominant. At pH < pK_a, the ozone reactivity of the amine moiety significantly decreases due to protonation (Section 4.5). In this case, the main reaction site is shifted to another moiety that is not affected by pH (e.g., olefin).

An example is tamoxifen (contains a tertiary amine and an olefin) of which species-specific k_{O3} for the neutral and the protonated forms are 3.2 × 10^8 M^{-1}s^{-1} and 1.6 × 10^4 M^{-1}s^{-1}, respectively (Knoop et al., 2018). In contrast to the typical k_{O3} of < 0.1 M^{-1}s^{-1} for the protonated form of simple aliphatic amines (von Sonntag and von Gunten, 2012), the k_{O3} of the protonated tamoxifen is still very high, indicating the shift of the reaction site from the amine moiety to the olefin, the second reactive moiety. In this sense, the species-specific k_{O3} for the neutral and protonated forms of tamoxifen can be considered the moiety-specific k_{O3} for the amine and olefin moieties, respectively.

By combining the moiety-specific k_{O3} of the two reaction sites (amine and olefin) with the degree of protonation of the amine moiety, the fraction of ozone attacking at the amine moiety of tamoxifen at a specific pH can be expressed as (Eq. 6):

$$\textit{fraction of ozone attack at amine} = \frac{\left(k_{O3,amine-N}\ (1-\alpha) + k_{O3,amine-NH+}(\alpha)\right)}{\left(k_{O3,\ amine-N}\ (1-\alpha) + k_{O3,amine-NH+}\ (\alpha) + k_{O3,olefin}\right)} \quad (6)$$

where $\alpha = \frac{[H^+]}{([H^+]+K_a)}$ is the degree of protonation of the amine moiety of tamoxifen ($R_3NH^+ \leftrightarrow R_3N$) based on the reported pK_a = 9.49 (Knoop et al., 2018). $k_{O3,amine\text{-}N}$ is the moiety-specific k_{O3} for the amine moiety (neutral form), i.e., 3.2 × 10^8 M^{-1}s^{-1} (Knoop et al., 2018). $k_{O3,olefin}$ is the moiety-specific k_{O3} for the olefin moiety, approximated by the reported species-specific k_{O3} for the protonated tamoxifen, i.e., 1.6 × 10^4 M^{-1}s^{-1} (Knoop et al., 2018). $k_{O3,amine\text{-}NH+}$ is the moiety-specific k_{O3} for the amine moiety as the protonated form, arbitrarily given 0.1 M^{-1}s^{-1} according to the typical k_{O3} for protonated amines.

Fig. 14 shows the calculated % ozone attack at the amine moiety for selected pharmaceuticals containing multiple reaction sites based on Eq. 6, by extending the approximation to other secondary reaction sites (aromatic and sulfur moieties).

Depending on the difference of moiety-specific k_{O3}, the main reaction site at a specific pH can differ significantly (Fig. 14). For tamoxifen, the moiety-specific k_{O3} for the neutral tertiary amine is about four orders of magnitude higher than for the olefin (3.2 × 10^8 M^{-1}s^{-1} and 1.6 × 10^4 M^{-1}s^{-1}, respectively (Knoop et al., 2018)). This results in 98 % of ozone attack at the tertiary amine at pH 7, despite the predominance of the protonated form of the amine (tamoxifen pK_a = 9.5). In contrast, for nortriptyline with a comparable pK_a of 10.2, the difference in the moiety-specific k_{O3} is smaller (k_{O3} = 4.3 × 10^5 M^{-1}s^{-1} for the neutral secondary amine and 2.1 × 10^3 M^{-1}s^{-1} for the olefin (Benitez et al., 2013)). As a consequence, at pH 7, nortriptyline is oxidized by ozone mostly at the olefin moiety.

The pK_a of amine moieties also plays a role in determining the main reaction site for a given pH. The k_{O3} of the thiazine moiety of cephalexin is as high as the k_{O3} of the primary amine moiety (8.2 × 10^4 M^{-1}s^{-1} and 9.3 × 10^4 M^{-1}s^{-1}, respectively (Dodd et al., 2006); see the structure in Figure S1, SI). At pH 7, cephalexin is attacked by ozone at the amine moiety with a moderate proportion (33%), because of a pK_a of 7.1, more acidic than typical primary amines due to the presence of a carbonyl as a neighboring group. At higher pH, the thiazine and the amino groups

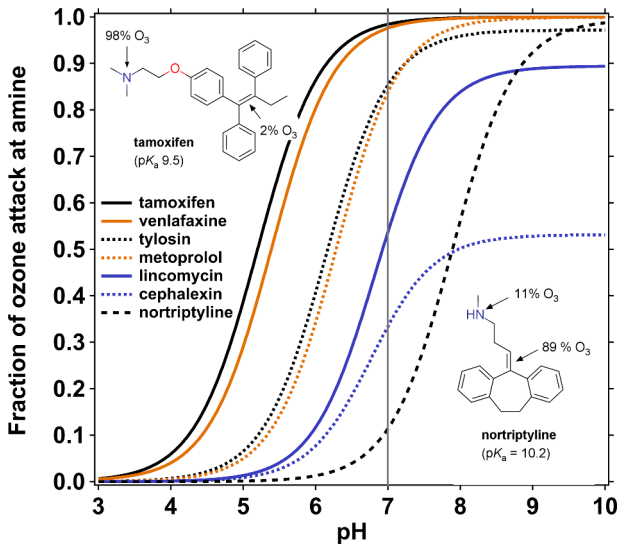

Fig. 14. Pharmaceutical compounds with multiple reaction sites for ozone: pH-dependent fraction of ozone attack at the amine moiety. The compounds containing amine and olefin moieties are shown as black lines, amine and aromatic moieties are shown as orange lines, and amine and sulfur moieties are shown as blue lines. Tamoxifen and nortriptyline are highlighted as examples for pH 7. The moiety-specific second-order rate constants and pK_a values used for the calculation for all pharmaceuticals are presented in Figure S1 (SI).

contribute similarly to the oxidation of cephalexin by ozone, due to the similar k_{O3} for the two moieties.

Many heterocyclic moieties contain an ionizable nitrogen as well as a carbon-carbon double bond within a cyclic structure. Therefore, identifying the main ozone reaction site within a heterocyclic moiety can be challenging. Regioselectivity prediction by quantum chemical computations could be especially useful in these cases. Computed molecular descriptors such as average local ionization energies, orbital energies, and bond dissociation energies can describe where the ozone reaction would preferentially take place within a molecule (Tentscher et al., 2019) and have been applied recently in an ozone pathway prediction system (Lee et al., 2017a) and for studying the ozone reaction for selected heterocyclic compounds (Chen et al., 2019; Yao et al., 2020).

5. Kinetics of the reaction of ozone with macromolecules: Antibiotic resistance gene (ARG) inactivation and DNA oxidation

Some macromolecules (e.g., DOM) are highly heterogeneous and therefore their reactions with ozone are largely assessed in terms of the effect on bulk parameters (e.g., specific UV absorbance, EDC, etc.) or elemental ratios (see Section 3.2). However, because biomolecules (e.g., proteins, nucleic acids) are often macromolecules consisting of known sequences of discrete subunits (e.g., amino acids, nucleobases), they present an opportunity to predict the kinetics of macromolecule in ozonation as the aggregation of reactions with individual subunits, for which reactivities with ozone are generally known. One example is the reaction of ozone with antibiotic resistance genes, discussed below.

5.1. Ozonation of Antibiotic Resistant Bacteria

Concerns about the potential for wastewater treatment facilities to act as breeding grounds for antibiotic resistant bacteria (Dodd, 2012; Pruden et al., 2013; Rizzo et al., 2013; Zarei-Baygi et al., 2019) have led to interest in the use of ozone, and other disinfectants, for antibiotic resistance control. Antibiotic resistance inactivation presents a special challenge for chemical disinfectants. For ordinary microorganisms the outcome is agnostic of the means of action (i.e., inactivating a bacterium by oxidizing its cell membrane proteins and/or its DNA both achieve the same outcome). However, for antibiotic resistant bacteria, inactivating the organism does not guarantee loss of the potential for antibiotic resistance, as multiple mechanisms of antibiotic resistance gene (ARG) horizontal transfer exist, including uptake by non-resistant organisms of ARGs from dead cells, particularly if their cell membranes are lysed during disinfection (Dodd, 2012). Additionally, several studies have indicated the possibility for antibiotic resistance 'rebound' after disinfection, in which the absolute and/or relative abundance of antibiotic resistant bacteria (ARB) increases after disinfection (Czekalski et al., 2016; Iakovides et al., 2019). Finally, the disinfection process may select for ARBs over non-resistant populations (Alexander et al., 2016). Therefore, in addition to the interest in ARB inactivation, attention has more recently been focused on inactivation of the ARGs themselves, which is the primary subject of this critical review.

As with most microorganisms, ozone rapidly inactivates antibiotic resistant bacteria (Pak et al., 2016), achieving for instance 3 – 4-log inactivation of sulfonamide-resistant *E. coli* J53 after application of 0.08 mg/L ozone in buffered deionized water (Czekalski et al., 2016). ARB inactivation in secondary wastewater effluent is also highly effective. ~2-log inactivation of trimethoprim- or sulfamethoxazole-resistant *E. coli* was achieved with specific ozone doses as low as 0.25 mg O_3/mg DOC in secondary effluent, and was unaffected by the addition of hydrogen peroxide (Iakovides et al., 2019).

5.2. Ozonation of Antibiotic Resistance Genes

Inactivation of ARGs by ozone has been widely measured, including in clean systems (Czekalski et al., 2016; He et al., 2019), secondary wastewater effluent (Alexander et al., 2016; Ben et al., 2017; Czekalski et al., 2016; Iakovides et al., 2019; Lamba and Ahammad, 2017; Zheng et al., 2017; Zhuang et al., 2015), sludge (Pei et al., 2016), and cow manure (Cengiz et al., 2010). Early quantification of ARG depletion by quantitative polymerase chain reaction in clean systems reported ~1.5-log abatement of the ARG *sul1* with an ozone dose of 0.2 mg/L applied to ARG-containing *E. coli* at a contact time of >30 minutes (i.e., complete ozone depletion) in buffered ultrapurified water at pH 7.4 (Czekalski et al., 2016). Ozonation conducted at rapid time scales with quench-flow kinetics revealed that ARG inactivation happens subsequent to cell inactivation (Czekalski et al., 2016), potentially supporting the hypothesis that cell membranes must first be ruptured to expose ARGs to bulk solution before they can be inactivated (Dodd, 2012). However, previous studies on bacterial inactivation by ozone found nearly complete inactivation at very low specific ozone doses (0.2 mg O_3/mg DOC for 15 s) occurring prior to cell membrane destruction (Ramseier et al., 2011b), leaving open the possibility of ozone diffusion into the cell leading to ARG oxidation. A study aiming to measure the ozonation kinetics of ARGs themselves ozonated extracellular DNA extracted from an antibiotic-resistant strain of *Bacillus subtilis* in buffered deionized water. The k_{O3} of four amplicons (266 – 1017 base pairs) of the ARG *blt* were measured to be (1.8 – 6.9) × 10^4 $M^{-1}s^{-1}$, corresponding to an average per-base k_{O3} of 65 $M^{-1}s^{-1}$ (He et al., 2019). Based on the average of the k_{O3} of the four amplicons, a pseudo-first order rate constant with 0.04 mM (2 mg/L) ozone would be 2.1 s^{-1}, corresponding to a half-life of 0.33 s.

Previously, the k_{O3} of calf DNA oxidation was measured and the per-base k_{O3} was 410 $M^{-1}s^{-1}$ (Theruvathu et al., 2001). The rate of DNA oxidation by ozone was slower than would be predicted if DNA strands reacted equivalently to a mixture of their component nucleobases. If it is assumed that a reaction between ozone and any of the nucleobases on a strand of DNA is sufficient to degrade it (measured by PCR signal), then degradation kinetics should be controlled by the sum of the reactions between each of its nucleobases and ozone as follows (Eqs. 7 and 8 explained in Text S1, SI):

$$\frac{d[DNA]}{dt} = -[DNA][O_3]k_{O3,DNA} \quad (7)$$

$$k_{O3,DNA} = mk_A + nk_G + qk_C + pk_T \quad (8)$$

where m, n, q, and p are the sums of adenine (A), guanine (G), cytosine (C), and thymine (T) bases per strand of DNA, and k_A, k_G, k_C, and k_T, are the respective second-order rate constants for their reactions with ozone.

Before calculating the overall predicted rate of DNA oxidation, the acid-base speciation of nucleobases must be accounted for by converting species-specific k_{O3} to pH-dependent $k_{O3,\ app}$ for each nucleobase, as shown in Table S7 (SI). Computing this overall predicted k_{O3} from the shortest (266 bp) amplicon in (He et al., 2019), leads to an overall expected k_{O3} for the reaction between ozone and the amplicon of 6.49×10^6 $M^{-1}s^{-1}$ and a specific (per nucleobase) k_{O3} of 2.40×10^4 $M^{-1}s^{-1}$ (Table S8, SI), approximately 370 times higher than that observed by (He et al., 2019), and 59 times higher than observed with calf DNA (Theruvathu et al., 2001).

The reasons for this discrepancy between the predicted and observed k_{O3} for DNA in clean systems are not immediately clear, but several possibilities exist. One option is analytical artifacts: DNA abatement during disinfection is commonly monitored by qPCR (McKinney and Pruden, 2012; Yoon et al., 2017), but a single modification at certain sites may be insufficient to eliminate or drastically reduce amplification efficiency (Sikorsky et al., 2004; 2007), leading to underprediction of the extent of DNA damage. Additionally, different amplification efficiencies of damaged DNA are observed when using different polymerase reagent kits (Hajibabaei et al., 2005), and certain polymerase reagents are specifically designed to amplify damaged DNA (Robertson et al., 2014). Another possibility is tertiary structure leading to reduced reactivity due to steric shielding of ozone targets from the bulk solution, as is observed during protein oxidation, in which some oxidizable residues may be buried in the hydrophobic core of the protein and unavailable for oxidation reactions (Choe et al., 2015; Jensen et al., 2012; Lundeen and McNeill, 2013; Sivey et al., 2013). Finally, one possibility to explain the dramatically lower k_{O3} observed for DNA than would be predicted based on the sum of the constituent nucleobases is an increase in the pK_a of nucleobases, due to a combination of hydrogen bonding between bases and pi-stacking interactions. These interactions have been reported to increase the pK_a of protonated nucleobases by up to 3–4 orders of magnitude, which in some cases (A, C), could convert the majority of the bases from their neutral or negatively-charged reactive forms to their charged forms, which are nearly inert (Tang et al., 2007; Wilcox et al., 2011). However, performing the same calculation as in Table S7 (SI) but assuming that the pK_a of all nucleobases is 1–4 units higher produces only a modest decrease in calculated $k_{O3,\ app}$. Therefore, this pK_a shift alone is unlikely to explain the discrepancy between calculated and observed k_{O3} of DNA ozonation. The reason that a dramatic pK_a shift fails to produce a major change in outcome is likely that overall reactivity appears dominated by thymine (Table S7, SI), and the protonated form of thymine is still quite reactive with ozone ($k_{O3} = 4.2 \times 10^4$ $M^{-1}s^{-1}$).

In contrast to ozonation of ARBs in clean systems or of extracted DNA, inactivation of antibiotic resistance genes in real wastewater effluent and sludge is relatively ineffective (Alexander et al., 2016; Ben et al., 2017; Cengiz et al., 2010; Iakovides et al., 2019; Lamba and Ahammad, 2017; Pei et al., 2016; Zheng et al., 2017; Zhuang et al., 2015). ARB and ARG inactivation generally require comparable doses as ~80% abatement of Group I and Group II micropollutants identified by (Lee et al., 2013) as being highly ($k_{O3,app,pH7} > 10^5$ $M^{-1}s^{-1}$) and moderately ($10\ M^{-1}s^{-1} < k_{O3,app,pH7} < 10^5\ M^{-1}s^{-1}$) reactive with ozone (Fig. 15). In Fig. 15, Group II is further divided into Group IIA ($10^3\ M^{-1}s^{-1} < k_{O3,app,pH7} < 10^5\ M^{-1}s^{-1}$) and Group IIB ($10\ M^{-1}s^{-1} < k_{O3,app,pH7} < 10^3\ M^{-1}s^{-1}$) using micropollutant abatement data from Bourgin et al. (2018). Ozone doses are often constrained in practice by bromate formation, which strongly depends on the specific ozone doses (Soltermann et al., 2017). Specific ozone doses shown to achieve 2-log inactivation of ARB (~0.4 mg O_3/mg DOC) (Czekalski et al., 2016) are generally at or below the threshold for moderate bromate formation (Soltermann et al., 2017), while specific ozone doses to achieve 2-log abatement of ARGs (Alexander et al., 2016; Czekalski et al., 2016) are in the ozone dose range with moderate to high bromate yields (Fig. 15).

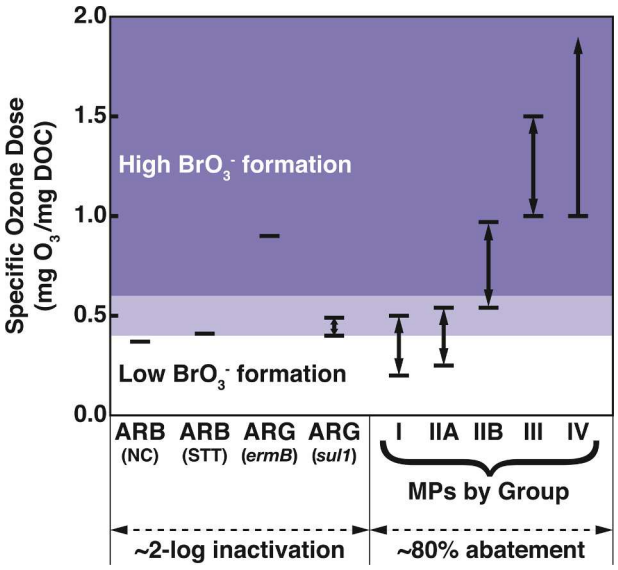

Fig. 15. Specific ozone doses in wastewater effluent required for 2-log inactivation of ARBs and ARGs, and specific ozone dose ranges required for ~80% abatement of the four categories of micropollutants (MPs) discussed in (Lee et al., 2013), arranged from easiest to most difficult to abate. Groupings are based on the apparent second-order rate constants for the reactions with ozone and •OH at pH 7 (Group I: $k_{O3,app,pH7} > 10^5$ $M^{-1}s^{-1}$; Group IIA: $10^3 < k_{O3,app,pH7} < 10^5$ $M^{-1}s^{-1}$; Group IIB: $10 < k_{O3,app,pH7} < 10^3$ $M^{-1}s^{-1}$; Group III: $k_{O3,app,pH7} < 10$ $M^{-1}s^{-1}$ and $k_{•OH} > 5 \times 10^9$ $M^{-1}s^{-1}$; Group IV: 10^9 $M^{-1}s^{-1} < k_{•OH} < 5 \times 10^9$ $M^{-1}s^{-1}$). NC refers to norfloxacin/ceftazidime-resistant and STT refers to sulfamethoxazole/trimethoprim/tetracycline-resistant bacteria present in the wastewater effluent prior to ozonation. *ermB* and *sul1* are the names of eritromycine and sulfonamide antibiotic resistance genes measured in Czekalski et al., (2016). The light blue shaded region refers to specific dose range associated with moderate bromate yields from bromide (~2 – 3%), while the dark blue range is associated with high bromate yields (~3 – 15%).

Reconciling the paradox of effective ARG inactivation in clean systems or with extracted DNA with relatively ineffective inactivation in practical systems will require further studies. Possible contributors to this discrepancy include the location of the ARGs (chromosomal vs. plasmid, intracellular vs. extracellular) (Dodd, 2012), and issues potentially related to the lower reactivity of DNA than one would predict as discussed above.

6. Conclusions

Due to a significant knowledge gain in the ozone chemistry in aqueous solution and shifts in application of ozonation processes, this critical review highlights the most important aspects of the ozone chemistry and applications as follows:

- A paradigm shift in the application of ozone for impaired water qualities (enhanced wastewater treatment, water reuse) needs a new focus on higher levels and different types of dissolved organic matter (DOM) than for typical drinking water applications. Furthermore, bromate formation has to be carefully monitored due to sometimes higher and variable levels of bromide.
- Several bulk parameters (UV absorbance, electron donating capacity) and high resolution mass spectrometry can be applied to elucidate changes in DOM properties and/or used as proxies to monitor and control ozonation processes for micropollutant abatement.

- An updated compilation of the kinetics and mechanisms of the reactions of the main reactive functional groups (olefins, activated aromatic compounds, nitrogen-containing compounds, sulfur-containing compounds) and relatively less known functional groups (carbanions, hydrocarbons, β-diketones) with ozone is provided. The kinetics of ozone reactions have been used to assess the main reaction site of the organic compounds containing multiple reactive functional groups to anticipate the formation of transformation products.
- The inactivation of antibiotic resistant bacteria and antibiotic resistance genes by ozone are discussed in comparison to the reactivity of DNA and a paradox of different reaction kinetics is highlighted.
- The consequences of the formation of oxidation byproducts from DOM and transformation products from micropollutants are not discussed in this review. However, this compilation of ozone reaction mechanisms will be the basis to predict oxidation byproducts and transformation products and assess the (eco)toxicological consequences and their potential biodegradability.

Declaration of Competing interest

The authors declare that they have no known competing financial interests or personal relationships that could have appeared to influence the work reported in this paper.

Acknowledgements

We acknowledge support from the Swiss National Science Foundation (SNSF) for financial support (project N° 200021-181975) and the U. S. National Science Foundation (CBET-1944810). We thank Keith Reber of Towson University for a helpful suggestion to explain the reactivity difference between isomers of 1,2-dichloroethene and Peter Tentscher for quantum chemical computations. This review was initiated as a lockdown project during the Covid-19 pandemic.

Supplementary materials

Supplementary material associated with this article can be found, in the online version, at doi:10.1016/j.watres.2022.118053.

References

Acero, J.L., von Gunten, U., 2001. Characterization of oxidation processes: Ozonation and the AOP O_3/H_2O_2. J. Amer. Water Works Assoc. 93 (10), 90–100.
Adams, C.D., Cozzens, R.A., Kim, B.J., 1997. Effects of ozonation on the biodegradability of substituted phenols. Water Research 31 (10), 2655–2663.
Aeschbacher, M., Sander, M., Schwarzenbach, R.P., 2010. Novel Electrochemical Approach to Assess the Redox Properties of Humic Substances. Environmental Science & Technology 44 (1), 87–93.
Agopovich, J.W., Gillies, C.W., 1980. The ozonolysis of trifluoroethylene, 1,1-difluoroethylene, and perfluoroethylene. Epoxide and ozonide formation. Journal of the American Chemical Society 102 (25), 7572–7574.
Aieta, E.M., Reagan, K.M., Lang, J.S., McReynolds, L., Kang, J.-W., Glaze, W.H., 1988. Advanced Oxidation Processes for Treating Groundwater Contaminated With TCE and PCE: Pilot-Scale Evaluations. Journal - AWWA 80 (5), 64–72.
Alexander, J., Knopp, G., Dotsch, A., Wieland, A., Schwartz, T., 2016. Ozone treatment of conditioned wastewater selects antibiotic resistance genes, opportunistic bacteria, and induce strong population shifts. Science of the Total Environment 559, 103–112.
Allard, S., Nottle, C.E., Chan, A., Joll, C., von Gunten, U., 2013. Ozonation of iodide-containing waters: Selective oxidation of iodide to iodate with simultaneous minimization of bromate and I-THMs. Water Research 47 (6), 1953–1960.
Andersson, A., Lavonen, E., Harir, M., Gonsior, M., Hertkorn, N., Schmitt-Kopplin, P., Kylin, H., Bastviken, D, 2020. Selective removal of natural organic matter during drinking water production changes the composition of disinfection by-products. Environmental Science-Water Research & Technology 6 (3), 779–794.
Andreozzi, R., Insola, A., Caprio, V., Damore, M.G., 1991. Ozonation of Pyridine in Aqueous-Solution - Mechanistic and Kinetic Aspects. Water Research 25 (6), 655–659.
Andreozzi, R., Caprio, V., Damore, M.G., Insola, A., 1992a. Reactivity Towards Ozone of 2-Hydroxypyridine in Aqueous-Solution. Ozone-Science & Engineering 14 (2), 177–184.
Andreozzi, R., Insola, A., Caprio, V., Damore, M.G., 1992b. Quinoline Ozonation in Aqueous-Solution. Water Research 26 (5), 639–643.
Andrzejewski, P., Kasprzyk-Hordern, B., Nawrocki, J., 2008. N-nitrosodimethylamine (NDMA) formation during ozonation of dimethylamine-containing waters. Water Research 42 (4-5), 863–870.
Angeles, L.F., Mullen, R.A., Huang, I.J., Wilson, C., Khunjar, W., Sirotkin, H.I., McElroy, A.E., Aga, D.S., 2020. Assessing pharmaceutical removal and reduction in toxicity provided by advanced wastewater treatment systems. Environmental Science: Water Research & Technology 6 (1), 62–77.
Anslyn, E.V., Dougherty, D.A., 2006. Modern physical organic chemistry. University Science, Sausalito, CA.
Bahr, C., Schumacher, J., Ernst, M., Luck, F., Heinzmann, B., Jekel, M., 2007. SUVA as control parameter for the effective ozonation of organic pollutants in secondary effluent. Water Science and Technology 55 (12), 267–274.
Bailey, P.S., Lane, A.G., 1967. Competition between complete and partial cleavage during ozonation of olefins. Journal of the American Chemical Society 89 (17), 4473–4479.
Beggs, K.M.H., Billica, J.A., Korak, J.A., Rosario-Ortiz, F.L., McKnight, D.M., Summers, R. S., 2013. Spectral evaluation of watershed DOM and DBP precursors. Journal American Water Works Association 105 (4), 49–50.
Ben, W.W., Wang, J., Cao, R.K., Yang, M., Zhang, Y., Qiang, Z.M., 2017. Distribution of antibiotic resistance in the effluents of ten municipal wastewater treatment plants in China and the effect of treatment processes. Chemosphere 172, 392–398.
Benitez, F.J., Acero, J.L., Garcia-Reyes, J.F., Real, F.J., Roldan, G., Rodriguez, E., Molina-Díaz, A., 2013. Determination of the Reaction Rate Constants and Decomposition Mechanisms of Ozone with Two Model Emerging Contaminants: DEET and Nortriptyline. Industrial & Engineering Chemistry Research 52 (48), 17064–17073.
Benner, J., Ternes, T.A., 2009a. Ozonation of Propranolol: Formation of Oxidation Products. Environmental Science & Technology 43 (13), 5086–5093.
Benner, J., Ternes, T.A., 2009b. Ozonation of Metoprolol: Elucidation of Oxidation Pathways and Major Oxidation Products. Environmental Science & Technology 43 (14), 5472–5480.
Berger, P., Karpel Vel Leitner, N., Dore, M., Legube, B, 1999. Ozone and Hydroxyl Radicals Induced Oxidation of Glycine. Water Research 33, 433–441.
Bichsel, Y., von Gunten, U., 1999. Oxidation of iodide and hypoiodous acid in the disinfection of natural waters. Environ. Sci. Technol. 33, 4040–4045.
Bollmann, A.F., Seitz, W., Prasse, C., Lucke, T., Schulz, W., Ternes, T., 2016. Occurrence and fate of amisulpride, sulpiride, and lamotrigine in municipal wastewater treatment plants with biological treatment and ozonation. Journal of Hazardous Materials 320, 204–215.
Borowska, E., Bourgin, M., Hollender, J., Kienle, C., McArdell, C.S., von Gunten, U., 2016. Oxidation of cetirizine, fexofenadine and hydrochlorothiazide during ozonation: Kinetics and formation of transformation products. Water Research 94, 350–362.
Bourgin, M., Beck, B., Boehler, M., Borowska, E., Fleiner, J., Salhi, E., Teichler, R., von Gunten, U., Siegrist, H., McArdell, C.S., 2018. Evaluation of a full-scale wastewater treatment plant upgraded with ozonation and biological post-treatments: Abatement of micropollutants, formation of transformation products and oxidation by-products. Water Research 129, 486–498.
Broséus, R., Vincent, S., Aboulfadl, K., Daneshvar, A., Sauve, S., Barbeau, B., Prevost, M., 2009. Ozone oxidation of pharmaceuticals, endocrine disruptors and pesticides during drinking water treatment. Water Research 43 (18), 4707–4717.
Buffle, M.O., Galli, S., von Gunten, U., 2004. Enhanced bromate control during ozonation: The chlorine-ammonia process. Environmental Science & Technology 38 (19), 5187–5195.
Buffle, M.O., Schumacher, J., Meylan, S., Jekel, M., von Gunten, U., 2006a. Ozonation and advanced oxidation of wastewater: Effect of O-3 dose, pH, DOM and HO.-scavengers on ozone decomposition and HO. generation. Ozone-Science & Engineering 28 (4), 247–259.
Buffle, M.O., Schumacher, J., Salhi, E., Jekel, M., von Gunten, U., 2006b. Measurement of the initial phase of ozone decomposition in water and wastewater by means of a continuous quench-flow system: Application to disinfection and pharmaceutical oxidation. Water Research 40 (9), 1884–1894.
Bühler, R.E., Staehelin, J., Hoigné, J., 1984. Ozone Decomposition in Water Studied by Pulse Radiolysis +. HO2/O2- and HO3/O3- as Intermediates. J. Phys. Chem. 88, 2560–2564.
Cengiz, M., Uslu, M.O., Balcioglu, I., 2010. Treatment of E. coli HB101 and the tetM gene by Fenton's reagent and ozone in cow manure. Journal of Environmental Management 91 (12), 2590–2593.
Chan, W.F., Larson, R.A., 1991. Mechanisms and Products of Ozonolysis of Aniline in Aqueous-Solution Containing Nitrite Ion. Water Research 25 (12), 1539–1544.
Chedeville, O., Debacq, M., Porte, C., 2009. Removal of phenolic compounds present in olive mill wastewaters by ozonation. Desalination 249 (2), 865–869.
Chen, S.Y., Blaney, L., Chen, P., Deng, S.S., Hopanna, M., Bao, Y.X., Yu, G., 2019. Ozonation of the 5-fluorouracil anticancer drug and its prodrug capecitabine: Reaction kinetics, oxidation mechanisms, and residual toxicity. Frontiers of Environmental Science & Engineering 13 (4), 59.
Chen, W., Westerhoff, P., Leenheer, J.A., Booksh, K., 2003. Fluorescence excitation - Emission matrix regional integration to quantify spectra for dissolved organic matter. Environmental Science & Technology 37 (24), 5701–5710.
Chen, W.R., Wu, C., Elovitz, M.S., Linden, K.G., Mel Suffet, I.H., 2008. Reactions of thiocarbamate, triazine and urea herbicides, RDX and benzenes on EPA Contaminant Candidate List with ozone and with hydroxyl radicals. Water Res 42 (1-2), 137–144.
Chen, Z., Valentine, R.L., 2008. The Influence of the Pre-Oxidation of Natural Organic Matter on the Formation of N-Nitrosodimethylamine (NDMA). Environmental Science & Technology 42 (14), 5062–5067.

Cheng, Z., Yang, B., Chen, Q., Tan, Y., Gao, X., Yuan, T., Shen, Z., 2018. 2D-QSAR and 3D-QSAR simulations for the reaction rate constants of organic compounds in ozone-hydrogen peroxide oxidation. Chemosphere 212, 828–836.
Choe, J.K., Richards, D.H., Wilson, C.J., Mitch, W.A., 2015. Degradation of Amino Acids and Structure in Model Proteins and Bacteriophage MS2 by Chlorine, Bromine, and Ozone. Environmental Science & Technology 49 (22), 13331–13339.
Chon, K., Lee, Y., Traber, J., von Gunten, U., 2013. Quantification and characterization of dissolved organic nitrogen in wastewater effluents by electrodialysis treatment followed by size-exclusion chromatography with nitrogen detection. Water Research 47 (14), 5381–5391.
Chon, K., Salhi, E., von Gunten, U., 2015. Combination of UV absorbance and electron donating capacity to assess degradation of micropollutants and formation of bromate during ozonation of wastewater effluents. Water Research 81 (0), 388–397.
Chuang, Y.-H., Szczuka, A., Shabani, F., Munoz, J., Aflaki, R., Hammond, S.D., Mitch, W. A., 2019. Pilot-scale comparison of microfiltration/reverse osmosis and ozone/biological activated carbon with UV/hydrogen peroxide or UV/free chlorine AOP treatment for controlling disinfection byproducts during wastewater reuse. Water Research 152, 215–225.
Chys, M., Audenaert, W.T.M., Deniere, E., Mortier, S.T.F.C., Van Langenhove, H., Nopens, I., Demeestere, K., Van Hulle, S.W.H., 2017a. Surrogate-Based Correlation Models in View of Real-Time Control of Ozonation of Secondary Treated Municipal Wastewater—Model Development and Dynamic Validation. Environmental Science & Technology 51 (24), 14233–14243.
Chys, M., Demeestere, K., Ingabire, A.S., Dries, J., Van Langenhove, H., Van Hulle, S.W. H., 2017b. Enhanced treatment of secondary municipal wastewater effluent: comparing (biological) filtration and ozonation in view of micropollutant removal, unselective effluent toxicity, and the potential for real-time control. Water Science and Technology 76 (1), 236–246.
Courbat, R., Ramseier, S., Walther, J.L., Gaille, P., Jordan, R., Kaiser, H.-P., Revelly, P., Stettler, R., von Gunten, U., 1999. Utilisation de l'ozone pour le traitement des eaux potables en Suisse. GWA Gas, Wasser, Abwasser 843–852.
Criegee, R., 1975. Mechanism of Ozonolysis. Angewandte Chemie International Edition in English 14 (11), 745–752.
Crone, B.C., Speth, T.F., Wahman, D.G., Smith, S.J., Abulikemu, G., Kleiner, E.J., Pressman, J.G., 2019. Occurrence of per- and polyfluoroalkyl substances (PFAS) in source water and their treatment in drinking water. Critical Reviews in Environmental Science and Technology 49 (24), 2359–2396.
Czekalski, N., Imminger, S., Salhi, E., Veljkovic, M., Kleffel, K., Drissner, D., Hammes, F., Burgmann, H., von Gunten, U., 2016. Inactivation of Antibiotic Resistant Bacteria and Resistance Genes by Ozone: From Laboratory Experiments to Full-Scale Wastewater Treatment. Environmental Science & Technology 50 (21), 11862–11871.
Dantas, R.F., Canterino, M., Marotta, R., Sans, C., Esplugas, S., Andreozzi, R., 2007. Bezafibrate removal by means of ozonation: Primary intermediates, kinetics, and toxicity assessment. Water Research 41 (12), 2525–2532.
de Vera, G.A., Gernjak, W., Weinberg, H., Farre, M.J., Keller, J., von Gunten, U., 2017. Kinetics and mechanisms of nitrate and ammonium formation during ozonation of dissolved organic nitrogen. Water Research 108, 451–461.
Deborde, M., Rabouan, S., Mazellier, P., Duguet, J.-P., Legube, B., 2008. Oxidation of bisphenol A by ozone in aqueous solution. Water Research 42 (16), 4299–4308.
Deborde, M., von Gunten, U., 2008. Reactions of chlorine with inorganic and organic compounds during water treatment-Kinetics and mechanisms: a critical review. Water Res 42 (1-2), 13–51.
Derco, J., Melicher, M., Kassai, A., Dudas, J., Valicková, M., 2011. Removal of Benzothiazoles by Ozone Pretreatment. Environmental Engineering Science 28 (11), 781–785.
Dodd, M.C., Buffle, M.O., von Gunten, U., 2006. Oxidation of antibacterial molecules by aqueous ozone: Moiety-specific reaction kinetics and application to ozone-based wastewater treatment. Environmental Science & Technology 40 (6), 1969–1977.
Dodd, M.C., Kohler, H.-P.E., von Gunten, U., 2009. Oxidation of Antibacterial Compounds by Ozone and Hydroxyl Radical: Elimination of Biological Activity during Aqueous Ozonation Processes. Environmental Science & Technology 43 (7), 2498–2504.
Dodd, M.C., Rentsch, D., Singer, H.P., Kohler, H.P.E., von Gunten, U., 2010. Transformation of beta-Lactam Antibacterial Agents during Aqueous Ozonation: Reaction Pathways and Quantitative Bioassay of Biologically-Active Oxidation Products. Environmental Science & Technology 44 (15), 5940–5948.
Dodd, M.C., 2012. Potential impacts of disinfection processes on elimination and deactivation of antibiotic resistance genes during water and wastewater treatment. Journal of Environmental Monitoring 14 (7), 1754–1771.
Domenjoud, B., Gonzalez Ospina, A., Vulliet, E., Baig, S., 2017. Innovative Coupling of Ozone Oxidation and Biodegradation for Micropollutants Removal from Wastewater. Ozone: Science & Engineering 39 (5), 296–309.
Domino, M.M., Pepich, B.V., Munch, D.J., Fair, P.S. and Xie, Y. (2003) Method 552.3 Determination of Haloacetic Acids and Dalapon in Drinking Water by Liquid-Liquid Microextraction, Derivatization, and Gas Chromatography with Electron Capture Detection. USEPA (ed).
Dong, H., Qiang, Z., Richardson, S.D., 2019. Formation of Iodinated Disinfection Byproducts (I-DBPs) in Drinking Water: Emerging Concerns and Current Issues. Accounts of Chemical Research 52 (4), 896–905.
Dong, S., Masalha, N., Plewa, M.J., Nguyen, T.H., 2017. Toxicity of Wastewater with Elevated Bromide and Iodide after Chlorination, Chloramination, or Ozonation Disinfection. Environmental Science & Technology 51 (16), 9297–9304.
Dowideit, P., von Sonntag, C., 1998. Reaction of Ozone with Ethene and Its Methyl- and Chlorine-Substituted Derivatives in Aqueous Solution. Environmental Science & Technology 32 (8), 1112–1119.
Duguet, J.P., Bernazeau, F., Mallevialle, J., 1990. Research Note: Removal of Atrazine by Ozone and Ozone-Hydrogen Peroxide Combinations in Surface Water. Ozone: Science & Engineering 12 (2), 195–197.
Eggen, R.I.L., Hollender, J., Joss, A., Schärer, M., Stamm, C., 2014. Reducing the Discharge of Micropollutants in the Aquatic Environment: The Benefits of Upgrading Wastewater Treatment Plants. Environmental Science & Technology 48 (14), 7683–7689.
Eidinoff, M.L., 1945. Dissociation Constants of Acetylacetone, Ethyl Acetoacetate and Benzoylacetone. Journal of the American Chemical Society 67 (12), 2072–2073.
Einhorn, J., Einhorn, C., Luche, J.L., 1991. A Mild and Efficient Sonochemical Tert-Butoxycarbonylation of Amines from Their Salts. Synlett (1), 37–38.
Elovitz, M.S., von Gunten, U., 1999. Hydroxyl radical ozone ratios during ozonation processes. I-The R-ct concept. Ozone-Science & Engineering 21 (3), 239–260.
Elovitz, M.S., von Gunten, U. and Kaiser, H.P. (2000a) Natural Organic Matter and Disinfection By-Products. Barrett, S.E., Krasner, S.W. and Amy, G.L. (eds), pp. 248-269.
Elovitz, M.S., von Gunten, U., Kaiser, H.P., 2000b. Hydroxyl radical/ozone ratios during ozonation processes. II. The effect of temperature, pH, alkalinity, and DOM properties. Ozone-Science & Engineering 22 (2), 123–150.
Erickson, R.E., Myszkiewicz, T.M., 1965. Mechanism of Ozonation Reactions. Nitrones. Journal of Organic Chemistry 30, 4326.
Escher, B.I., Bramaz, N., Ort, C., 2009. JEM Spotlight: Monitoring the treatment efficiency of a full scale ozonation on a sewage treatment plant with a mode-of-action based test battery. Journal of Environmental Monitoring 11 (10), 1836–1846.
Essaïed, K.-A., Brown, L.V., von Gunten, U., 2022. Reactions of amines with ozone and chlorine: Two novel oxidative methods to evaluate the N-DBP formation potential from dissolved organic nitrogen. Water Research 209, 117864.
EU (1998) Official Journal of the European Community L 330: Directive 98/83/EG.
Favier, M., Dewil, R., Van Eyck, K., Van Schepdael, A., Cabooter, D, 2015. High-resolution MS and MSn investigation of ozone oxidation products from phenazone-type pharmaceuticals and metabolites. Chemosphere 136, 32–41.
Flyunt, R., Theruvathu, J.A., Leitzke, A., Sonntag, C.v., 2002. The reactions of thymine and thymidine with ozone. Journal of the Chemical Society, Perkin Transactions 2 (9), 1572–1582.
Funke, J., Prasse, C., Dietrich, C., Ternes, T.A., 2021. Ozonation products of zidovudine and thymidine in oxidative water treatment. Water Research X 11, 100090.
Gallen, C., Eaglesham, G., Drage, D., Nguyen, T.H., Mueller, J.F., 2018. A mass estimate of perfluoroalkyl substance (PFAS) release from Australian wastewater treatment plants. Chemosphere 208, 975–983.
Genena, A.K., Luiz, D.B., Gebhardt, W., Moreira, R.F.P.M., Jose, H.J., Schroder, H.F., 2011. Imazalil Degradation upon Applying Ozone-Transformation Products, Kinetics, and Toxicity of Treated Aqueous Solutions. Ozone-Science & Engineering 33 (4), 308–328.
Gerrity, D., Gamage, S., Holady, J.C., Mawhinney, D.B., Quiones, O., Trenholm, R.A., Snyder, S.A., 2011. Pilot-scale evaluation of ozone and biological activated carbon for trace organic contaminant mitigation and disinfection. Water Research 45 (5), 2155–2165.
Gerrity, D., Snyder, S., 2011. Review of Ozone for Water Reuse Applications: Toxicity, Regulations, and Trace Organic Contaminant Oxidation. Ozone: Science & Engineering 33 (4), 253–266.
Gerrity, D., Gamage, S., Jones, D., Korshin, G.V., Lee, Y., Pisarenko, A., Trenholm, R.A., von Gunten, U., Wert, E.C., Snyder, S.A., 2012. Development of surrogate correlation models to predict trace organic contaminant oxidation and microbial inactivation during ozonation. Water Research 46 (19), 6257–6272.
Gerrity, D., Pecson, B., Trussell, R.S., Trussell, R.R., 2013. Potable reuse treatment trains throughout the world. Journal of Water Supply: Research and Technology-Aqua 62 (6), 321–338.
Gerrity, D., Owens-Bennett, E., Venezia, T., Stanford, B.D., Plumlee, M.H., Debroux, J., Trussell, R.S., 2014. Applicability of Ozone and Biological Activated Carbon for Potable Reuse. Ozone: Science & Engineering 36 (2), 123–137.
Gerrity, D., Pisarenko, A.N., Marti, E., Trenholm, R.A., Gerringer, F., Reungoat, J., Dickenson, E., 2015. Nitrosamines in pilot-scale and full-scale wastewater treatment plants with ozonation. Water Research 72, 251–261.
Gilbert, E., Hoffmann-Glewe, S., 1990. Ozonation of Sulfur-Containing Aliphatic Compounds in Aqueous Solution. I. Ozone: Science & Engineering 12 (3), 315–327.
Glaze, W.H., Koga, M., Cancilla, D, 1989. Ozonation Byproducts. 2. Improvement of an Aqueous-Phase Dervatization Method for the Detection of Formaldehyde and Other Carbonyl Compounds Formed by the Ozonation of Drinking Water. Environ. Sci. Technol. 23, 838–847.
Gonsior, M., Schmitt-Kopplin, P., Stavklint, H., Richardson, S.D., Hertkorn, N., Bastviken, D, 2014. Changes in Dissolved Organic Matter during the Treatment Processes of a Drinking Water Plant in Sweden and Formation of Previously Unknown Disinfection Byproducts. Environmental Science & Technology 48 (21), 12714–12722.
Gross, K.C., Seybold, P.G., 2001. Substituent effects on the physical properties and pKa of phenol. International Journal of Quantum Chemistry 85 (4-5), 569–579.
Gulde, R., Clerc, B., Rutsch, M., Helbing, J., Salhi, E., McArdell, C.S., von Gunten, U., 2021a. Oxidation of 51 micropollutants during drinking water ozonation: Formation of transformation products and their fate during biological post-filtration. Water Research 207, 117812.
Gulde, R., Rutsch, M., Clerc, B., Schollée, J.E., von Gunten, U., McArdell, C.S., 2021b. Formation of transformation products during ozonation of secondary wastewater effluent and their fate in post-treatment: From laboratory- to full-scale. Water Research 200, 117200.
Haag, W.R., Hoigné, J., 1983a. Ozonation of water containing chlorine or chloramines - Reaction products and kinetics. Water Research 17 (10), 1397–1402.

Haag, W.R., Hoigné, J., 1983b. Ozonation of bromide-containing waters: kinetics of formation of hypobromous acid and bromate. Environmental Science & Technology 17 (5), 261–267.
Haag, W.R., Hoigné, J., Bader, H., 1984. Improved ammonia oxidation by ozone in the presence of bromide ion during water treatment. Water Research 18 (9), 1125–1128.
Hajibabaei, M., DeWaard, J.R., Ivanova, N.V., Ratnasingham, S., Dooh, R.T., Kirk, S.L., Mackie, P.M., Hebert, P.D.N., 2005. Critical factors for assembling a high volume of DNA barcodes. Philosophical Transactions of the Royal Society B-Biological Sciences 360 (1462), 1959–1967.
Hammes, F., Salhi, E., Koster, O., Kaiser, H.P., Egli, T., von Gunten, U., 2006. Mechanistic and kinetic evaluation of organic disinfection by-product and assimilable organic carbon (AOC) formation during the ozonation of drinking water. Water Research 40 (12), 2275–2286.
Hammes, F., Meylan, S., Salhi, E., Koster, O., Egli, T., von Gunten, U., 2007. Formation of assimilable organic carbon (AOC) and specific natural organic matter (NOM) fractions during ozonation of phytoplankton. Water Research 41 (7), 1447–1454.
Harkness, J.S., Dwyer, G.S., Warner, N.R., Parker, K.M., Mitch, W.A., Vengosh, A., 2015. Iodide, Bromide, and Ammonium in Hydraulic Fracturing and Oil and Gas Wastewaters: Environmental Implications. Environmental Science & Technology 49 (3), 1955–1963.
He, H., Zhou, P.R., Shimabuku, K.K., Fang, X.Z., Li, S., Lee, Y.H., Dodd, M.C., 2019. Degradation and Deactivation of Bacterial Antibiotic Resistance Genes during Exposure to Free Chlorine, Monochloramine, Chlorine Dioxide, Ozone, Ultraviolet Light, and Hydroxyl Radical. Environmental Science & Technology 53 (4), 2013–2026.
Heeb, M.B., Kristiana, M., Trogolo, D., Arey, J.S., von Gunten, U., 2017. Formation and reactivity of inorganic and organic chloramines and bromamines during oxidative water treatment. Water Research 110, 91–101.
Henry, L.K., Puspitasari-Nienaber, N.L., Jaren-Galan, M., van Breemen, R.B., Catignani, G.L., Schwartz, S.J., 2000. Effects of ozone and oxygen on the degradation of carotenoids in an aqueous model system. Journal of Agricultural and Food Chemistry 48 (10), 5008–5013.
Her, N., Amy, G., McKnight, D., Sohn, J., Yoon, Y.M., 2003. Characterization of DOM as a function of MW by fluorescence EEM and HPLC-SEC using UVA, DOC, and fluorescence detection. Water Research 37 (17), 4295–4303.
Hermes, N., Jewell, K.S., Falas, P., Lutze, H.V., Wick, A., Ternes, T.A., 2020. Ozonation of Sitagliptin: Removal Kinetics and Elucidation of Oxidative Transformation Products. Environmental Science & Technology 54 (17), 10588–10598.
Hoigné, J., Bader, H., 1975. Ozonation of water: role of hydroxyl radicals as oxidizing intermediates. Science 190, 782–784 (Journal Article).
Hoigné, J., Bader, H., 1983a. Rate constants of reactions of ozone with organic and inorganic compounds in water–II dissociating organic compounds. Water Research 17 (2), 185–194.
Hoigné, J., Bader, H., 1983b. Rate constants of reactions of ozone with organic and inorganic compounds in water–I non-dissociating organic compounds. Water Research 17 (2), 173–183.
Hoigné, J., Bader, H., Haag, W.R., Staehelin, J., 1985. Rate constants of reactions of ozone with organic and inorganic compounds in water. III. Inorganic compounds and radicals. Water Res 19, 993–1004.
Hoigné, J., Bader, H., 1988. The formation of trichloronitromethane (chloropicrin) and chloroform in a combined ozonation/chlorination treatment of drinking water. Water Research 22 (3), 313–319.
Hoigné, J., Bader, H., 1994. Kinetics of reactions of chlorine dioxide (OClO) in water—I. Rate constants for inorganic and organic compounds. Water Research 28 (1), 45–55.
Hoigné, J. (1998) The Handbook of Environmental Chemistry Quality and Treatment of Drinking Water. Hubrec, J. (ed), Springer, Berlin.
Hollender, J., Zimmermann, S.G., Koepke, S., Krauss, M., McArdell, C.S., Ort, C., Singer, H., von Gunten, U., Siegrist, H., 2009. Elimination of Organic Micropollutants in a Municipal Wastewater Treatment Plant Upgraded with a Full-Scale Post-Ozonation Followed by Sand Filtration. Environmental Science & Technology 43 (20), 7862–7869.
Hong, P.K.A., Zeng, Y., 2002. Degradation of pentachlorophenol by ozonation and biodegradability of intermediates. Water Research 36 (17), 4243–4254.
Hooper, J., Funk, D., Bell, K., Noibi, M., Vickstrom, K., Schulz, C., Machek, E., Huang, C.-H., 2020. Pilot testing of direct and indirect potable water reuse using multi-stage ozone-biofiltration without reverse osmosis. Water Research 169, 115178.
Hopkins, Z.R., Snowberger, S., Blaney, L., 2017. Ozonation of the oxybenzone, octinoxate, and octocrylene UV-filters: Reaction kinetics, absorbance characteristics, and transformation products. Journal of Hazardous Materials 338, 23–32.
Houska, J., Salhi, E., Walpen, N., von Gunten, U., 2021. Oxidant-reactive carbonous moieties in dissolved organic matter: Selective quantification by oxidative titration using chlorine dioxide and ozone. Water Research 207, 117790.
Hu, J., Song, H., Karanfil, T., 2010. Comparative Analysis of Halonitromethane and Trihalomethane Formation and Speciation in Drinking Water: The Effects of Disinfectants, pH, Bromide, and Nitrite. Environmental Science & Technology 44 (2), 794–799.
Hua, G., Reckhow, D.A., 2013. Effect of pre-ozonation on the formation and speciation of DBPs. Water Research 47 (13), 4322–4330.
Huang, Y., Li, T., Zheng, S., Fan, L., Su, L., Zhao, Y., Xie, H.-B., Li, C., 2020. QSAR modeling for the ozonation of diverse organic compounds in water. Science of The Total Environment 715, 136816.
Huber, M.M., Canonica, S., Park, G.Y., von Gunten, U., 2003. Oxidation of pharmaceuticals during ozonation and advanced oxidation processes. Environmental Science & Technology 37 (5), 1016–1024.
Huber, M.M., Ternes, T.A., von Gunten, U., 2004. Removal of estrogenic activity and formation of oxidation products during ozonation of 17 alpha-ethinylestradiol. Environmental Science & Technology 38 (19), 5177–5186.
Huber, M.M., Gobel, A., Joss, A., Hermann, N., Loffler, D., McArdell, C.S., Ried, A., Siegrist, H., Ternes, T.A., von Gunten, U., 2005a. Oxidation of pharmaceuticals during ozonation of municipal wastewater effluents: A pilot study. Environmental Science & Technology 39 (11), 4290–4299.
Huber, M.M., Korhonen, S., Ternes, T.A., von Gunten, U., 2005b. Oxidation of pharmaceuticals during water treatment with chlorine dioxide. Water Research 39 (15), 3607–3617.
Hübner, U., Seiwert, B., Reemtsma, T., Jekel, M., 2014. Ozonation products of carbamazepine and their removal from secondary effluents by soil aquifer treatment - Indications from column experiments. Water Research 49, 34–43.
Hübner, U., von Gunten, U., Jekel, M., 2015. Evaluation of the persistence of transformation products from ozonation of trace organic compounds – A critical review. Water Research 68, 150–170.
Hunt, N.K., Marinas, B.J., 1999. Inactivation of Escherichia coli with ozone: Chemical and inactivation kinetics. Water Research 33 (11), 2633–2641.
Iakovides, I.C., Michael-Kordatou, I., Moreira, N.F.F., Ribeiro, A.R., Fernandes, T., Pereira, M.F.R., Nunes, O.C., Manaia, C.M., Silva, A.M.T., Fatta-Kassinos, D, 2019. Continuous ozonation of urban wastewater: Removal of antibiotics, antibiotic-resistant Escherichia coli and antibiotic resistance genes and phytotoxicity. Water Research 159, 333–347.
Inyang, M., Dickenson, E.R.V., 2017. The use of carbon adsorbents for the removal of perfluoroalkyl acids from potable reuse systems. Chemosphere 184, 168–175.
Itzel, F., Gehrmann, L., Bielak, H., Ebersbach, P., Boergers, A., Herbst, H., Maus, C., Simon, A., Dopp, E., Hammers-Wirtz, M., Schmidt, T.C., Tuerk, J., 2017. Investigation of full-scale ozonation at a municipal wastewater treatment plant using a toxicity-based evaluation concept. Journal of Toxicology and Environmental Health, Part A 80 (23-24), 1242–1258.
Itzel, F., Baetz, N., Hohrenk, L.L., Gehrmann, L., Antakyali, D., Schmidt, T.C., Tuerk, J., 2020. Evaluation of a biological post-treatment after full-scale ozonation at a municipal wastewater treatment plant. Water Research 170, 115316.
Jáky, M., Szammer, J., Simon-Trompler, E., 2006. Kinetics and mechanism of the oxidation of acetylacetone by permanganate ion. International Journal of Chemical Kinetics 38 (7), 444–450.
Janex, M.L., Savoye, P., Roustan, M., Do-Quang, Z., Laîné, J.M., Lazarova, V., 2000. Wastewater Disinfection by Ozone: Influence of Water Quality and Kinetics Modeling. Ozone: Science & Engineering 22 (2), 113–121.
Jans, U., Prasse, C., von Gunten, U., 2021. Enhanced Treatment of Municipal Wastewater Effluents by Fe-TAML/H2O2: Efficiency of Micropollutant Abatement. Environmental Science & Technology 55 (5), 3313–3321.
Jensen, R.L., Arnbjerg, J., Ogilby, P.R., 2012. Reaction of Singlet Oxygen with Tryptophan in Proteins: A Pronounced Effect of the Local Environment on the Reaction Rate. Journal of the American Chemical Society 134 (23), 9820–9826.
Jeon, D., Kim, J., Shin, J., Hidayat, Z.R., Na, S., Lee, Y., 2016. Transformation of ranitidine during water chlorination and ozonation: Moiety-specific reaction kinetics and elimination efficiency of NDMA formation potential. Journal of Hazardous Materials 318, 802–809.
Jiang, J.L., Yue, X.A., Chen, Q.F., Gao, Z., 2010. Determination of ozonization reaction rate constants of aromatic pollutants and QSAR study. Bulletin of environmental contamination and toxicology 85 (6), 568–572.
Jin, X.H., Peldszus, S., Huck, P.M., 2012. Reaction kinetics of selected micropollutants in ozonation and advanced oxidation processes. Water Research 46 (19), 6519–6530.
Joss, A., Siegrist, H., Ternes, T.A., 2008. Are we about to upgrade wastewater treatment for removing organic micropollutants? Water Science and Technology 57 (2), 251–255.
Joule, J.A., Mills, K., 2012. Heterocyclic chemistry at a glance. Wiley, Chichester, West Sussex; Hoboken.
Kaiser, H.-P., Köster, O., Gresch, M., Périsset, P.M.J., Jäggi, P., Salhi, E., von Gunten, U., 2013. Process Control For Ozonation Systems: A Novel Real-Time Approach. Ozone: Science & Engineering 35 (3), 168–185.
Keay, R.E., Hamilton, G.A., 1976. Alkene epoxidation by intermediates formed during the ozonation of alkynes. Journal of the American Chemical Society 98 (21), 6578–6582.
Khan, M.H., Bae, H., Jung, J.-Y., 2010. Tetracycline degradation by ozonation in the aqueous phase: Proposed degradation intermediates and pathway. Journal of Hazardous Materials 181 (1), 659–665.
Kim, M.S., Lee, C., 2019. Ozonation of Microcystins: Kinetics and Toxicity Decrease. Environmental Science & Technology 53 (11), 6427–6435.
Knoop, O., Hohrenk, L.L., Lutze, H.V., Schmidt, T.C., 2018. Ozonation of tamoxifen and toremifene – Reaction kinetics and transformation products. Environmental Science & Technology 52 (21), 12583–12591.
Knopp, G., Prasse, C., Ternes, T.A., Cornel, P., 2016. Elimination of micropollutants and transformation products from a wastewater treatment plant effluent through pilot scale ozonation followed by various activated carbon and biological filters. Water Research 100, 580–592.
Kolonko, K.J., Shapiro, R.H., Barkley, R.M., Sievers, R.E., 1979. Ozonation of Caffeine in Aqueous-Solution. Journal of Organic Chemistry 44 (22), 3769–3778.
Kosaka, K., Asami, M., Konno, Y., Oya, M., Kunikane, S., 2009. Identification of Antiyellowing Agents as Precursors of N-Nitrosodimethylamine Production on Ozonation from Sewage Treatment Plant Influent. Environmental Science & Technology 43 (14), 5236–5241.
Kosaka, K., Asami, M., Ohkubo, K., Iwamoto, T., Tanaka, Y., Koshino, H., Echigo, S., Akiba, M., 2014. Identification of a New N-Nitrosodimethylamine Precursor in

Sewage Containing Industrial Effluents. Environmental Science & Technology 48 (19), 11243–11250.
Krasner, S.W., Glaze, W.H., Weinberg, H.S., Daniel, P.A., Najm, I.N., 1993. Formation and Control of Bromate During Ozonation of Waters Containing Bromide. Journal (American Water Works Association) 85 (1), 73–81.
Krasner, S.W., 2009. The formation and control of emerging disinfection by-products of health concern. Philosophical Transactions of the Royal Society a-Mathematical Physical and Engineering Sciences 367 (1904), 4077–4095.
Krasner, S.W., Mitch, W.A., McCurry, D.L., Hanigan, D., Westerhoff, P., 2013. Formation, precursors, control, and occurrence of nitrosamines in drinking water: A review. Water Research 47 (13), 4433–4450.
Krasner, S.W., Westerhoff, P., Mitch, W.A., Hanigan, D., McCurry, D.L., von Gunten, U., 2018. Behavior of NDMA precursors at 21 full-scale water treatment facilities. Environmental Science: Water Research & Technology 4 (12), 1966–1978.
Krauss, M., Longree, P., Dorusch, F., Ort, C., Hollender, J., 2009. Occurrence and removal of N-nitrosamines in wastewater treatment plants. Water Research 43 (17), 4381–4391.
Lamba, M., Ahammad, S.Z., 2017. Performance comparison of secondary and tertiary treatment systems for treating antibiotic resistance. Water Research 127, 172–182.
Lange, F., Cornelissen, S., Kubac, D., Sein, M.M., von Sonntag, J., Hannich, C.B., Golloch, A., Heipieper, H.J., Moder, M., von Sonntag, C., 2006. Degradation of macrolide antibiotics by ozone: A mechanistic case study with clarithromycin. Chemosphere 65 (1), 17–23.
Lavonen, E.E., Kothawala, D.N., Tranvik, L.J., Gonsior, M., Schmitt-Kopplin, P., Kohler, S.J., 2015. Tracking changes in the optical properties and molecular composition of dissolved organic matter during drinking water production. Water Research 85, 286–294.
Le Lacheur, R.M., Glaze, W.H, 1996. Reactions of ozone and hydroxyl radicals with serine. Environmental Science & Technology 30 (4), 1072–1080.
Lee, C., Schmidt, C., Yoon, J., von Gunten, U., 2007a. Oxidation of N-nitrosodimethylamine (NDMA) precursors with ozone and chlorine dioxide: Kinetics and effect on NDMA formation potential. Environmental Science & Technology 41 (6), 2056–2063.
Lee, C., Yoon, J., von Gunten, U., 2007b. Oxidative degradation of N-nitrosodimethylamine by conventional ozonation and the advanced oxidation process ozone/hydrogen peroxide. Water Research 41 (3), 581–590.
Lee, M., Zimmermann-Steffens, S.G., Arey, J.S., Fenner, K., von Gunten, U., 2015. Development of Prediction Models for the Reactivity of Organic Compounds with Ozone in Aqueous Solution by Quantum Chemical Calculations: The Role of Delocalized and Localized Molecular Orbitals. Environmental Science & Technology 49 (16), 9925–9935.
Lee, M., Blum, L.C., Schmid, E., Fenner, K., von Gunten, U., 2017a. A computer-based prediction platform for the reaction of ozone with organic compounds in aqueous solution: kinetics and mechanisms. Environmental Science: Processes & Impacts 19 (3), 465–476.
Lee, M., Merle, T., Rentsch, D., Canonica, S., von Gunten, U., 2017b. Abatement of Polychoro-1,3-butadienes in Aqueous Solution by Ozone, UV Photolysis, and Advanced Oxidation Processes (O3/H2O2 and UV/H2O2). Environmental Science & Technology 51 (1), 497–505.
Lee, Y., Escher, B.I., von Gunten, U., 2008. Efficient Removal of Estrogenic Activity during Oxidative Treatment of Waters Containing Steroid Estrogens. Environ. Sci. Technol. 42 (17), 6333–6339.
Lee, Y., Zimmermann, S.G., Kieu, A.T., von Gunten, U., 2009. Ferrate (Fe(VI)) Application for Municipal Wastewater Treatment: A Novel Process for Simultaneous Micropollutant Oxidation and Phosphate Removal. Environmental Science & Technology 43 (10), 3831–3838.
Lee, Y., von Gunten, U., 2010. Oxidative transformation of micropollutants during municipal wastewater treatment: Comparison of kinetic aspects of selective (chlorine, chlorine dioxide, ferrateVI, and ozone) and non-selective oxidants (hydroxyl radical). Water Research 44 (2), 555–566.
Lee, Y., von Gunten, U., 2012. Quantitative structure-activity relationships (QSARs) for the transformation of organic micropollutants during oxidative water treatment. Water Res 46 (19), 6177–6195.
Lee, Y., Gerrity, D., Lee, M., Bogeat, A.E., Salhi, E., Gamage, S., Trenholm, R.A., Wert, E. C., Snyder, S.A., von Gunten, U., 2013. Prediction of Micropollutant Elimination during Ozonation of Municipal Wastewater Effluents: Use of Kinetic and Water Specific Information. Environmental Science & Technology 47 (11), 5872–5881.
Lee, Y., Kovalova, L., McArdell, C.S., von Gunten, U., 2014. Prediction of micropollutant elimination during ozonation of a hospital wastewater effluent. Water Research 64 (0), 134–148.
Lee, Y., Gerrity, D., Lee, M., Gamage, S., Pisarenko, A., Trenholm, R.A., Canonica, S., Snyder, S.A., von Gunten, U., 2016a. Organic Contaminant Abatement in Reclaimed Water by UV/H2O2 and a Combined Process Consisting of O3/H2O2 Followed by UV/H2O2: Prediction of Abatement Efficiency, Energy Consumption, and Byproduct Formation. Environmental Science & Technology 50 (7), 3809–3819.
Lee, Y., Imminger, S., Czekalski, N., von Gunten, U., Hammes, F., 2016b. Inactivation efficiency of Escherichia coli and autochthonous bacteria during ozonation of municipal wastewater effluents quantified with flow cytometry and adenosine triphosphate analyses. Water Research 101, 617–627.
Lee, Y., von Gunten, U., 2016. Advances in predicting organic contaminant abatement during ozonation of municipal wastewater effluent: reaction kinetics, transformation products, and changes of biological effects. Environmental Science: Water Research & Technology 2 (3), 421–442.
Legube, B., Nompex, P., Doré, M., 1987. Ozonation des bases puriques en milieu aqueux: etudes cinetiques de la reaction. Water Research 21 (9), 1101–1107.
Leitzke, A., von Sonntag, C., 2009. Ozonolysis of Unsaturated Acids in Aqueous Solution: Acrylic, Methacrylic, Maleic, Fumaric and Muconic Acids. Ozone: Science & Engineering 31 (4), 301–308.
Leresche, F., McKay, G., Kurtz, T., von Gunten, U., Canonica, S., Rosario-Ortiz, F.L., 2019. Effects of Ozone on the Photochemical and Photophysical Properties of Dissolved Organic Matter. Environmental Science & Technology 53 (10), 5622–5632.
Leresche, F., Torres-Ruiz, J.A., Kurtz, T., von Gunten, U., Rosario-Ortiz, F.L., 2021. Optical properties and photochemical production of hydroxyl radical and singlet oxygen after ozonation of dissolved organic matter. Environmental Science: Water Research & Technology 7 (2), 346–356.
Lester, Y., Mamane, H., Zucker, I., Avisar, D, 2013. Treating wastewater from a pharmaceutical formulation facility by biological process and ozone. Water Research 47 (13), 4349–4356.
Leviss, D.H., Van Ry, D.A., Hinrichs, R.Z., 2016. Multiphase Ozonolysis of Aqueous alpha-Terpineol. Environmental Science & Technology 50 (21), 11698–11705.
Li, J., Jiang, J., Pang, S.Y., Cao, Y., Zhou, Y., Guan, C., 2020. Oxidation of iodide and hypoiodous acid by non-chlorinated water treatment oxidants and formation of iodinated organic compounds: A review. Chemical Engineering Journal 386, 123822.
Lim, S., Lee, W., Na, S., Shin, J., Lee, Y., 2016. N-nitrosodimethylamine (NDMA) formation during ozonation of N,N-dimethylhydrazine compounds: Reaction kinetics, mechanisms, and implications for NDMA formation control. Water Research 105, 119–128.
Lim, S., McArdell, C.S., von Gunten, U., 2019. Reactions of aliphatic amines with ozone: Kinetics and mechanisms. Water Research 157, 514–528.
Liu, X.K., Liu, R.R., Zhu, B., Ruan, T., Jiang, G.B., 2020. Characterization of Carbonyl Disinfection By-Products During Ozonation, Chlorination, and Chloramination of Dissolved Organic Matters. Environmental Science & Technology 54 (4), 2218–2227.
Liu, Z.S., Craven, C.B., Huang, G., Jiang, P., Wu, D., Li, X.F., 2019. Stable Isotopic Labeling and Nontarget Identification of Nanogram/Liter Amino Contaminants in Water. Analytical Chemistry 91 (20), 13213–13221.
Lundeen, R.A., McNeill, K., 2013. Reactivity Differences of Combined and Free Amino Acids: Quantifying the Relationship between Three-Dimensional Protein Structure and Singlet Oxygen Reaction Rates. Environmental Science & Technology 47 (24), 14215–14223.
Lutze, H.V., Brekenfeld, J., Naumov, S., von Sonntag, C., Schmidt, T.C., 2018. Degradation of perfluorinated compounds by sulfate radicals – New mechanistic aspects and economical considerations. Water Research 129, 509–519.
Lyon, B.A., Cory, R.M., Weinberg, H.S., 2014. Changes in dissolved organic matter fluorescence and disinfection byproduct formation from UV and subsequent chlorination/chloramination. Journal of Hazardous Materials 264, 411–419.
Magdeburg, A., Stalter, D., Schlüsener, M., Ternes, T., Oehlmann, J., 2014. Evaluating the efficiency of advanced wastewater treatment: Target analysis of organic contaminants and (geno-)toxicity assessment tell a different story. Water Research 50 (0), 35–47.
Manasfi, T., McArdell, C.S., Hollender, J. and von Gunten, U. 2022 (In prep.) Non-targeted analysis reveals novel transformation products during ozonation of wastewater: Formation of nitro compounds in the presence of nitrite.
Marron, E.L., Mitch, W.A., von Gunten, U., Sedlak, D.L., 2019. A Tale of Two Treatments: The Multiple Barrier Approach to Removing Chemical Contaminants During Potable Water Reuse. Accounts of Chemical Research 52 (3), 615–622.
Marron, E.L., Prasse, C., Van Buren, J., Sedlak, D.L., 2020. Formation and Fate of Carbonyls in Potable Water Reuse Systems. Environmental Science & Technology 54 (17), 10895–10903.
Marti, E.J., Pisarenko, A.N., Peller, J.R., Dickenson, E.R.V., 2015. N-nitrosodimethylamine (NDMA) formation from the ozonation of model compounds. Water Research 72, 262–270.
Matsui, M., Kamiya, K., Shibata, K., Muramatsu, H., Nakazumi, H., 1990. Ozonolysis of Substituted Uracils. Journal of Organic Chemistry 55 (4), 1396–1399.
Mawhinney, D.B., Vanderford, B.J., Snyder, S.A., 2012. Transformation of 1H-Benzotriazole by Ozone in Aqueous Solution. Environmental Science & Technology 46 (13), 7102–7111.
McCurry, D.L., Krasner, S.W., von Gunten, U., Mitch, W.A., 2015. Determinants of disinfectant pretreatment efficacy for nitrosamine control in chloraminated drinking water. Water Research 84, 161–170.
McCurry, D.L., Quay, A.N., Mitch, W.A., 2016. Ozone Promotes Chloropicrin Formation by Oxidizing Amines to Nitro Compounds. Environ Sci Technol 50 (3), 1209–1217.
McDowell, D.C., Huber, M.M., Wagner, M., von Gunten, U., Ternes, T.A., 2005. Ozonation of Carbamazepine in Drinking Water: Identification and Kinetic Study of Major Oxidation Products. Environmental Science & Technology 39 (20), 8014–8022.
McKay, G., Korak, J.A., Rosario-Ortiz, F.L., 2018. Temperature Dependence of Dissolved Organic Matter Fluorescence. Environmental Science & Technology 52 (16), 9022–9032.
McKinney, C.W., Pruden, A., 2012. Ultraviolet Disinfection of Antibiotic Resistant Bacteria and Their Antibiotic Resistance Genes in Water and Wastewater. Environmental Science & Technology 46 (24), 13393–13400.
McMurry, J.E., Melton, J., Padgett, H., 1974. New method for converting nitro compounds into carbonyls. Ozonolysis of nitronates. Journal of Organic Chemistry 39, 259–260.
Merel, S., Lege, S., Heras, J.E.Y., Zwiener, C., 2017. Assessment of N-Oxide Formation during Wastewater Ozonation. Environmental Science & Technology 51 (1), 410–417.

Merle, T., Pronk, W., von Gunten, U., 2017. MEMBRO3X, a Novel Combination of a Membrane Contactor with Advanced Oxidation (O3/H2O2) for Simultaneous Micropollutant Abatement and Bromate Minimization. Environmental Science & Technology Letters 4 (5), 180–185.
Mestankova, H., Escher, B., Schirmer, K., von Gunten, U., Canonica, S., 2011. Evolution of algal toxicity during (photo)oxidative degradation of diuron. Aquatic Toxicology 101 (2), 466–473.
Mestankova, H., Schirmer, K., Escher, B.I., von Gunten, U., Canonica, S., 2012. Removal of the antiviral agent oseltamivir and its biological activity by oxidative processes. Environmental Pollution 161, 30–35.
Mestankova, H., Schirmer, K., Canonica, S., von Gunten, U., 2014. Development of mutagenicity during degradation of N-nitrosamines by advanced oxidation processes. Water Research 66, 399–410.
Miklos, D.B., Remy, C., Jekel, M., Linden, K.G., Drewes, J.E., Hübner, U., 2018. Evaluation of advanced oxidation processes for water and wastewater treatment – A critical review. Water Research 139, 118–131.
Minakata, D., Crittenden, J., 2011. Linear Free Energy Relationships between Aqueous phase Hydroxyl Radical Reaction Rate Constants and Free Energy of Activation. Environmental Science & Technology 45 (8), 3479–3486.
Mitch, W.A., Sedlak, D.L., 2002. Formation of N-nitrosodimethylamine (NDMA) from Dimethylamine during Chlorination. Environ. Sci. Technol. 26, 588–595.
Mitch, W.A., Gerecke, A.C., Sedlak, D.L., 2003a. A N-nitrosodimethylamine (NDMA) precursor analysis for chlorination of water and wastewater. Water Research 37 (15), 3733–3741.
Mitch, W.A., Sharp, J.O., Trussell, R.R., Valentine, R.L., Alvarez-Cohen, L., Sedlak, D.L., 2003b. N-nitrosodimethylamine (NDMA) as a drinking water contaminant: A review. Environmental Engineering Science 20 (5), 389–404.
Moriyasu, M., Kato, A., Hashimoto, Y., 1986. Kinetic studies of fast equilibrium by means of high-performance liquid chromatography. Part 11. Keto–enol tautomerism of some β-dicarbonyl compounds. Journal of the Chemical Society 2 (4), 515–520. Perkin Transactions.
Morrison, C., Hogard, S., Pearce, R., Gerrity, D., von Gunten, U. and Wert, E.C. submitted, Ozone disinfection of waterborne pathogens and their surrogates: A critical review. Water Research.
Muñoz, F., Mvula, E., Braslavsky, S.E., von Sonntag, C., 2001. Singlet dioxygen formation in ozone reactions in aqueous solution. Journal of the Chemical Society 2 (7), 1109–1116. Perkin Transactions.
Mutseyekwa, M.E., Dogan, S., Pirgalioglu, S., 2017. Ozonation for the removal of bisphenol A. Water Sci Technol 76 (9-10), 2764–2775.
Mvula, E., von Sonntag, C., 2003. Ozonolysis of phenols in aqueous solution. Organic & Biomolecular Chemistry 1 (10), 1749–1756.
Mvula, E., Naumov, S., von Sonntag, C., 2009. Ozonolysis of Lignin Models in Aqueous Solution: Anisole, 1,2-Dimethoxybenzene, 1,4-Dimethoxybenzene, and 1,3,5-Trimethoxybenzene. Environmental Science & Technology 43 (16), 6275–6282.
Najm, I.N., Trussell, R.R., 2001. NDMA Formation in Water and Wastewater. Journal AWWA 93 (2), 92–99.
Nanaboina, V., Korshin, G.V., 2010. Evolution of Absorbance Spectra of Ozonated Wastewater and Its Relationship with the Degradation of Trace-Level Organic Species. Environmental Science & Technology 44 (16), 6130–6137.
Nawrocki, J., Świetlik, J., Raczyk-Stanisławiak, U., Dąbrowska, A., Biłozor, S., Ilecki, W., 2003. Influence of Ozonation Conditions on Aldehyde and Carboxylic Acid Formation. Ozone: Science & Engineering 25 (1), 53–62.
Önnby, L., Salhi, E., McKay, G., Rosario-Ortiz, F.L., von Gunten, U., 2018a. Ozone and chlorine reactions with dissolved organic matter - Assessment of oxidant-reactive moieties by optical measurements and the electron donating capacities. Water Research 144, 64–75.
Önnby, L., Walpen, N., Salhi, E., Sander, M., von Gunten, U., 2018b. Two analytical approaches quantifying the electron donating capacities of dissolved organic matter to monitor its oxidation during chlorination and ozonation. Water Research 144, 677–689.
Onstad, G.D., Strauch, S., Meriluoto, J., Codd, G.A., von Gunten, U., 2007. Selective Oxidation of Key Functional Groups in Cyanotoxins during Drinking Water Ozonation. Environmental Science & Technology 41 (12), 4397–4404.
Orvik, J.A., 1980. Kinetics and Mechanism of Nitromethane Chlorination. A New Rate Expression. J Am Chem Soc 102, 740–743.
Oya, M., Kosaka, K., Asami, M., Kunikane, S., 2008. Formation of N-nitrosodimethylamine (NDMA) by ozonation of dyes and related compounds. Chemosphere 73 (11), 1724–1730.
Pak, G., Salcedo, D.E., Lee, H., Oh, J., Maeng, S.K., Song, K.G., Hong, S.W., Kim, H.C., Chandran, K., Kim, S., 2016. Comparison of Antibiotic Resistance Removal Efficiencies Using Ozone Disinfection under Different pH and Suspended Solids and Humic Substance Concentrations. Environmental Science & Technology 50 (14), 7590–7600.
Paraskeva, P., Graham, N.J.D., 2002. Ozonation of municipal wastewater effluents. Water Environment Research 74 (6), 569–581.
Park, M., Anumol, T., Daniels, K.D., Wu, S., Ziska, A.D., Snyder, S.A., 2017. Predicting trace organic compound attenuation by ozone oxidation: Development of indicator and surrogate models. Water Research 119, 21–32.
Parkin, G.F., McCarty, P.L., 1981. A comparison of the characteristics of soluble organic nitrogen in untreated and activated sludge treated wastewaters. Water Research 15 (1), 139–149.
Pehlivanoglu-Mantas, E., Sedlak, D.L., 2006. Wastewater-Derived Dissolved Organic Nitrogen: Analytical Methods, Characterization, and Effects—A Review. Critical Reviews in Environmental Science and Technology 36 (3), 261–285.
Pehlivanoglu-Mantas, E., Sedlak, D.L., 2008. Measurement of dissolved organic nitrogen forms in wastewater effluents: Concentrations, size distribution and NDMA formation potential. Water Research 42 (14), 3890–3898.
Pei, J., Yao, H., Wang, H., Ren, J., Yu, X.H., 2016. Comparison of ozone and thermal hydrolysis combined with anaerobic digestion for municipal and pharmaceutical waste sludge with tetracycline resistance genes. Water Research 99, 122–128.
Pérez-González, A., Urtiaga, A.M., Ibáñez, R., Ortiz, I., 2012. State of the art and review on the treatment technologies of water reverse osmosis concentrates. Water Research 46 (2), 267–283.
Peter, A., von Gunten, U., 2007. Oxidation kinetics of selected taste and odor compounds during ozonation of drinking water. Environmental Science & Technology 41 (2), 626–631.
Phungsai, P., Kurisu, F., Kasuga, I., Furumai, H., 2016. Molecular characterization of low molecular weight dissolved organic matter in water reclamation processes using Orbitrap mass spectrometry. Water Research 100, 526–536.
Phungsai, P., Kurisu, F., Kasuga, I., Furumai, H., 2018. Changes in Dissolved Organic Matter Composition and Disinfection Byproduct Precursors in Advanced Drinking Water Treatment Processes. Environmental Science & Technology 52 (6), 3392–3401.
Phungsai, P., Kurisu, F., Kasuga, I., Furumai, H., 2019. Molecular characteristics of dissolved organic matter transformed by O-3 and O-3/H2O2 treatments and the effects on formation of unknown disinfection by-products. Water Research 159, 214–222.
Pi, Y., Zhang, L., Wang, J., 2007. The formation and influence of hydrogen peroxide during ozonation of para-chlorophenol. J Hazard Mater 141 (3), 707–712.
Pierpoint, A.C., Hapeman, C.J., Torrents, A., 2001. Linear free energy study of ring-substituted aniline ozonation for developing treatment of aniline-based pesticide wastes. Journal of Agricultural and Food Chemistry 49 (8), 3827–3832.
Pinkernell, U., Luke, H.J., Karst, U., 1997. Selective photometric determination of peroxycarboxylic acids in the presence of hydrogen peroxide. Analyst 122 (6), 567–571.
Pinkernell, U., von Gunten, U., 2001. Bromate minimization during ozonation: mechanistic considerations. Environ. Sci. Technol. 35, 2525–2531.
Pisarenko, A.N., Marti, E.J., Gerrity, D., Peller, J.R., Dickenson, E.R.V., 2015. Effects of molecular ozone and hydroxyl radical on formation of N-nitrosamines and perfluoroalkyl acids during ozonation of treated wastewaters. Environmental Science: Water Research & Technology 1, 668–678.
Prasse, C., Wagner, M., Schulz, R., Ternes, T.A., 2012. Oxidation of the Antiviral Drug Acyclovir and Its Biodegradation Product Carboxy-acyclovir with Ozone: Kinetics and Identification of Oxidation Products. Environmental Science & Technology 46 (4), 2169–2178.
Prasse, C., Stalter, D., Schulte-Oehlmann, U., Oehlmann, J., Ternes, T.A., 2015. Spoilt for choice: A critical review on the chemical and biological assessment of current wastewater treatment technologies. Water Research 87, 237–270.
Price, C.C., Bullitt, O.H., 1947. Hydrolysis and Oxidation of Mustard Gas and Related Compounds in Aqueous Solution. Journal of Organic Chemistry 12 (2), 238–248.
Pruden, A., Larsson, D.G.J., Amezquita, A., Collignon, P., Brandt, K.K., Graham, D.W., Lazorchak, J.M., Suzuki, S., Silley, P., Snape, J.R., Topp, E., Zhang, T., Zhu, Y.G., 2013. Management Options for Reducing the Release of Antibiotics and Antibiotic Resistance Genes to the Environment. Environmental Health Perspectives 121 (8), 878–885.
Pryor, W.A., Giamalva, D.H., Church, D.F., 1984. Kinetics of Ozonation. 2. Amino Acids and Model Compounds in Water and Comparisons to Rates in Nonpolar Solvents. J Am Chem Soc 106, 7094.
Qiu, Y., Kuo, C.-H., Zappi, M.E., Fleming, E.C., 2004. Ozonation of 2, 6-, 3, 4-, and 3, 5-dichlorophenol isomers within aqueous solutions. Journal of Environmental Engineering 130 (4), 408–416.
Ramseier, M.K., von Gunten, U., 2009. Mechanisms of Phenol Ozonation—Kinetics of Formation of Primary and Secondary Reaction Products. Ozone: Science & Engineering 31 (3), 201–215.
Ramseier, M.K., Peter, A., Traber, J., von Gunten, U., 2011a. Formation of assimilable organic carbon during oxidation of natural waters with ozone, chlorine dioxide, chlorine, permanganate, and ferrate. Water Research 45 (5), 2002–2010.
Ramseier, M.K., von Gunten, U., Freihofer, P., Hammes, F., 2011b. Kinetics of membrane damage to high (HNA) and low (LNA) nucleic acid bacterial clusters in drinking water by ozone, chlorine, chlorine dioxide, monochloramine, ferrate(VI), and permanganate. Water Research 45 (3), 1490–1500.
Reckhow, D.A., Singer, P.C., 1984. The removal of organic halide precursors by preozonation and Alum coagulation. J. Amer. Water Works Assoc. 76 (4), 151–157.
Reckhow, D.A., Legube, B., Singer, P.C., 1986. The Ozonation of Organic Halide Precursors: Effect of Bicarbonate. Wat. Res. 20, 987–998.
Reisz, E., Fischbacher, A., Naumov, S., von Sonntag, C., Schmidt, T.C., 2014. Hydride Transfer: A Dominating Reaction of Ozone with Tertiary Butanol and Formate Ion in Aqueous Solution. Ozone-Science & Engineering 36 (6), 532–539.
Reisz, E., von Sonntag, C., Tekle-Rottering, A., Naumov, S., Schmidt, W., Schmidt, T.C., 2018. Reaction of 2-propanol with ozone in aqueous media. Water Res 128, 171–182.
Reisz, E., Tekle-Rottering, A., Naumov, S., Schmidt, W., Schmidt, T.C., 2019. Reaction of 1-propanol with Ozone in Aqueous Media. Int J Mol Sci 20 (17), 4165.
Remucal, C.K., Salhi, E., Walpen, N., von Gunten, U., 2020. Molecular-Level Transformation of Dissolved Organic Matter during Oxidation by Ozone and Hydroxyl Radical. Environmental Science & Technology 54 (16), 10351–10360.
Reungoat, J., Escher, B.I., Macova, M., Argaud, F.X., Gernjak, W., Keller, J., 2012. Ozonation and biological activated carbon filtration of wastewater treatment plant effluents. Water Research 46 (3), 863–872.

Rizzo, L., Manaia, C., Merlin, C., Schwartz, T., Dagot, C., Ploy, M.C., Michael, I., Fatta-Kassinos, D, 2013. Urban wastewater treatment plants as hotspots for antibiotic resistant bacteria and genes spread into the environment: A review. Science of the Total Environment 447, 345–360.
Robertson, J.M., Dineen, S.M., Scott, K.A., Lucyshyn, J., Saeed, M., Murphy, D.L., Schweighardt, A.J., Meiklejohn, K.A., 2014. Assessing PreCR (TM) repair enzymes for restoration of STR profiles from artificially degraded DNA for human identification. Forensic Science International-Genetics 12, 168–180.
Rook, J.J., 1974. Formation of haloforms during chlorination of natural waters. Water Treat. Exam. 23, 234–243.
Sarasa, J., Cortes, S., Ormad, P., Gracia, R., Ovelleiro, J.L., 2002. Study of the aromatic by-products formed from ozonation of anilines in aqueous solution. Water Research 36 (12), 3035–3044.
Scheurer, M., Godejohann, M., Wick, A., Happel, O., Ternes, T., Brauch, H.J., Ruck, W., Lange, F., 2012. Structural elucidation of main ozonation products of the artificial sweeteners cyclamate and acesulfame. Environmental Science and Pollution Research 19 (4), 1107–1118.
Schindler Wildhaber, Y., Mestankova, H., Schärer, M., Schirmer, K., Salhi, E., von Gunten, U., 2015. Novel test procedure to evaluate the treatability of wastewater with ozone. Water Research 75, 324–335.
Schmidt, C.K., Brauch, H.-J., 2008. N,N-Dimethylsulfamide as Precursor for N-Nitrosodimethylamine (NDMA) Formation upon Ozonation and its Fate During Drinking Water Treatment. Environ. Sci. Technol. 42 (17), 6340–6346.
Schollée, J.E., Bourgin, M., von Gunten, U., McArdell, C.S., Hollender, J., 2018. Non-target screening to trace ozonation transformation products in a wastewater treatment train including different post-treatments. Water Research 142, 267–278.
Schymanski, E.L., Jeon, J., Gulde, R., Fenner, K., Ruff, M., Singer, H.P., Hollender, J., 2014. Identifying Small Molecules via High Resolution Mass Spectrometry: Communicating Confidence. Environmental Science & Technology 48 (4), 2097–2098.
Serjeant, E.P., Dempsey, B., 1979. Ionisation constants of organic acids in aqueous solution. Pergamon, Pergamon.
Shah, A.D., Krasner, S.W., Lee, C.F.T., von Gunten, U., Mitch, W.A., 2012. Trade-Offs in Disinfection Byproduct Formation Associated with Precursor Preoxidation for Control of N-Nitrosodimethylamine Formation. Environmental Science & Technology 46 (9), 4809–4818.
Shi, J.L., McCurry, D.L., 2020. Transformation of N-Methylamine Drugs during Wastewater Ozonation: Formation of Nitromethane, an Efficient Precursor to Halonitromethanes. Environmental Science & Technology 54 (4), 2182–2191.
Shi, J.L., Plata, S.L., Kleimans, M., Childress, A.E., McCurry, D.L., 2021. Formation and Fate of Nitromethane in Ozone-Based Water Reuse Processes. Environmental Science & Technology 55, 6281–6289.
Shon, H.K., Vigneswaran, S., Snyder, S.A., 2006. Effluent Organic Matter (EfOM) in Wastewater: Constituents, Effects, and Treatment. Critical Reviews in Environmental Science and Technology 36 (4), 327–374.
Sikorsky, J.A., Primerano, D.A., Fenger, T.W., Denvir, J., 2004. Effect of DNA damage on PCR amplification efficiency with the relative threshold cycle method. Biochemical and Biophysical Research Communications 323 (3), 823–830.
Sikorsky, J.A., Primerano, D.A., Fenger, T.W., Denvir, J., 2007. DNA damage reduces Taq DNA polymerase fidelity and PCR amplification efficiency. Biochemical and Biophysical Research Communications 355 (2), 431–437.
Sivey, J.D., Howell, S.C., Bean, D.J., McCurry, D.L., Mitch, W.A., Wilson, C.J., 2013. Role of Lysine during Protein Modification by HOCl and HOBr: Halogen-Transfer Agent or Sacrificial Antioxidant? Biochemistry 52 (7), 1260–1271.
Snyder, S.A., 2008. Occurrence, Treatment, and Toxicological Relevance of EDCs and Pharmaceuticals in Water. Ozone: Science & Engineering 30 (1), 65–69.
Soltermann, F., Abegglen, C., Götz, C., von Gunten, U., 2016. Bromide Sources and Loads in Swiss Surface Waters and Their Relevance for Bromate Formation during Wastewater Ozonation. Environmental Science & Technology 50 (18), 9825–9834.
Soltermann, F., Abegglen, C., Tschui, M., Stahel, S., von Gunten, U., 2017. Options and limitations for bromate control during ozonation of wastewater. Water Research 116, 76–85.
Song, R., Donohoe, C., Minear, R., Westerhoff, P., Ozekin, K., Amy, G., 1996. Empirical Modeling of Bromate Formation during ozonation of Bromide-Containing Waters. Wat. Res. 30, 1161–1168.
Song, R., Westerhoff, P., Minear, R.A., Amy, G., 1997. Bromate minimization during ozonation. J. Amer. Water Works Assoc. 89 (6), 69–78.
Staehelin, J., Bühler, R.E., Hoigné, J., 1984. Ozone Decomposition in Water Studied by Pulse Radiolysis 2. OH and HO4 as Chain Intermediates. J. Phys. Chem. 88, 5999–6004.
Staehelin, J., Hoigné, J., 1985. Decomposition of Ozone in Water in the Presence of Organic Solutes Acting as Promoters and Inhibitors of Radical Chain Reactions. Environ. Sci. Technol. 19, 1206–1213.
Stalter, D., Magdeburg, A., Oehlmann, J., 2010a. Comparative toxicity assessment of ozone and activated carbon treated sewage effluents using an in vivo test battery. Water Research 44 (8), 2610–2620.
Stalter, D., Magdeburg, A., Weil, M., Knacker, T., Oehlmann, J., 2010b. Toxication or detoxication? In vivo toxicity assessment of ozonation as advanced wastewater treatment with the rainbow trout. Water Research 44 (2), 439–448.
Stapf, M., Miehe, U., Jekel, M., 2016. Application of online UV absorption measurements for ozone process control in secondary effluent with variable nitrite concentration. Water Research 104, 111–118.
Steinle-Darling, E., 2015. The Many Faces of DPR in Texas. Journal - AWWA 107 (3), 16–20.
Sudhakaran, S., Amy, G.L., 2013. QSAR models for oxidation of organic micropollutants in water based on ozone and hydroxyl radical rate constants and their chemical classification. Water Research 47 (3), 1111–1122.
Sun, Y., Angelotti, B., Brooks, M., Dowbiggin, B., Evans, P.J., Devins, B., Wang, Z.-W., 2018. A pilot-scale investigation of disinfection by-product precursors and trace organic removal mechanisms in ozone-biologically activated carbon treatment for potable reuse. Chemosphere 210, 539–549.
Sundaram, V., Pagilla, K., Guarin, T., Li, L., Marfil-Vega, R., Bukhari, Z., 2020. Extended field investigations of ozone-biofiltration advanced water treatment for potable reuse. Water Research 172, 115513.
Swietlik, J., Dabrowska, A., Raczyk-Stanislawiak, U., Nawrocki, J., 2004. Reactivity of natural organic matter fractions with chlorine dioxide and ozone. Water Research 38 (3), 547–558.
Swietlik, J., Sikorska, E., 2004. Application of fluorescence spectroscopy in the studies of natural organic matter fractions reactivity with chlorine dioxide and ozone. Water Research 38 (17), 3791–3799.
Swietlik, J., Raczyk-Stanislawiak, U., Nawrocki, J., 2009. The influence of disinfection on aquatic biodegradable organic carbon formation. Water Research 43 (2), 463–473.
Tang, C.L., Alexov, E., Pyle, A.M., Honig, B., 2007. Calculation of pK(a)s in RNA: On the structural origins and functional roles of protonated nucleotides. Journal of Molecular Biology 366 (5), 1475–1496.
Tekle-Röttering, A., Jewell, K.S., Reisz, E., Lutze, H.V., Ternes, T.A., Schmidt, W., Schmidt, T.C., 2016a. Ozonation of piperidine, piperazine and morpholine: Kinetics, stoichiometry, product formation and mechanistic considerations. Water Research 88, 960–971.
Tekle-Röttering, A., Reisz, E., Jewell, K.S., Lutze, H.V., Ternes, T.A., Schmidt, W., Schmidt, T.C., 2016b. Ozonation of pyridine and other N-heterocyclic aromatic compounds: Kinetics, stoichiometry, identification of products and elucidation of pathways. Water Research 102, 582–593.
Tekle-Röttering, A., von Sonntag, C., Reisz, E., vom Eyser, C., Lutze, H.V., Turk, J., Naumov, S., Schmidt, W., Schmidt, T.C., 2016c. Ozonation of anilines: Kinetics, stoichiometry, product identification and elucidation of pathways. Water Research 98, 147–159.
Tekle-Röttering, A., Lim, S., Reisz, E., Lutze, H.V., Abdighahroudi, M.S., Willach, S., Schmidt, W., Tentscher, P.R., Rentsch, D., McArdell, C.S., Schmidt, T.C., von Gunten, U., 2020. Reactions of pyrrole, imidazole, and pyrazole with ozone: kinetics and mechanisms. Environmental Science-Water Research & Technology 6 (4), 976–992.
Tentscher, P.R., Bourgin, M., von Gunten, U., 2018. Ozonation of *Para* -Substituted Phenolic Compounds Yields *p* -Benzoquinones, Other Cyclic α,β-Unsaturated Ketones, and Substituted Catechols. Environmental Science & Technology 52 (8), 4763–4773.
Tentscher, P.R., Lee, M., von Gunten, U., 2019. Micropollutant Oxidation Studied by Quantum Chemical Computations: Methodology and Applications to Thermodynamics, Kinetics, and Reaction Mechanisms. Accounts of Chemical Research 52 (3), 605–614.
Tentscher, P.R., Escher, B.I., Schlichting, R., König, M., Bramaz, N., Schirmer, K., von Gunten, U., 2021. Toxic effects of substituted p-benzoquinones and hydroquinones in in vitro bioassays are altered by reactions with the cell assay medium. Water Research 202, 117415.
Ternes, T., Joss, A., 2006. Human Pharmaceuticals, Hormones and Fragrances. The challenge of micropollutants in urban water management, IWA, London.
Ternes, T.A., 1998. Occurrence of drugs in German sewage treatment plants and rivers. Water Res 32, 3245–3260.
Ternes, T.A., Stuber, J., Herrmann, N., McDowell, D., Ried, A., Kampmann, M., Teiser, B., 2003. Ozonation: a tool for removal of pharmaceuticals, contrast media and musk fragrances from wastewater? Water Research 37 (8), 1976–1982.
Ternes, T.A., Joss, A., Siegrist, H., 2004. Peer Reviewed: Scrutinizing Pharmaceuticals and Personal Care Products in Wastewater Treatment. Environmental Science & Technology 38 (20), 392A–399A.
Ternes, T.A., Prasse, C., Eversloh, C.L., Knopp, G., Cornel, P., Schulte-Oehlmann, U., Schwartz, T., Alexander, J., Seitz, W., Coors, A., Oehlmann, J., 2017. Integrated Evaluation Concept to Assess the Efficacy of Advanced Wastewater Treatment Processes for the Elimination of Micropollutants and Pathogens. Environmental Science & Technology 51 (1), 308–319.
Theruvathu, J.A., Flyunt, R., Aravindakumar, C.T., von Sonntag, C., 2001. Rate constants of ozone reactions with DNA, its constituents and related compounds. Journal of the Chemical Society-Perkin Transactions 2 (3), 269–274.
These, A., Reemtsma, T., 2005. Structure-dependent reactivity of low molecular weight fulvic acid molecules during ozonation. Environmental Science & Technology 39 (21), 8382–8387.
Thibaud, H., de Laat, J., Merlet, N., Doré, M., 1987. Formation de chloropicrine en milieu aqueux: Influence des nitrites sur la formation de precurseurs par oxydation de composes organiques. Water Research 21 (7), 813–821.
Tian, Z., Zhao, H., Peter, K.T., Gonzalez, M., Wetzel, J., Wu, C., Hu, X., Prat, J., Mudrock, E., Hettinger, R., Cortina, A.E., Biswas, R.G., Kock, F.V.C., Soong, R., Jenne, A., Du, B., Hou, F., He, H., Lundeen, R., Gilbreath, A., Sutton, R., Scholz, N.L., Davis, J.W., Dodd, M.C., Simpson, A., McIntyre, J.K., Kolodziej, E.P., 2021. A ubiquitous tire rubber–derived chemical induces acute mortality in coho salmon. Science 371, 185–189.
Trogolo, D., Mishra, B.K., Heeb, M.B., von Gunten, U., Arey, J.S., 2015. Molecular Mechanism of NDMA Formation from N,N-Dimethylsulfamide During Ozonation: Quantum Chemical Insights into a Bromide-Catalyzed Pathway. Environmental Science & Technology 49 (7), 4163–4175.

Utsumi, H., Han, S.-K., Ichikawa, K., 1998. Enhancement of hydroxyl radical generation by phenols and their reaction intermediates during ozonation. Water Science and Technology 38 (6), 147–154.
Vaidya, R., Buehlmann, P.H., Salazar-Benites, G., Schimmoller, L., Nading, T., Wilson, C. A., Bott, C., Gonzalez, R., Novak, J.T., 2019. Pilot Plant Performance Comparing Carbon-Based and Membrane-Based Potable Reuse Schemes. Environmental Engineering Science 36 (11), 1369–1378.
Valdés, H., Zaror, C.A., Jekel, M., 2004. Kinetic study of reactions between ozone and benzothiazole in water. Water Science and Technology 48 (11-12), 505–510.
van der Kooij, D., Hijnen, W.A.M., Kruithof, J., 1989. The effects of ozonation, biological filtration and the distribution on the concentration of easily assimilable organic carbon (AOC) in drinking water. Ozone Sci. Eng. 11, 297.
van Ginkel, C.G., van Haperen, A.M., van der Togt, B., 2005. Reduction of bromate to bromide coupled to acetate oxidation by anaerobic mixed microbial cultures. Water Research 39 (1), 59–64.
Völker, J., Stapf, M., Miehe, U., Wagner, M., 2019. Systematic Review of Toxicity Removal by Advanced Wastewater Treatment Technologies via Ozonation and Activated Carbon. Environmental Science & Technology 53 (13), 7215–7233.
von Gunten, U., Hoigné, J., 1994. Bromate formation during ozonation of bromide-containing waters: Interaction of ozone and hydroxyl radical reactions. Environ. Sci. Technol. 28, 1234–1242.
von Gunten, U., Oliveras, Y., 1998. Advanced Oxidation of bromide-containing waters: bromate formation mechanisms. Environ. Sci. Technol. 32, 63–70.
von Gunten, U., 2003a. Ozonation of drinking water: Part II. Disinfection and by-product formation. Water Res 37, 1469–1487.
von Gunten, U., 2003b. Ozonation of drinking water: Part I. Oxidation kinetics and product formation. Water Research 37 (7), 1443–1467.
von Gunten, U., Salhi, E., Schmidt, C.K., Arnold, W.A., 2010. Kinetics and Mechanisms of N-Nitrosodimethylamine Formation upon Ozonation of N,N-Dimethylsulfamide-Containing Waters: Bromide Catalysis. Environmental Science & Technology 44 (15), 5762–5768.
von Gunten, U., 2018. Oxidation Processes in Water Treatment: Are We on Track? Environmental Science & Technology 52 (9), 5062–5075.
von Sonntag, C., von Gunten, U., 2012. Chemistry of ozone in water and wastewater treatment from basic principles to applications. IWA Publishing, London.
Voumard, M., Breider, F. and von Gunten, U., submitted, Effect of cetyltrimethyl ammonium chloride on various Escherichia coli strains and their inactivation by ozone and monochloramine. Water Research.
Walpen, N., Houska, J., Salhi, E., Sander, M., von Gunten, U., 2020. Quantification of the electron donating capacity and UV absorbance of disssolved organic matter during wastewater ozonation by an assay and an automated analyzer. Water Res 185 (15), 116235.
Walpen, N., Joss, A., von Gunten, U., 2022. Application of UV absorbance and electron-donating capacity as surrogates for micropollutant abatement during full-scale ozonation of secondary-treated wastewater. Water Research 209, 117858.
Wang, S., Wang, X., Chen, J., Qu, R., Wang, Z., 2017. Removal of the UV Filter Benzophenone-2 in Aqueous Solution by Ozonation: Kinetics, Intermediates, Pathways and Toxicity. Ozone: Science & Engineering 40 (2), 122–132.
Weishaar, J.L., Aiken, G.R., Bergamaschi, B.A., Fram, M.S., Fujii, R., Mopper, K., 2003. Evaluation of specific ultraviolet absorbance as an indicator of the chemical composition and reactivity of dissolved organic carbon. Environmental Science & Technology 37 (20), 4702–4708.
Wenk, J., Aeschbacher, M., Salhi, E., Canonica, S., von Gunten, U., Sander, M., 2013. Chemical Oxidation of Dissolved Organic Matter by Chlorine Dioxide, Chlorine, And Ozone: Effects on Its Optical and Antioxidant Properties. Environmental Science & Technology 47 (19), 11147–11156.
Wert, E.C., Rosario-Ortiz, F.L., Drury, D.D., Snyder, S.A., 2007. Formation of oxidation byproducts from ozonation of wastewater. Water Research 41 (7), 1481–1490.
Wert, E.C., Rosario-Ortiz, F.L., Snyder, S.A., 2009. Effect of ozone exposure on the oxidation of trace organic contaminants in wastewater. Water Research 43 (4), 1005–1014.
Wert, E.C., Rosario-Ortiz, F.L., 2011. Effect of Ozonation on Trihalomethane and Haloacetic Acid Formation and Speciation in a Full-Scale Distribution System. Ozone-Science & Engineering 33 (1), 14–22.
Westerhoff, P., Mash, H., 2002. Dissolved organic nitrogen in drinking water supplies: a review. Journal of Water Supply Research and Technology-Aqua 51 (8), 415–448.
White, E.H., Egger, N., 1984. Reaction of Sydnones with Ozone as a Method of Deamination On the Mechanism of Inhibition of Monoamine Oxidase by Sydnones. J Am Chem Soc 106, 3701–3703.
WHO, 2017. Guidelines for Drinking Water Quality, Fourth Edition. World Health Organization, Geneva.
Wilcox, J.L., Ahluwalia, A.K., Bevilacqua, P.C., 2011. Charged Nucleobases and Their Potential for RNA Catalysis. Accounts of Chemical Research 44 (12), 1270–1279.
Wildhaber, Y.S., Mestankova, H., Scharer, M., Schirmer, K., Salhi, E., von Gunten, U., 2015. Novel test procedure to evaluate the treatability of wastewater with ozone. Water Research 75, 324–335.
Witkowski, B., Jurdana, S., Gierczak, T., 2018. Limononic Acid Oxidation by Hydroxyl Radicals and Ozone in the Aqueous Phase. Environmental Science & Technology 52 (6), 3402–3411.
Witkowski, B., Al-sharafi, M., Gierczak, T., 2019. Ozonolysis of β-Caryophyllonic and Limononic Acids in the Aqueous Phase: Kinetics, Product Yield, and Mechanism. Environmental Science & Technology 53 (15), 8823–8832.
Wittmer, A., Heisele, A., McArdell, C.S., Böhler, M., Longree, P., Siegrist, H., 2015. Decreased UV absorbance as an indicator of micropollutant removal efficiency in wastewater treated with ozone. Water Science and Technology 71 (7), 980–985.
Wolf, C., von Gunten, U., Kohn, T., 2018. Kinetics of Inactivation of Waterborne Enteric Viruses by Ozone. Environmental Science & Technology 52 (4), 2170–2177.
Wolf, C., Pavese, A., von Gunten, U., Kohn, T., 2019. Proxies to monitor the inactivation of viruses by ozone in surface water and wastewater effluent. Water Research 166, 115088.
Wu, Q.-Y., Zhou, Y.-T., Li, W., Zhang, X., Du, Y., Hu, H.-Y., 2019. Underestimated risk from ozonation of wastewater containing bromide: Both organic byproducts and bromate contributed to the toxicity increase. Water Research 162, 43–52.
Xu, P., Janex, M.L., Savoye, P., Cockx, A., Lazarova, V., 2002. Wastewater disinfection by ozone: main parameters for process design. Wat. Res. 36, 1043–1055.
Yao, C.C.D., Haag, W.R., 1991. Rate Constants for Direct Reactions of Ozone with Several Drinking-Water Contaminants. Water Research 25 (7), 761–773.
Yao, Y., Xie, Y., Zhao, B., Zhou, L., Shi, Y., Wang, Y., Sheng, Y., Zhao, H., Sun, J., Cao, H., 2020. N-dependent ozonation efficiency over nitrogen-containing heterocyclic contaminants: A combined density functional theory study on reaction kinetics and degradation pathways. Chemical Engineering Journal 382, 122708.
Yoon, Y., Chung, H.J., Di, D.Y.W., Dodd, M.C., Hur, H.G., Lee, Y., 2017. Inactivation efficiency of plasmid-encoded antibiotic resistance genes during water treatment with chlorine, UV, and UV/H2O2. Water Research 123, 783–793.
Zarei-Baygi, A., Harb, M., Wang, P., Stadler, L.B., Smith, A.L., 2019. Evaluating Antibiotic Resistance Gene Correlations with Antibiotic Exposure Conditions in Anaerobic Membrane Bioreactors. Environmental Science & Technology 53 (7), 3599–3609.
Zhang, H.F., Zhang, Y.H., Shi, Q., Ren, S.Y., Yu, J.W., Ji, F., Luo, W.B., Yang, M., 2012. Characterization of low molecular weight dissolved natural organic matter along the treatment trait of a waterworks using Fourier transform ion cyclotron resonance mass spectrometry. Water Research 46 (16), 5197–5204.
Zhang, K., Zhang, Z.-h., Wang, H., Wang, X.-m., Zhang, X.-h., Xie, Y.F., 2020. Synergistic effects of combining ozonation, ceramic membrane filtration and biologically active carbon filtration for wastewater reclamation. Journal of Hazardous Materials 382, 121091.
Zheng, J., Su, C., Zhou, J.W., Xu, L.K., Qian, Y.Y., Chen, H., 2017. Effects and mechanisms of ultraviolet, chlorination, and ozone disinfection on antibiotic resistance genes in secondary effluents of municipal wastewater treatment plants. Chemical Engineering Journal 317, 309–316.
Zhu, H., Shen, Z., Tang, Q., Ji, W., Jia, L., 2014. Degradation mechanism study of organic pollutants in ozonation process by QSAR analysis. Chemical Engineering Journal 255, 431–436.
Zhu, H., Guo, W., Shen, Z., Tang, Q., Ji, W., Jia, L., 2015. QSAR models for degradation of organic pollutants in ozonation process under acidic condition. Chemosphere 119, 65–71.
Zhuang, Y., Ren, H.Q., Geng, J.J., Zhang, Y.Y., Zhang, Y., Ding, L.L., Xu, K., 2015. Inactivation of antibiotic resistance genes in municipal wastewater by chlorination, ultraviolet, and ozonation disinfection. Environmental Science and Pollution Research 22 (9), 7037–7044.
Zimmermann, S.G., Wittenwiler, M., Hollender, J., Krauss, M., Ort, C., Siegrist, H., von Gunten, U., 2011. Kinetic assessment and modeling of an ozonation step for full-scale municipal wastewater treatment: Micropollutant oxidation, by-product formation and disinfection. Water Research 45 (2), 605–617.
Zimmermann, S.G., Schmukat, A., Schulz, M., Benner, J., von Gunten, U., Ternes, T.A., 2012. Kinetic and Mechanistic Investigations of the Oxidation of Tramadol by Ferrate and Ozone. Environmental Science & Technology 46 (2), 876–884.
Zoumpouli, G.A., Zhang, Z., Wenk, J., Prasse, C., 2021. Aqueous ozonation of furans: Kinetics and transformation mechanisms leading to the formation of α,β-unsaturated dicarbonyl compounds. Water Research 203, 117487.
Zucker, I., Mamane, H., Riani, A., Gozlan, I., Avisar, D, 2018. Formation and degradation of N-oxide venlafaxine during ozonation and biological post-treatment. Science of the Total Environment 619, 578–586.
Zürcher, F., Bader, H. and Hoigne, J. (1978) Verhalten organischer Spurenstoffe bei der Ozonung von Trinkwasser., pp. 198-213, Berlin.